The Hong Kong Polytechnic University

Department of Building Services Engineering

Diagnosis and Robust Control of Complex Building Central Chilling Systems for Enhanced Energy Performance

GAO Diance

A thesis submitted in partial fulfillment of the requirements

for the Degree of Doctor of Philosophy

April, 2012

CERTIFICATE OF ORIGINALITY

I hereby declare that this thesis is my own work and that, to the best of my knowledge and belief, it reproduces no materials previously published or written, nor material that has been accepted for the award of any other degree or diploma, except where due acknowledgement has been made in the text.

I also declare that the intellectual content of this thesis is the product of my own work, except to the extent that assistance from others in the project's design and conception or in style, presentation and linguistic expression is acknowledged.

GAO Diance

Department of Building Services Engineering

The Hong Kong Polytechnic University

Hong Kong, P.R. China

April, 2012

ABSTRACT

Abstract of thesis entitled: Diagnosis and Robust Control of Complex Building Central Chilling Systems for Enhanced Energy Performance

Submitted by : GAO Diance

For the degree of : Doctor of Philosophy

at The Hong Kong Polytechnic University in April, 2012

Low delta-T syndrome (i.e., low chilled water temperature difference disease) and deficit flow problem (i.e., the required flow rate of secondary loop exceeds that of the primary loop) widely exist in many building chilled water systems, which make the system fail to operate as efficient as anticipated, degrading the overall building energy performance. This thesis focuses on developing diagnosis and robust control strategies to avoid or improve the low delta-T syndrome and enhance the operation and energy performance of chilled water systems.

The main contributions of this thesis include an in-situ case study to diagnose the low delta-T syndrome in a complex building chilled water system, an online optimal control strategy for complex chilled water systems involving heat exchangers, a fault-tolerant control strategy for secondary chilled water systems, and a fault diagnosis strategy integrated with energy impact evaluation method for low delta-T syndrome. These proposed strategies are developed based on an actual chilling

system in a super high-rise building, and are tested and validated on a dynamic simulation platform developed in this study prior to site implementation.

Firstly, an in-situ case study to diagnose the low delta-t syndrome and deficit flow problem that frequently occurred in the studied super high-rise building is conducted. An in-situ diagnosis method of low delta-t syndrome for practical applications is proposed, which involves history operation data analysis and experimental validation. The reasons for low delta-T syndrome in this studied system are detected and identified, and corresponding suggestions are provided as well.

Secondly, based on the causes that resulted in low delta-T syndrome found in the actual super high-rise building under study, an adaptive optimal control strategy for online control of complex chilled water systems involving intermediate heat exchangers is developed. This optimal control strategy searches for the optimal settings of the outlet water temperature after heat exchangers and the required operating number of heat exchangers and pumps in order to minimize the total energy consumption of pumps under various working conditions. The strategy has enhanced control robustness and reliability including avoiding deficit flow problem when compared with the conventional strategies. An adaptive method is utilized to update the key parameters of the proposed models online. The proposed strategy is validated to be robust and reliable to eliminate deficit flow problem when facing disturbances. The test results also demonstrate that the proposed strategy can accurately identify the optimal control settings. Significant energy of pumps

therefore can be saved when compared with other conventional methods for online practical applications.

Thirdly, a fault-tolerant control strategy for secondary chilled water pumps is developed not only for eliminating the low delta-T syndrome and deficit flow problem but also for enhancing the energy efficiency of the chilled water distribution systems. This fault-tolerant strategy employs the developed flow-limiting technique that is activated when deficit flow tends to occur and eliminates it by resetting the differential pressure set-point for pumps control. This strategy also integrates optimal differential pressure set-point that can minimize flow resistance of chilled water loop while still satisfying cooling energy demand. The performance of this proposed strategy is evaluated in a simulated environment representing a chilled water system in a super high-rise commercial building by comparing it with two conventional control strategies. Results show that the proposed strategy can effectively eliminate the deficit flow in the bypass at both starting and normal operation periods.

Fourthly, a fault detection and diagnosis (FDD) strategy integrated with an energy impact evaluation method for low delta-at syndrome is developed to identify the low delta-T problem caused by cooling coils under various working conditions, and predict its energy impact on the pumps using a model-based method.

Fifthly, an in-situ approach is presented for experimental validation of the possibility by using a check valve (i.e., putting a one-direction check valve in the chilled water by-pass line) in the studied super high-rise building to solve the deficit flow problem

and thus to enhance the overall operational performance. The experimental tests were carried out on the complex central chilled water system in a super high-rise building by using a ‘simulated’ check valve through fully closing one of the butterfly valves in the by-pass line when the system operated with significant excess flow demand and experienced with low delta-T problems. The results showed that the system operational performance can be improved greatly when the ‘simulated’ check valve was used as compared to that without using the check valve.

Lastly, the software tools and implementation guidelines for applying these online supervisory and optimal control strategies in practice are presented.

PUBLICATIONS ARISING FROM THIS THESIS

Journal Papers Published

2013 Wang S.W., **Gao D.C.**, Sun Y.J. and Xiao F. 2013. An online adaptive optimal control strategy for complex building chilled water systems involving intermediate heat exchangers. *Applied Thermal Engineering* 50(1): 614-628.

2012 **Gao D.C.**, Wang S.W., Sun Y.J. and Xiao F. 2012. Diagnosis of the low temperature difference syndrome in the chilled water system of a super high-rise building: a case study. *Applied Energy* 98(1): 597-606.

2011 **Gao D.C.**, Wang S.W., and Sun Y.J. 2011. A fault-tolerant and energy efficient control strategy for primary–secondary chilled water systems in buildings. *Energy and buildings* 43(12): 3646–3656.

2010 Wang S.W., Ma Z.J. and **Gao D.C.** 2010. Performance enhancement of a complex chilled water system using a check valve: Experimental validations, *Applied Thermal Engineering* 30(17-18):2827-2832.

Journal Papers under preparation

2012 **Gao D.C.**, Wang S.W. and Xiao F. Fault diagnosis and energy impact evaluation of low delta-T syndrome in building chilled water system.

2012 **Gao D.C.**, Wang S.W. and Xiao F. Evaluation and solutions of low delta-T syndrome in building chilled water system: A review.

Conference Paper

2012 **Gao D.C.**, Wang S.W. and Xiao F. 2012. Online robust control of chilled water systems of buildings for energy performance enhancement. The 6th

Asian Conference on Refrigeration and Air Conditioning (ACRA), August 26-28, 2012. *Xi'an, China.*

Patent

2011 Wang S.W. and **Gao D.C.** Secondary chilled water flow limiting system and strategy, China patent (filed): No. 201110202193.5.

ACKNOWLEDGEMETNS

First and foremost, I would like to express my heartfelt gratitude to my supervisor, Prof. Shengwei Wang, Chair professor, both for his intellectual guidance and for his warm and constant encouragement during the course of this research. Also, I would like to thank my co-supervisors, Dr. Fu Xiao, Assistant Professor, for her valuable suggestions over entire process of my PhD study.

My special thanks go to Sun Hung Kai Real Properties Limited for the essential support to this research work. I would also like to thank all colleagues, especially Dr. Sun Yongjun, Dr. Ma Zhenjun and Dr. Zhou Qiang, in the research team. The long road to accomplish this research is memorable because of their help and support.

Lastly, I would like to express my deepest appreciation to my wife, my parents, my daughter, and my mother-in-law, for their understanding, support and encouragement in the past years.

TABLE OF CONTENTS

Page

LIST OF FIGURES

Page

LIST OF TABLES

Page

NOMENCLATURE

A	Area (m^2)
a_0-a_2	Coefficients
B	Ratio of the impeller channel depth at intake to that at exhaust
b_0-b_2	Coefficients
c	Specific heat {kJ/(kg·K)}
C	Capacity flow rate (kW/K)
COP	Coefficient of performance
c_{01}-c_{03}, c_{11}-c_{13}	Coefficients
c_0-c_2	Coefficients
C_c	Overall thermal capacity of a coil (kW/K)
c_i	Vapor velocity at the impeller exhaust (m/s)
c_{r2}	Impeller exit radial velocity (m/s)
DP1	Differential pressure at supply side (kPa)
DP2	Differential pressure at remote side (kPa)
d_0-d_1	Coefficient
E	Coefficient
e_0-e_3	Coefficients
Freq	Frequency (Hz)
G	Coefficient
h	Enthalpy (kJ/kg)
H	Head (m or kPa)
h_{hyd}	Hydrodynamic losses (kW/kg)
h_{pol}	Polytropical compression work (kW/kg)
$h_{g,w}$	Enthalpy of water above reference state for liquid water at T_{re} (kJ/kg)
$h_{s,w}$	Saturation air enthalpy with respect to the temperature of the water surface (kJ/kg)

h_{th}	Compressor theoretical head (kW/kg)
J	Cost function
$LMTD$	Log mean temperature difference (°C)
Le	Lewis number
m	Index
M	Flow rate (kg/s or m^3/s)
n	Index
N	Number
NTU	Number of transfer units
P	Power (kW)
PD	Pressure drop/pressure differential (kPa or m)
Q	Heat transfer rate (kW)
R	Heat transfer resistance (k/kW)
r_i	Residual of the ith performance index
$\widetilde{r}_i$	Estimator of the residual of the ith performance index
S	Flow resistance ($kPa \times s^2/l^2$)
SG	Specific gravity of the fluid being pumped
SHR	Sensible heat ratio
T	Temperature (°C)
T'	Temperature after introducing dynamic effects (°C)
Th	Threshold
t_c	Mean temperature of the coil (°C)
T_{ref}	Reference temperature for zero enthalpy of liquid water (°C)
$TYPE\ XX$	Component type number
u_2	Impeller tip speed (m/s)
U	Uncertainty
UA	Overall heat transfer coefficient (kW/K)
v	Flow velocity (m/s)
W	Power consumption (kW)

Greek symbols

α	Coefficient
β	Impeller blades angle
ρ	Fluid density at the mean temperature (kg/m^3)
ε	Heat transfer effectiveness
ω	Capacity flow rate ratio
ω_a	Air humidity ratio
$\omega_{s,w}$	Saturation air humidity ratio with respect to the temperature of the water surface
$\omega_{s,w,e}$	Effective saturation air humidity ratio with respect to the temperature of the water surface
θ	Inlet guide vane angle
ξ	Flow resistance of a component
ζ, χ	Constants
ψ_1, ψ_2	Constants
η	Efficiency (%)
υ_1	Specific volume at the impeller intake (m^3/kg)
υ_i	Specific volume at the impeller exhaust (m^3/kg)
Δ	Time interval
τ	Time
φ_1-φ_5	Converting factors
σ	Standard variance
$\tilde{\sigma}^2_{\tilde{r}_i - r}$	the estimated variance of $\tilde{r}_i - r_i$
$t_{\alpha/2, n-p}$	*t* distribution with *n-p* degrees of freedom at a confidence level of (1-α)

Subscripts

a	Air
adj	Adjusted
ahx	After heat exchanger(at the secondary side of heat exchanger)
AHU	Air handling unit

a,o	Air outlet
bench	Benchmark
bhx	Before heat exchanger(at the primary side of heat exchanger)
bp	Bypass
c	Cold
cd	Condenser
ch	Chiller
com	Compressor
ct	Cooling tower
des	Design
ev	Evaporator
fic	Fictitious
h	Hot
hx	Heat exchanger
i	Individual
imp	Impeller
in	Inlet
indi	Individual
inter	Internal
LL	Lower limit
m	Motor
max	Maximum
meas	Measurement
min	Minimum
out	Outlet
p	Pressure
pf	Pump fitting
pipe	Pipeline
pri	Primary
pu	Pump

ref	Refrigerant
reg	Regressor
rtn	Return
sec	Secondary
set	Set-point
sup	Supply
term	Terminal
tot	Total
UL	Upper limit
VFD	Variable frequency drive
w	Water
wb	Wet-bulb
z1	Zone 1
z2	Zone 2
Z3	Zone 3
Z4	Zone 4

Superscripts

a_0-a_3	Coefficients
b_0-b_3	Coefficients
c_0-c_5	Coefficients
d_0-d_2	Coefficients
e_0-e_1	Coefficients
k	k^{th} time step
T	Transpose

CHAPTER 1 INTRODUCTION

1.1 Motivation

Energy crisis and global warming have made the whole world pay more attention to the problems of energy and environment. How to reduce the energy consumption and CO_2 emission while still enhancing life and environmental quality becomes the major challenge confronted by professionals.

According to the 2010 buildings energy data book provided by the U.S. Department of Energy, the buildings sector consumes 74% of U.S. electric energy in 2010, among which the residential sector and the commercial sector consumed 39% and 36%, respectively. While in Hong Kong, the proportion of the energy consumption of buildings occupies 90% of the total electric energy consumption in 2008, highly surpassing the other sectors, such as industry and transport. Within the building sector, heating, ventilating, and air-conditioning systems (HVAC) are the biggest energy consumers. The statistical data show that HVAC systems account for 44.4% of U.S. total building energy usage in 2010, while lighting and water heating merely occupy 13.4% and 9.1%, respectively (2010 buildings energy data book).

Meanwhile, the HVAC market has grown dramatically in recent years as a result of the increasing demand for better indoor thermal comfort. The rapidly growing HVAC energy consumption aggraded the world energy and environment crisis. In

general, energy saving, energy efficiency improvement, and promotion of using renewable energy sources are the three key instruments to alleviate this crisis. Therefore, enhancing the overall energy efficiency of HVAC systems has become one of the hot topics in HVAC field.

In many existing HVAC systems, the equipment cannot work at desired high efficiency due to various faults, such as improper design, lack of proper commissioning, improper control, poor maintenance, etc. Although HVAC systems were properly designed in the design period and accurately commissioned after installation, they also might not operate under anticipant states. The HVAC systems were originally designed based on the full load condition. When working conditions changed, the overall energy performance is difficult to maintain high, especially under low part load, if there is no proper control. Studies and investigations have shown that the overall building energy consumption can be reduced 20% [Kissock 1993, Claridge and Liu et al. 1996, Claridge and Culp et al. 2000], even 50% under some conditions [Liu and Athar et al. 1994], by eliminating the faults and employing optimal control. It also can be seen in ASHRAE handbook of application that it can improve the building energy performance and increase the indoor environment quality by implementing optimal and supervisory control strategies.

Chilled water system plays an important role in the entire HVAC systems. It mainly consists of chillers, distributing pumps, heat exchangers, terminal units, pipelines, water valves, and so on. The main functions of chilled water system are to generate

the chilled water (by chillers) and deliver them to the terminal units (by pumps) to meet the desired cooling load. Over the last two decades, primary-secondary chilled water systems have been widely employed to offer comfortable indoor environment in commercial buildings, especially in large buildings, due to its higher energy efficiency than the traditional constant flow system. While in real applications, most of the primary-secondary systems, from time to time, cannot work as efficient as expected because of the excess secondary flow demand, which causes deficit flow problem (i.e. the required flow rate of secondary loop exceeds that of the primary loop). When the deficit flow problem exists, the temperature difference produced by the terminal units will be much lower than its design values, which is known as the low delta-T syndrome [Kirsner et al. 1994, Waltz 2000, Kirsner 1998, Avery 1998]. Kirsner [1994] pointed out that the low delta-T chilled water plant syndrome existed in almost all large distributed chilled water systems.

A series of operational problems might be caused by the deficit flow problem and low delta-T syndrome in practical applications, such as the high supply water temperature, the over-supplied chilled water, and the increased energy consumption of the secondary pumps. Existing studies [McQuay 2002, Taylor 2002, Durkin 2005] demonstrated a lot of potential causes for the deficit flow problem and the low delta-T syndrome. The causes mainly include improper set-points or poor control calibration, the use of three-way valves, improper coil and control valve selection, no control valve interlock, and uncontrolled process load, reduced coil effectiveness, outdoor air economizers and 100% outdoor air systems, and so on.

Measures to handle the low delta-T syndrome also have been proposed to enhance the energy performance of chilled water systems [Fiorino 1999, Fiorino 2002, Avery 2001, Taylor 2002, Luther 2002] from component selection criteria to configurations of distribution systems, such as proper selection and application of cooling coils, controls systems, distribution pumps, and piping systems. However, most of the studies pay more attention to analyzing the possible causes and solutions of this problem from the view of design and commissioning. In practice, even the HVAC systems were properly designed and well commissioned, deficit flow still cannot be completely avoided in the operation period due to some disturbances, such as improper control strategies, unreliable control settings, or sudden change in cooling load. There are no reliable, robust and secure solutions that can eliminate deficit flow in real applications. The research associated with proper control of secondary pumps to eliminate deficit flow and low delta-T syndrome for real applications is missing. Further more, many of the proposed solutions from the viewpoint of design might be only feasible to be adopted in new systems, while solutions from the viewpoint of operation and control are still insufficient, which will be practical and preferable for the large number of existing systems suffering from the deficit flow and low delta-T syndrome.

Therefore, this research focuses on how to eliminate the low delta-T syndrome and deficit flow problem by developing fault diagnosis and robust control strategies for enhancing the energy performance of complex chilled water systems during the operation period.

1.2 Aim and Objectives

The aim of this study is to develop proper solutions for chilled water systems to eliminate the low delta-T syndrome and deficit flow problem in order to enhance the operation and energy performances of chilled water systems. Three approaches, in terms of fault detection and diagnosis (FDD) strategies, proper control strategies and the use of check valve, are proposed for addressing the problems from different viewpoints and for different application cases.

Since low delta-T syndrome and deficit flow problem are the symptoms only, it is important to find out the real causes and then to correct them. Two fault diagnosis strategies are proposed to determine the exact causes resulting in the problems. One is the in-situ FDD method developed for preliminarily diagnosing the simple reasons, which is easy and convenient for in-situ implementation. Another advanced FDD method is proposed to determine the exactly potential reasons and evaluate the energy impact on the system.

Since the existing control strategies for chilled water distribution system is not robust and easily cause deficit flow problem when facing disturbances, two novel control strategies are proposed to control the chilled water system in proper operation to avoid the occurrence of low delta-T syndrome and deficit flow problem. One is the adaptive optimal control strategy for complex chilled water system involving heat exchangers, which provides optimal control settings with enhanced robustness that can ensure stable operation of the system even facing disturbances.

Another is the fault-tolerant control strategy, which can automatically eliminate the deficit flow in the bypass line when the deficit flow is detected, and therefore enhance the system energy performance even faults still exist.

Since the check valve is a solution that is discussed and not fully accepted in the field, this study evaluates the feasibility of using check valve in a real complex chilled water system, and assess its energy benefits. It is noticed that the proposed FDD strategies and control strategies can be implemented in a system simultaneously. The check valve and the fault-tolerant control strategy are not for the use at the same time as they handle the same problem by two different means.

The detailed objectives and subtasks of this research are listed below:

(1) Establish a dynamic simulation platform for complex building central chilling systems to test and analyze the control performances and economic feasibilities of different control strategies;

(2) Develop an in-situ fault diagnosis method and conduct a case study on diagnosing the low delta-T problem resulted from the deficit flow that frequently occurred in the chilled water system of a super high-rise building at operation stage;

(3) Develop an optimal control strategy for complex chilled water systems involving intermediate heat exchangers, which can determine the optimal control settings for variable speed pumps and heat exchangers to achieve energy efficient operation and to avoid low delta-T syndrome and deficit flow problem;

(4) Develop a fault-tolerant control strategy for variable speed pumps to eliminate the deficit flow in the chilled water systems, which can avoid too low chilled water temperature difference and ensure a relatively high energy performance of a system although the occurrence of faults in system might cause the deficit flow.

(5) Develop a fault diagnosis strategy and an energy impact evaluation method for low delta-T syndrome resulted from performance degradation of cooling coils and/or heat exchangers, which can identify the degraded system temperature difference under various working conditions and evaluate its energy impact on the pumps using a model-based method;

(6) Conduct an in-situ experimental validation of feasibility by using a check valve to eliminate the deficit flow and enhance the operational performance of the complex chilled water system.

1.3 Organization of This Thesis

This chapter outlines the motivation of this study. The motivation is to eliminate the low delta-T syndrome and deficit flow problem by developing fault diagnosis and robust control strategies for enhancing the energy performance of complex chilled water systems during the operation period. It also presents the aim and objectives of this thesis. The subsequent chapters are organized as follows.

Chapter 2 presents a literature review on the existing studies on the low delta-T syndrome, fault diagnosis strategies, robust and optimal control strategies, etc, for

enhancing the operation and energy performance of HVAC systems. The analysis and evaluation of these studies are provided as well.

Chapter 3 describes a complex central chilling system of a super high-rise building under study. A dynamic simulation platform is established based on this studied building chilling system, which is implemented as a tool to test and analyze the control performances and economic feasibilities of different control strategies.

In Chapter 4, an in-situ fault diagnosis method and a case study to diagnose the low delta-T syndrome and deficit flow problem in a real chilled water system of a super high-rise building are presented. Improper set-point reset of the outlet water temperature at the secondary sides of heat exchangers were finally to be determined as the exact fault that caused the deficit flow problem, which is also confirmed by the in-situ tests.

Chapter 5 presents an optimal control strategy for online control of complex chilled water systems involving intermediate heat exchangers to enhance their operation and energy performances. This optimal control strategy searches for the optimal settings of the outlet water temperature after heat exchangers and the required operating number of heat exchangers and pumps in order to minimize the total energy consumption of pumps under various working conditions. The control robustness and reliability of eliminating deficit flow problem is also considered as the constraints in this strategy.

Chapter 6 presents a fault-tolerant and energy efficient control strategy for secondary pumps to eliminate deficit flow problem of the primary-secondary chilled water systems concerning both operating efficiency and tolerance to unhealthy and faulty balances of chilled water systems. The performance of this strategy is validated on a simulated dynamic system constructed based on the real system in a supper-high-rise building.

In Chapter 7, a fault diagnosis strategy is presented to diagnose the low delta-T syndrome and the deficit flow problem resulted from the degraded cooling coils. Meanwhile, an energy impact evaluation method is also developed to evaluate the energy impact of pumps in a complex building chilled water system when suffering from low delta-T syndrome.

Chapter 8 presents an approach for experimental validation of the possibility by using a check valve (i.e., putting a one-direction check valve in the chilled water by-pass line) in the studied super high-rise building to solve the deficit flow problem and thus to enhance the overall operational performance.

Chapter 9 presents the implementation of the developed fault diagnosis strategy and online control strategies for robust and optimal control of the complex building chilling system in practice.

Chapter 10 summarizes the main work and contributions of this study, and gives recommendations for future application and research in the related areas.

CHAPTER 2 LITERATURE REVIEW

Since this study mainly focuses on providing solutions and measures to solve the low delta-T syndrome and the deficit flow problem in chilled water systems by means of diagnosis and control strategies, a brief review on the studies and researches concerning the low delta-T syndrome, optimal and robust control, as well as fault detection and diagnosis (FDD) in HVAC systems will be presented.

Section 2.1 presents the existing studies on the low delta-T syndrome, including some causes and solutions. In Section 2.2, researches on optimal and robust control for HVAC systems are summarized. Section 2.3 presents the studies on the FDD methods applied in the HVAC system. Section 2.4 provides the discussions on the existing studies of low delta-T syndrome, control methods, and FDD methods. A summary of this chapter is given in Section 2.5.

2.1 The low delta-T syndrome in chilled water systems

2.1.1 An overview

Over the last decades, primary-secondary chilled water systems have been widely used in commercial buildings. In a typical primary-secondary chilled water system, the primary constant speed pumps ensure the chillers operate with constant flow rate, and the secondary variable speed pumps vary the flow rate according to the cooling

demands of the terminals. It is an energy efficient configuration when compared with a constant flow system [Wang 2010]. While in real applications, most of the primary-secondary systems, from time to time, do not work as efficient as expected due to the excess secondary flow demand, which causes deficit flow problem (i.e. the required flow rate of secondary loop exceeds that of the primary loop). The excess return water flow rate will flow through the bypass line and mix with the main supply chilled water, resulting in increased temperature of water supplied to building and thus higher flow demand from terminals. Since the cooling coils are selected to produce a temperature rise at full load that is equal to the temperature differential selected for the chillers. The flow rate of secondary loop should be therefore equal to that of the primary loop under full load condition and should be less than that of primary loop under part load condition. When the deficit flow problem exists, the temperature differential produced by the terminals might be much lower than its design values, which is known as low delta-T syndrome [Kirsner et al. 1994, Waltz 2000, Kirsner 1998, Avery 1998]. Kirsner [1994] pointed out that low delta-T chilled water plant syndrome exists in almost all large distributed chilled water systems.

The deficit flow may cause a series of operational problems, such as the high supply water temperature, the over-supplied chilled water, and the increased energy consumption of the secondary pumps. If such phenomenon cannot be eliminated, a vicious circle in the secondary loop may be caused. It means that, when the deficit flow occurs, the mixing of the return chilled water to the supply chilled water results in higher temperature of chilled water supplied to the terminal air-handling units

(AHU). The increased temperature of the supply chilled water consequently leads to an increased chilled water flow rate which further worsens the deficit flow. The deficit flow will not disappear until the flow rate in the primary loop is increased greatly (e.g. an additional chiller is switched on).

2.1.2 Causes and solutions for low delta-T syndrome

During the past two decades, many possible reasons and solutions for low delta-T syndrome have been investigated.

Kirsner [1996] stated that the standard primary-secondary chilled water design cannot solve the low delta-T syndrome and a new paradigm with variable-flow primary pumps should be adopted for chilled water design. Three problems of the typical primary-secondary chilled water system were presented. The first problem is that the primary-secondary control scheme is "blinded" by low delta-T syndrome in the systems where the chillers are staged on and off based on the flow rate of the bypass line. Secondly, a constant-flow primary chilled water system with one fixed flow pump per chiller cannot response effectively to low delta-T syndrome. Thirdly, secondary pumping is not the most efficient pumping distribution scheme. Based on the analysis, it is proposed that a variable-flow design, including primary and secondary pumps, can response to the low delta-T syndrome, and it is needed to replace the conventional primary-secondary scheme.

Taylor [2002] presented some causes that result in low delta-T syndrome and

proposed some corresponding solutions. It was pointed out that some causes can be avoided, such as improper set-point or controls calibration, the use of three-way valves, improper coil and control valve selection, no control valve interlock, and uncontrolled process load, etc.. While some causes cannot be avoided, such as reduced coil effectiveness, outdoor air economizers and 100% outdoor air systems. The detailed description of causes and solutions for low delta-T syndrome is summarized in Table 2.1.

Taylor [2007] also stated that some causes can be resolved by proper design and component selection and proper operation and maintenance. But some of the causes of low delta-T are either impossible or not practical to eliminate. Therefore, the system must be designed to accommodate low delta-Ts in an efficient manner while still meeting all coil loads. The measures to accommodate low delta-T syndrome are proposed in Table 1.2. This can be done by using variable-speed-driven chillers, which are so efficient at part load that under all but the lowest load conditions, it is more efficient to run more chillers than are required to meet the load. Thus, additional flow resulting from degrading delta-T will have no impact on chiller energy use. To mitigate degrading delta-T for fixed-speed chiller plants, the design must allow the chillers to be over pumped (supplied with more than design flow) so that they can be more fully loaded before staging on the next chiller. Installing a check valve in the common leg of the primary-secondary connection is one way to force increased flow through chillers since it places the primary and secondary pumps in series. Other options include sizing primary pumps for increased flow

either using unequally sized pumps or with a lower design primary loop delta-T.

Table 2.1 List of causes and solutions for low delta-T syndrome

Category	Causes	Solutions
Causes that can be avoided by proper design or operation	Improper set-point or controls calibration	Check set-points regularly and adjust to design levels or higher.
	Use of three-way valves	Never use three-way valves in variable-flow systems, except perhaps for one or two valves to ensure that pumps are never dead-headed
	Improper coil selection	Document the plant design delta-T and chilled water supply temperature well and ensure that designers select coils for equal or higher delta-Ts.
	Improperly selected control valves	Proper sizing of control valves.
	No Control Valve Interlock	Control valves must be interlocked to shut off flow when the associated air handler shuts off
	Improperly Piped Coils	Coils must be piped counter flow.
	Improper tertiary connection and control	Ensure that the set-point of the controller maintaining supply water temperature to the building is several degrees above the chilled water temperature being delivered to building. Or, place a check valve in the common leg.
	Uncontrolled Process Loads	The designer should work with the process equipment supplier to determine if controls are present, and if not, whether external, field mounted shutoff valves may be installed.
Causes that can be resolved but may not result in overall energy savings	Laminar flow	The laminar flow "problem" so often referenced in the literature does not appear to be a real problem.
	Chilled water reset	The best chilled water reset strategy will vary depending on the plant design, chiller performance characteristics, and the nature of coil loads. Smaller plants, those with low pumping distribution losses, will usually benefit from chilled water reset. For large plants with high pumping distribution losses, raising chilled water temperature will increase pumping energy more than it reduces chiller energy, resulting in a net increase in plant energy usage.
Causes that cannot be avoided	Reduced coil effectiveness	Water-side fouling is easily controlled with water treatment at the time the system is filled. Air-side fouling is usually minimized by good filtration.
	Outdoor air economizers and 100% outdoor air systems	The impact of low coil entering air temperature can be mitigated by using a lower design delta-T. However, this will increase pump energy under all operating conditions, so it clearly is not a reasonable solution.

Table 2.2 Measures to accommodate low delta-T syndrome

	Causes	Solutions
Causes that can be avoided by proper design or operation	Improper set-point or controls calibration	Check set-points regularly and adjust to design levels or higher.
	Use of three-way valves	Never use three-way valves in variable-flow systems, except perhaps for one or two valves to ensure that pumps are never dead-headed.
	Improper coil selection	Document the plant design delta-T and chilled water supply temperature well and ensure that designers select coils for equal or higher delta-Ts.

Laminar flow is usually considered as one of the causes that results in the low delta-T syndrome because a sudden drop in heat transfer coefficient will occur when flow goes from the turbulent regime to the laminar flow regime when the Reynolds number drops below about 2000. However, Taylor [2002] stated that laminar flow effects are unlikely to be a major source of degrading delta-T syndrome. Figure 2.1 shows this effect on heat transfer factor J (defined as $S_t P_r^{2/3} (\mu_s/\mu)^{0.18}$ where S_t is the Stanton number, P_r is the Prandtl number, and the subscript s refers to the conditions at the inside surface of the tube) for two typical coils, one 12 feet long and one 2 feet long. At high turbulent flow rates, J is the same for both coils. As velocity decreases into the transition region, the heat transfer factor begins to fall, but less so for the shorter coil because the tube bends tend to keep flow more turbulent. At the onset laminar flow, the heat transfer factor begins to rise. Figure 2.2 shows the same data with the heat transfer factor converted to percent of design of the film heat transfer resistance at the inside surface of the tube and Reynolds number converted to percent of design flow rate. Film heat transfer resistance is only a small portion of the overall air-to-water heat transfer resistance at the design flow rate, but as water velocity falls,

this resistance rises until, at laminar flow conditions, it accounts for almost 90% of the overall resistance.

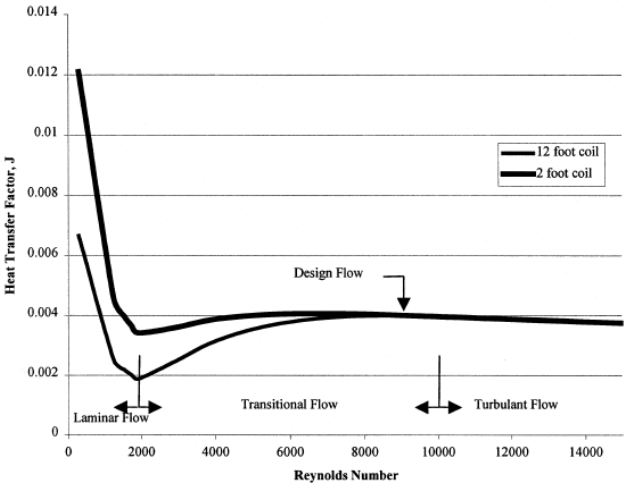

Figure 2.1 Heat transfer factor as flow varies (Taylor 2002)

(This coil was selected for 3 fps design velocity with 5/8 in. tubes. In this case, the coil never experiences fully developed turbulent flow; the design condition is already in the transition region. Laminar flow occurs at 0.5 to 0.8 fps, roughly 20% to 25% of design flow. Data obtained from coil manufacturer selection program correlated to measured coil data under low flow conditions.)

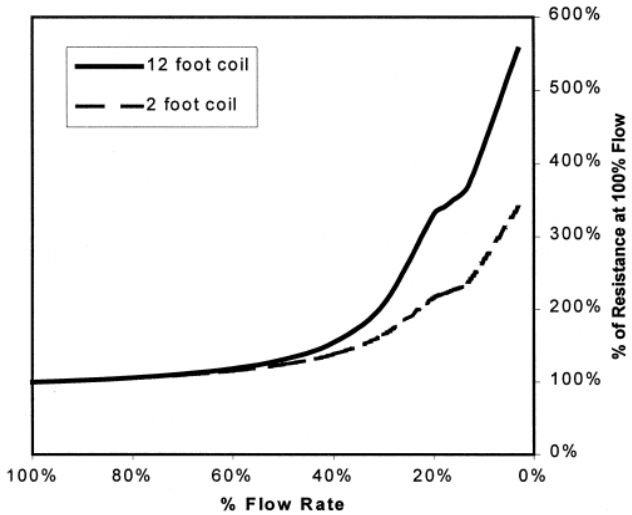

Figure 2.2 Percent of Heat transfer resistance as flow varies (Taylor 2002)

(This coil is the same as the one in the previous figure with heat transfer factor converted to percent of design the film heat transfer resistance at the inside surface of the tube and Reynolds number converted to percent of design flow rate.)

Fiorino [1999] indicated strongly that a higher delta-T can be achieved by proper

application of cooling coils, controls systems, distribution pumps, and piping systems. Up to 25 practical methods are recommended to achieve high chilled water delta-T ranging from component selection criteria to configurations of distribution systems, shown in Table 2.3.

Table 2.3 List of solutions for low delta-T syndrome

Number	Solutions
1	Select cooling/dehumidifying coils for high ΔTs.
2	Specify modulating two-way globe-style control valves with equal-percentage plugs for linear control of cooling coils.
3	Specify control valve actuators capable of accurately positioning the plug and shutting off flow at the highest ΔP that the chilled water distribution pump can apply at low flow conditions.
4	Specify control valve cages, trim, plugs, and seals capable of withstanding the erosion and cavitation present when throttling flow at the highest ΔP that the chilled water distribution pump can apply at low flow conditions.
5	Omit external balancing devices. Best practices 3 and 4 make these devices unnecessary.
6	Specify digital control for more precise control valve positioning.
7	Use chilled water multiple times before allowing it to return to the central water chilling plant.
8	Use chilled glycol for low-temperature/humidity applications that would require excessively close approach temperatures and/or subset supply temperatures if chilled water were used.
9	Use non-bypass blend-water systems rather than water-to-water heat exchangers to supply non-condensing (sensible) cooling water.
10	Treat sensible cooling and cooling/dehumidifying separately.
11	Use two cooling coils in series.
12	Use run-around pre-cooling/pre-heating coils for make-up air.
13	Replace three-way bypass control valves with two-way control valves.
14	Close control valves when air-handling unit fans are off.
15	Calibrate temperature and humidity sensors.
16	Protect temperature and humidity set-points.
17	Minimize water-side fouling and air-side restrictions.
18	Reduce chilled water distribution pump speeds at partial cooling loads.
19	Use multi-zone and primary/secondary chilled water distribution pumping.
20	Reduce differential chilled water pressure set-points at partial cooling loads.
21	Elevate chilled water supply temperatures at partial cooling loads.
22	Design reverse-return and loop-style chilled water distribution systems.
23	Eliminate constant speed chilled water “booster” pumps.
24	Replace marginally performing cooling coils and heat exchangers.
25	Monitor chilled water ΔTs and take corrective actions.

Hyman and Little (2004) analyzed the central chilled water system of the University of California Riverside (UCR) campus which also consists of a primary-secondary-tertiary pumping network. Due to inconsistent design standards over the years, some of the building (tertiary) loops were piped in series with the campus distribution (secondary) loop while others were connected with decoupling bypasses. This created negative pressure differences across the distribution mains at buildings remote from the chiller plant while, at buildings near the chiller plant, excessive positive pressure differences caused water to short-circuit back to the plant. These problems contributed to "low delta-T syndrome" which occurs when the temperature difference between the water supplied by the chiller plant and the water returning from the distribution network is noticeably lower than the designed temperature difference. Low delta-T syndrome limits the chiller capacity, resulting in inadequate cooling to the buildings served by the system. To alleviate the problems, some of the recommendations included installing variable frequency drives (VFDs) to run the pumps at reduced speeds, hydraulically decoupling the buildings that were piped in series, and installing pressure-independent control valves at locations close to the plant to eliminate leaking through the control valves.

Besides the approaches concerning the design and commissioning, the implementation of check valve on the bypass line has attracted more attention. The check valve actually is a one way valve, which only permits the water flow direction from the supply side to the return side and avoids the flow at the reverse direction in the bypass line. The major benefit of using the check valve is that an additional

chiller is not brought online simply to provide additional primary flow before the operating chillers are fully loaded [Severini 2004]. Severini [2004] described that his philosophy for designing and operation of primary-secondary chiller plants included using a check valve, which has been proved successfully in many projects. Based on a parametric study, Bahnfleth and Peyer [2004] presented that the addition of a check valve to a primary-secondary system can result in a total plant energy saving of up to 4% and a life cycle cost saving of up to 2%. Savings occurred only when the chilled water temperature differences were less than the design value. The authors pointed out that if the secondary pumps are not capable of handling the increased head and flow in the primary loop, the use of the check valve will be an unacceptable option as a retrofit. Kirsner [1998] presented that the use of a check valve is a cheap and simple improvement to the primary-secondary system. It allows a plant to efficiently deal with the low delta-T syndrome while preserving the protective features of the primary-secondary design. Avery [1998] installed a check valve in a real cooling plant for system retrofits and upgrading. The actual operation results showed that as much as 20% chiller plant energy and 28% annual chiller utilization hours were reduced due to the inclusion of the check valve as compared with that prior to the installation of the check valve. Taylor [2002A, 2002B] presented that the use of a check valve is recommended for fixed speed chiller plants, but not recommended for variable speed chiller plants since the efficiency of variable speed chillers is high at part-load conditions. The author pointed out that one disadvantage of having a check valve is that if the primary pumps are off and chiller isolation valves are closed while

the secondary pumps are on, the secondary pumps will be deadheaded. This can be avoided by shutting off the secondary pumps whenever all primary pumps are switched off.

Compared to above studies recommended to use check valves, several studies [McQuay 2002, Luther 2002, Coad 1998] argued that the use of the check valve will destroy the philosophy of the primary-secondary designs and designers will fell uncomfortably with forcing pumps into series operation and hence, the inclusion of a check valve was not recommended as part of the design of the primary-secondary systems. However, these studies failed to provide any persuasive proof indicating that the use of a check valve is not feasible. The application guide of McQuay [2002] stated that adding a check valve effectively makes the system variable primary flow during low delta-T intervals and the system control will become more complicated. Rishel [1998] presented that the low delta-T central plant syndrome is a complicated problem that cannot be easily fixed by using a check valve and the check valve is not suitable for all primary-secondary systems, such as for the systems utilizing special energy storage systems or water side economizers, etc.

2.2 The optimal and robust control in HVAC systems

Optimal and robust control, which addresses the energy or cost-efficient control of HVAC systems while providing the desired indoor comfort and healthy environment under the dynamic working conditions, is attracting more attention of the building professionals and the society and provides incentives to make more efforts in

developing more extensive and robust control methods for HVAC systems. In the control of HVAC systems, optimal and robust control aims at seeking the minimum energy input or operating cost to provide the satisfied indoor comfort and healthy environment, taking into account the ever-changing indoor and outdoor conditions as well as the characteristics of HVAC systems.

2.2.1 Sub-system optimal controls

Sub-system optimal controls aim to optimizing the subsystems locally in HVAC systems, such as multiple chillers system, cooling tower system, chilled water system, air-handling units system, etc.

Sun et al. (2010) presented a model-based optimal start control strategy for multi-chiller plants in commercial buildings, which considers both the recovery ability and the cooling load condition as the optimizing variables. A simplified building model has been used for predicting building cooling load, based on which the optimal operating chiller number and the related pre-cooling lead time can be identified. The new strategy is realized in two steps. The first step is to predict the building cooling load using a simplified building model, and identify a feasible set for the operating chiller number. The second step is to estimate the pre-cooling lead time using the simplified building model for each number inside the feasible range identified in the first step, and calculate the corresponding energy consumption. The number and its corresponding pre-cooling lead time which yields the least energy consumption constitute the optimal start operation. The proposed strategy, validated

through case studies, can be used in practical applications to select the optimal number of operating chillers and determine the associated pre-cooling lead time in order to achieve minimum energy consumption in the pre-cooling period.

Braun (2007) developed and evaluated a set of operating strategies that provide near-optimal performance for hybrid cooling plants in terms of operating costs. A hybrid chiller plant employs a combination of chillers that are "powered" by electricity and natural gas. Operating cost minimization for hybrid plants must account for effects of electrical and gas energy costs, electrical demand costs, and differences in maintenance costs associated with different chillers. Control strategy development was facilitated by separating hourly energy cost minimization from the problem of determining trade-offs between monthly energy and demand costs. A demand constraint is set for each month based upon a heuristic strategy and energy cost optimal strategies that attempt to satisfy the demand constraint are applied for cooling tower and chiller control at each decision interval. Simulated costs associated with the individual control strategies compare well with costs for optimal control.

A model-based supervisory control strategy for online control and operation of building central cooling water systems is presented by Ma and Wang (2008). Simplified semi-physical chiller and cooling tower models are used in the strategy to predict the system energy performance. The supervisory control strategy seeks the minimum energy input to provide adequate cooling energy for buildings, taking into

account the characteristics and interactions of central cooling water systems as well as the requirements and constraints of practical application. Simplified semi-physical chiller and cooling tower models are used to predict the system energy performance and environment quality as well as the system response to changes of control settings. A hybrid optimization technique, namely the PMES (performance map and exhaustive search) based method, is developed and utilized to seek optimal solutions to the optimization problem. The control performance and energy performance of this model based supervisory control strategy are evaluated on the central cooling water system of a high rise commercial office building by comparing with other conventional control strategies for cooling water systems in terms of energy efficiency, control accuracy, computational cost etc. The results show that this strategy is more energy efficient and computational cost effective than other methods for online practical applications.

Wang and Jin (2000) presented a supervisory control strategy using a system approach for VAV air-conditioning systems in which simplified physical models were utilized to predict the overall system performance, and genetic algorithm (GA) was used to solve the optimization problem of multiple control variables. It is the first application of GA in solving an optimal control problem formulated using a system approach in HVAC field. The simulation results showed that this online supervisory control strategy can improve the overall system energy and environment performance since it takes into consideration the system level characteristics and interactions among the system variables.

Some studies focused on the energy efficient control for the chilled water system. Among the existing studies, Moore and Fisher [2003] stated that the speed of pumps could be controlled to maintain at least one chilled water valve of cooling coils 90% open to save pumps energy consumption under part cooling load conditions. Wang and Ma (2010) developed a control strategy for variable speed pumps distributing chilled water to the heat exchangers in super high-rise buildings. A cascade control method was employed to generate a variable water flow set-point for pump speed control. The results showed that up to 16.01% of the pumps can be saved using this control strategy. Jin et al. (2007) presented three optimal control strategies for chilled water systems, i.e., the control of the supply head of secondary pumps, the control of the chilled water supply temperature set-point and the control of both in series. The simulation results based on a small scale HVAC system in the selected typical summer day and spring day showed that these three strategies can save about 3.85–3.90%, 2.53–3.38% and 1.98–15.96% of the total system energy consumption, respectively, as compared with the conventional strategies using the fixed temperature and/or fixed pressure differential set-points.

Ma and Wang (2009) presented the optimal control strategies, including the speed control strategy and the sequence control strategy, for variable speed pumps with different configurations in complex building air-conditioning systems to enhance their energy efficiencies. Through a detailed analysis of the system characteristics, the pressure drop models for different water networks in complex air-conditioning systems are developed and then used to formulate an optimal pump sequence control

strategy. This sequence control strategy determines the optimal number of pumps in operation taking into account their power consumptions and maintenance costs. The variable speed pumps in complex air-conditioning systems can be classified into two groups: the pumps distributing water to terminal units and pumps distributing water to heat exchanges. The speeds of pumps distributing water to terminal units are controlled by resetting the pressure differential set-point using the online opening signals of water control valves. The speeds of pumps distributing water to heat exchanges are controlled using a water flow controller. The performances of these strategies are tested and evaluated in a simulated virtual environment representing the complex air-conditioning system in a super high-rise building by comparing with that of other reference strategies. The results show that about 12–32% of pump energy could be saved by using these optimal control strategies.

2.2.2 Global optimal controls

Some other researchers [Braun 1989, Lu et al. 2005, Ma et al. 2009, Austin 1993, Hydeman 2007, Fong 2006, Jin 2007, Ma 2000] paid more attention to the global optimization of the whole chilled water systems.

Braun et al. (1989) presented two methodologies for determining the optimal control settings for chilled water systems without storage. One was a component model-based nonlinear optimization algorithm, in which the power consumptions of major components in the chilled water system were expressed as quadratic relationships. This methodology was used as a simulation tool for investigating the

system performance. The other was a system-based near optimal strategy, in which the total power consumption of the overall chiller plant was expressed as a quadratic relationship.

Lu et al. (2004) developed a model based optimization method for global optimization of overall HVAC systems. A modified genetic algorithm was developed to solve the optimization problem for overall HVAC systems through finding the optimal set points of the independent variables. A general procedure was provided for implementation of the proposed optimization solution for different application environments. Simulations based on a HVAC pilot plant showed that the energy usage could be substantially reduced compared with the traditional methods.

Yao and Ye (2010) developed a global optimization model for the overall energy-saving control of the central air-conditioning system based on the local energy models of equipments. The method of decomposition–coordination, an effective way to settle the high dimensional optimization problems, is introduced to solve the global model possibly concerned to a large-scale air-conditioning system in which a large number of decision variables are to be optimized. The global optimization model has been used to study a central air-conditioning system located in Changsha city (Hunan Province, China). The results of SCOP (system coefficient of performance) under optimal operation and non-optimal operation show that the energy saving brought by the global optimization scheme will become more significant under the lower load operation of the air-conditioning system.

2.2.3 Robust controls

Robust controls for HVAC systems aim to ensure the system to operate more stably and reliably concerning unexpected uncertainties and disturbances.

Wang (2002) presented a robust control strategy for combining DCV control with economizer control. The freezing transition control scheme can significantly increase the control stability in the transient region between the total free cooling mode and partial free cooling mode. The use of gain scheduling in the scheme can further improve the control stability in the transient region. The transition control scheme with I-term reset diminishes the alternation and oscillation in the transient region between the total free cooling mode and DCV mode. The use of gain scheduling (i.e. the robust transition control scheme with I-term reset and gain scheduling) further reduces the possibility of alternation and oscillation in the transient region. The feedback transition control scheme with I-term reset achieves better control stability in the transition process between the partial free cooling mode and DCV mode by avoiding the instable control during the initial stage of the DCV based fresh air damper control. The strategy with these schemes allows the controls of different processes to be tuned individually according to the characteristics of the individual processes and the change of process parameters near the upper and lower limits. The freezing and I-term reset ensure smooth handover between different control processes. The gain scheduling stabilizes the process control near the fully open or closed position of the valve/ damper in the transient regions. The use of them in the AHU control strategy combining DCV control and economizer control makes the

strategy robust when changing from one control process to another that could be rather frequent in practical systems due to the change of working conditions and measurement uncertainty, resulting in alternation and oscillation of the system control.

Huang and Wang (2008) developed a method for utilizing the fused measurement of the building cooling load to improve the reliability of the chiller sequencing control. The fused measurement is obtained by combining the complementary advantages of two different approaches to measuring the building cooling load. One approach is the direct measurement, which calculates the building cooling load directly, using the differential water temperature and water flow rate measurements. The other is the indirect measurement, which is the building cooling load calculated based on chiller models using the instantaneous chiller electrical power input, etc. The combination strategy is tested using the field data collected from the central plant of the air-conditioning system in a high-rise building in Hong Kong. The confidence degree associated with the fused measurement is systematically evaluated. Periodic update of the fusion algorithm parameters is also developed to improve the performance of the fusion strategy and the chiller sequencing control.

Sun and Wang (2009) presented a robust strategy for improving the reliability and the energy efficiency of chiller sequencing control based on the total cooling load measurement of centralized multiple centrifugal chiller plants. The improvement is achieved as follows. Firstly, a fused measurement of building cooling load is used to

replace the direct/indirect measurement. Secondly, the maximum cooling capacity of individual chillers is computed online using a simplified centrifugal chiller model. Thirdly, the online estimated maximum cooling capacity is calibrated according to the quality of the fused measurement in order to deal with the possible misbehaviors in measurement instruments. A simplified model for computing the maximum cooling capacity is developed and validated using field data. The performance of the proposed chiller sequencing control strategy is tested and compared with a conventional chiller sequencing control algorithm. Test results are presented showing that the proposed strategy can effectively improve the reliability of chiller sequencing control and reduce the energy consumption of chiller plants.

2.3 Fault detection and diagnosis for HVAC systems

Fault detection and diagnostics (FDD) is an area of investigation concerned with automating the processes of detecting faults with physical systems and diagnosing their causes. The primary objective of an FDD system is early detection of faults and diagnosis of their causes, enabling correction of the faults before additional damage to the system or loss of service occurs. This is accomplished by continuously monitoring the operations of a system, using FDD to detect and diagnose abnormal conditions and the faults associated with them, then evaluating the significance of the detected faults, and deciding how to respond.

Katipamula et al. (2005) presented a review on the methods for fault detection, diagnostics for building systems. A generic application of fault detection and

diagnostics to operation and maintenance of engineered system was described as shown in Figure 2.3. The first step is to monitor the physical system or device and detect any abnormal conditions (problems). This step is generally referred to as fault detection. When an abnormal condition is detected, fault diagnosis is used to evaluate the fault and determine its causes. These two steps constitute the FDD process. Following diagnosis, fault evaluation assesses the size and significance of the impact on system performance (in terms of energy use, cost, availability, or effects on other performance indicators). Based on the fault evaluation, a decision is then made on how to respond to the fault (e.g., by taking a corrective action or possibly even no action). These four steps together enable condition-based maintenance, which is referred to as an automated FDD system in this paper. In most cases, detection of faults is relatively easier than diagnosing the cause of the fault or evaluating the impacts arising from the fault.

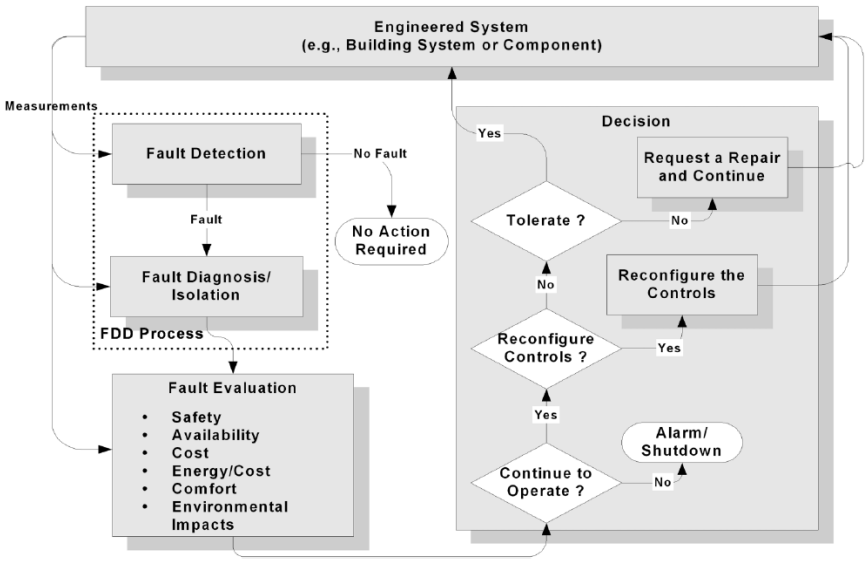

Figure 2.3 Generic applications of fault detection and diagnostics to operation and maintenance of engineered system (Katipamula et al. 2005)

FDD methods can also be roughly classified into two groups based on the work of Gertler (1998), i.e. model-free methods and model-based methods. Model-free method does not need a mathematical or experiential model as the performance reference to be compared with the actual performance while model-based method needs a model as the performance benchmark as shown in Figure 2.4.

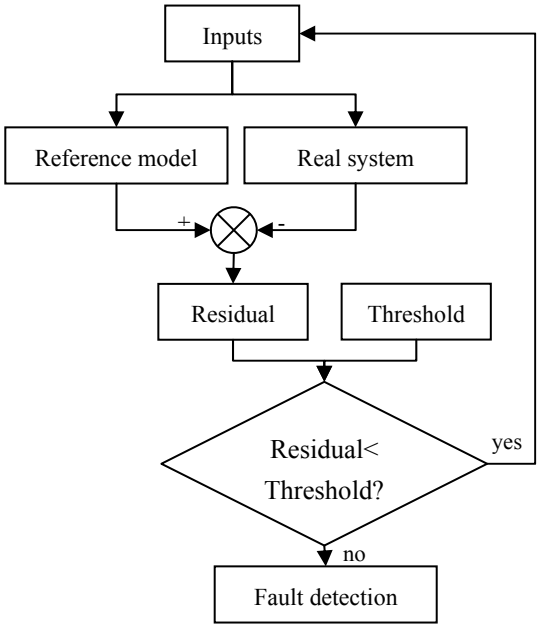

Figure 2.4 Flowchart of model-based FDD methods

Over the last two decades, there have been considerable research and development targeted toward developing FDD methods for HVAC equipments.

FDD methods for air-handling units (AHUs) and variable air volume (VAV) terminals are a hot research area. Yoshida et al. (1996) discussed some typical AHU faults i.e. outdoor air damper malfunction, fouling on cooling coils, air leakage through ductwork, fan motor malfunction and stuffing air filers. The autoregressive

model with exogenous input (ARX) and extended Kalman Filter were compared to detect a sudden failure in AHU control loop. Yoshida and Kumar (1999) discussed the ARX model and adaptive forgetting through multiple models (AFMM). They were applied in the on-line FDD for real VAV systems. Compared with ARX models, AFMM models need longer window length but more sensitive to the system changes. The author concluded that ARX models were more robust. Lee et al. (1996a and 1996b) carried out the FDD for AHUs using autoregressive moving average with exogenous input (ARMX), ARX and ANN. The concerned faults were complete failure of the supply and return fans, failure of the chilled water circulation pumps, stuck cooling coil valves, failure of temperature sensors, static pressure sensors, and air flow stations. Lee et al. (1997) extended the previous work in improving the ANN models for AHU FDD. More faults including several abrupt and performance degradation faults were considered in the AHU by Lee et al. (2004) using general regression neural-network (GRNN) models for FDD. Dexter and Ngo (2001) improved the previous work using a multi-step fuzzy model to detect and diagnose the AHU faults. Compared with the generic fuzzy reference models, the new approach could prevent false alarms and be able to isolate the valve leakage and fouling faults. As a part of ASHRAE research project (RP-1020), Norford et al. (2002) applied two FDD methods for AHU faults. One was first-principle model-based, and the other was semi-empirical polynomial regression-based. Wang and Xiao (2004) presented a FDD strategy for AHU sensor faults based on principal component analysis (PCA). Two PCA models were built based on the heat transfer

balance and pressure-flow balance in air-handling process. For each PCA model, the related sensors with a fixed bias could be detected and diagnosed. Qin and Wang (2005) conducted a survey on the VAV faults, and found 20.9% of VAV terminals were ineffective and ten main faults existed in the VAV systems. A PCA-based method was used to detect the flow sensor and reconstruct it. The other faults were isolated by integration of recognition, expert rules and performance indices.

Wang and Zhou (2010) developed a system-level FDD strategy for HVAC systems. It involves two schemes, system FDD scheme and sensor FDD&E scheme. Two schemes are involved in the system-level FDD strategy, i.e. system FDD scheme and sensor fault detection, diagnosis and estimation (FDD&E) scheme. It is found that the sensor FDD&E method can work well in identifying biased sensors and recovering biases even if system faults coexist, and the system FDD method is effective in diagnosing the system-level faults using processed measurements by the sensor FDD&E.

Upadhyayaa and Eryurekb (2006) proposed a group method of data handling (GMDH) to diagnose the sensor fault and tube fouling on a tube-and-shell heat exchanger. Weyer et al. (2000) proposed a method based on a first principle model to track the heat transfer coefficient and diagnose the settled material breakage. Six faults were studied by Persin and Tovornik (2005) including four sensor faults, tube clog and vessel leakage. A velocity-based linearization and a linear observer based on the energy balance were proposed to detect and diagnose these faults.

Transferable belief model (TBM) was developed to improve the inconsistency of data to make diagnosis more stable.

2.4 Discussions

Firstly, for low delta-T syndrome of chilled water system, the existing studies demonstrate that low delta-T syndrome and deficit flow problem widely existed in the primary-secondary chilled water system and the elimination of this problem can improve the energy efficiency of the chilled water systems. However, most of the studies pay more attention to analyzing the possible causes and solutions of this problem from the view of design and commissioning. In practice, even the HVAC systems were properly designed and well commissioned, deficit flow still cannot be completely avoided in the operation period due to some disturbances, e.g. improper control. There are no reliable, robust and secure solutions that can eliminate deficit flow in real applications. The research associated with proper control of secondary pumps to eliminate deficit flow and low delta-T syndrome for real applications is missing. Further more, many of the proposed solutions from the view point of design might be only feasible to be adopted in new design, solutions from the view point of operation and control are practical and preferable for the large number of existing systems suffering from the deficit flow and low delta-T syndrome.

Secondly, for practical applications, it is essential to find the causes before fully correcting them. However, the detailed study for detection and diagnosis of the low delta-T syndrome and deficit flow problem, particularly in real applications, is still

insufficient.

Thirdly, the above studies demonstrated that the potential energy savings associated with the optimal control in the typical chilled water systems. However, most of the control strategies are suitable only for typical chilled water systems with simple configurations, and fail to investigate the real-time applications in the complex chilled water systems. For instance, in a complex chilled water system using heat exchangers to transfer cooling energy from the low zones to high zones of a high-rise building, the outlet water temperature on the secondary sides of heat exchangers and the operating number of heat exchangers could not be optimized in the above studies. In such complex systems, the existing control strategies could not ensure the robust control for variable speed pumps to avoid deficit flow problem (i.e., the chilled water delivered to buildings exceeds the total flow of the chillers) that often occurred in primary–secondary systems [Wang et al. 2010] when certain faults or uncertainties occurred, such as sudden rise of inlet water temperature before heat exchangers.

Lastly, there is also no universal conclusion that whether the use of a check valve is a good practice and is worthy of consideration to deal with the low delta-T syndrome in a particular primary-secondary system. It is also noted that the studies supporting to use the check valves failed to provide the details how the check valve can help to deal with the low delta-T problems and achieve energy efficient operation.

2.5 Summary

This chapter provides the literature reviews on the existing studies related to the low delta-T syndrome, control and diagnosis strategies of HVAC systems. The discussions and basic assessment of the current studies have been presented. It is demonstrated that fault diagnosis and proper control are the two useful tools for enhancing the performance of HVAC systems. It is also clearly shown that the current research on solving the low delta-T syndrome is still inadequate in the following two aspects: (1) most of the studies paid more attention to analyzing the possible causes and solutions of this problem from the view of design and commissioning, robust and secure solutions that can eliminate low delta-T syndrome and deficit flow problem in real operations are still inadequate. (2) many of the proposed solutions from the viewpoint of design might be only feasible to be adopted in new systems, while solutions from the viewpoint of operation and control are still insufficient, which will be practical and preferable for the large number of existing systems suffering from the deficit flow and low delta-T syndrome besides new buildings.

The following chapters will present more feasible solutions for solving low delta-T syndrome and deficit flow problem for improving the insufficiencies of current studies.

CHAPTER 3 THE BUILDING SYSTEM AND DYNAMIC SIMULATION PLATFORM

A dynamic simulation platform, based on TRNSYS, for the complex building central chilling systems constructed in this study is presented in this chapter. This platform is utilized to evaluate and test the energy performance and operation robustness under the optimal control strategies developed in this study. The proposed FDD strategies are validated using this platform as well.

Section 3.1 briefly introduces a super high-rise commercial building and its complex central chilling system concerned in this study. Section 3.2 presents a dynamic simulation platform based on this complex central chilling system. The major component models and their interconnections used to construct the complex dynamic simulation platform are presented as well. A summary of this chapter is given in Section 3.3.

3.1 Building and HVAC System

In-situ tests are conducted to validate and compare the strategies developed. Since it is costly and inconvenient to do many site test, it is also hard to accurately compare various control strategies in real HVAC systems due to repeatability of test conditions and measurement accuracy, a dynamic simulation platform, namely virtual building system in this thesis, is developed to be regarded as a real-time

simulation tool for a building and/or its HVAC system. It can provide a convenient platform for testing and analyzing the control, environmental and energy performances of different control strategies under dynamic working conditions to determine the most promising strategies for the optimal control and operation of HVAC systems prior to site implementation. It is also a valuable tool for evaluating the performances of various fault detection and diagnosis (FDD) strategies.

Compared to some popular commercial simulation software packages, such as EnergyPlus (Crawley et al. 2000), DOE-2 (Lawrence Berkeley Laboratory 1982), etc., TRNSYS was selected in this study to construct the dynamic simulation platform because it is a complete and extensible simulation environment for the transient simulation of multi-zone building systems. TRNSYS is also capable of completing the building cooling load calculation, water system simulation and air system simulation with one single simulation package.

The building concerned in this research is a super high-rise building of approximately 490m height (currently the tallest building in Hong Kong) and 440,000 m^2 of floor area, consisting of a basement of four floors, a block building of 6 floors and a tower building of 112 floors, as shown in Figure 3.1. The basement is used mainly for parking with about 24,000 m^2. The block building from the ground floor to the fifth floor mainly serves as the commercial center including hotel ballrooms, shopping arcades and arrival lobbies. The gross area is about 67,000 m^2. The tower building consists of 349,000 m^2 for commercial offices and a six star hotel

on the upper floors. The whole building is constructed primary of reinforced steel concrete. The external walls are mostly the steel glass curtain with the heat transfer coefficient of 1.32 W/ (m^2K). The floor is made of 125mm slab of reinforced steel concrete.

Figure 3.1 Profile of International Commercial Center (ICC)

The central chilling systems of this building is divided into five zones to avoid the chilled water pipelines and terminal units from suffering extremely high static pressure (i.e., the highest static pressure of more than 40 bar and the designed working pressure of nearly 60 bar). The floors from ground floor to the sixth floor are Zone 1. Zone 2 involves the floors from the seventh floor to 41st floor. Zone 3 is from the 43rd to 77th floor and Zone 4 is from the 79th to 98th floor. Zone 5, from

100th to 118th floor, is the six-star hotel located on the upper floors of the building. The 6th, 42nd, 78th and 99th floors are used as the mechanical floors to accommodate the mechanical equipment such as chillers, cooling towers, heat exchangers, pumps, PAUs (Primary Air Units) and fans, etc. Considering the usage characteristics of the hotel, separate air-cooled chillers located on the 99th floor are designed to provide the chilled water for Zone 5. For the other zones, the cooling source is provided by the water-cooled chillers on the sixth floor. The schematics of the central chilling system of Zone 1 to Zone 4 are illustrated in Figure 3.2.

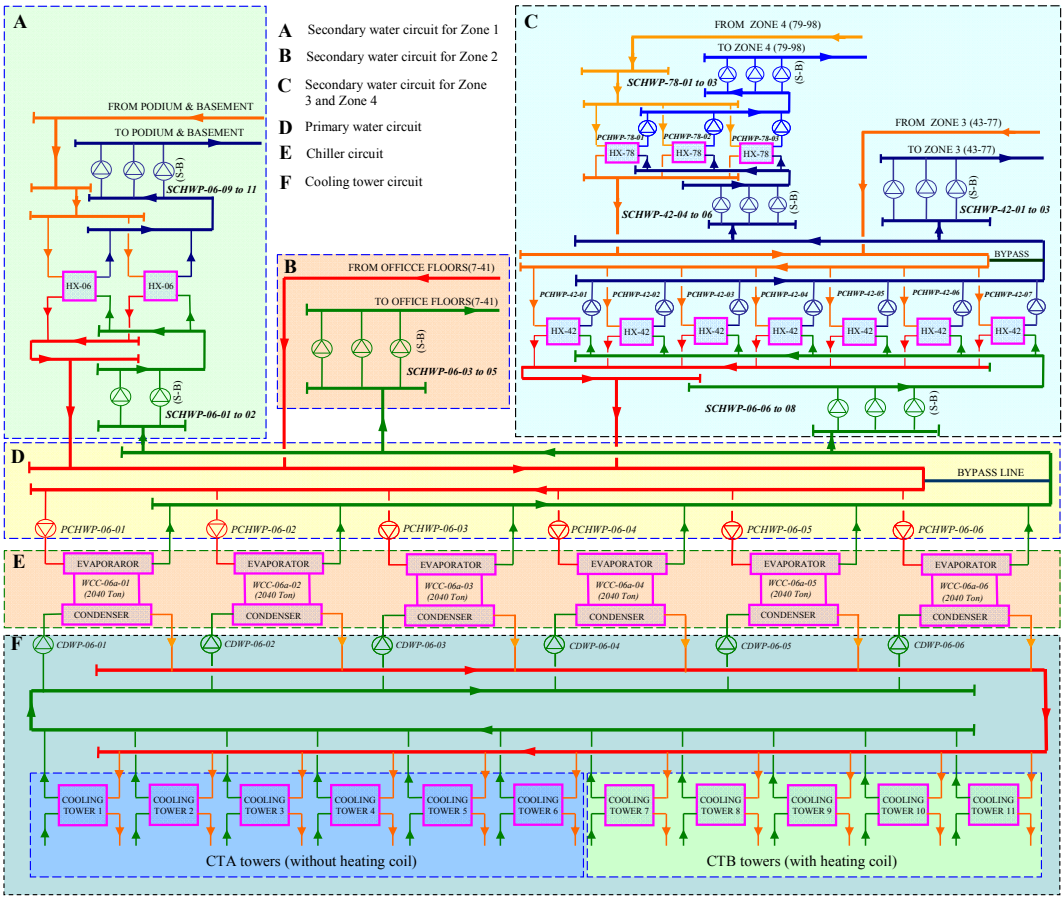

Figure 3.2 Schematics of the central chilling system.

In this central chilling system, six identical high voltage (10,000V) centrifugal chillers are employed to supply cooling energy for the building. The rated cooling

capacity and power consumption of each chiller are 7230 kW and 1346 kW respectively. The design chilled water supply and return temperatures for chillers are 5.5°C and 10.5°C respectively. Each chiller is associated with one constant condenser water pump and one constant primary chilled water pump. The heat generated from the chiller condensers is rejected by eleven evaporative water cooling towers with a total design capacity of 51,709 kW. All the cooling towers, on the sixth floor, are divided in two groups in order to avoid the plume. Each of the CTB towers are installed with a heating coil at the air exhaust for the plume abatement purpose. CTA towers are the towers without heating coils. Each of the CTA towers (total of six) has a heat rejection capacity of 5,234 kW and a nominal power consumption of 152 kW at the design condition. The rated water flow rate and air flow rate of each CTA tower are 250 L/s and 157.2m^3/s, respectively. Each of the CTB towers (total of five) has a heat rejection capacity of 4,061 kW and a nominal power consumption of 120 kW at the design condition. The rated water flow rate and air flow rate of each CTB tower are 194 L/s and 127.0m^3/s, respectively. Due to the space constraint, all cooling towers designed are crossover flow towers.

A typical primary-secondary chilled water system is employed in this central chilling system. In the primary loop, each chiller is associated with a constant speed primary water pump to guarantee the fixed water flow through the chiller. The secondary loop is decoupled from the primary loop through the bypass line. In the secondary chilled water system, only Zone 2 (indicated as B in Figure 3.2) is supplied with the chilled water from chillers directly. The design cooling load of Zone 2 is about 30%

of the design total cooling load. The heat exchangers are employed to transfer cooling energy from chillers to occupied zones in Zone 1, Zone 3 and Zone 4 to avoid extremely high static pressure on the chilled water pipelines and terminal units. Zone 1 (indicated as A in Figure 3.2) is supplied with the secondary chilled water through the heat exchangers located on the sixth floor while the chilled water from chillers serves as the cooling source of the heat exchangers. The design cooling load of this zone is about 19% of the design total cooling load. The design inlet and outlet water temperatures at the secondary side of heat exchangers are 11.3°C and 6.3°C, respectively. Zone 3 and Zone 4 (indicated as C in Figure 3.2) are supplied with the secondary chilled water through the first stage heat exchangers (HX-42 in Figure 3.2) located on the 42nd floor. Some of the chilled water after the first stage heat exchangers is delivered to Zone 3 by the secondary chilled water pumps (SCHWP-42-01 to 03) located on the 42nd floor. Some water is delivered to the second stage heat exchangers (HX-78 in Figure 3.2) located on the 78th floor by the secondary chilled water pumps (SCHWP-42-04 to 06) located on the 42nd floor. The design inlet and outlet water temperatures at the secondary side of the first stage heat exchangers are 11.3°C and 6.3°C, respectively. The original pumping configurations after HX-42 and HX-78 are also primary-secondary arrangement , which employs primary constant speeds pumps (PCHWP-42-01 to 07 and PCHWP-78-01 to 03) to deliver chilled water from the heat exchangers (HX-42) to the secondary variable speed pumps that deliver the chilled water to terminal units. All pumps in the chilled water system are equipped with VFDs (variable frequency drivers) to allow the

energy efficiency except that the primary chilled water pumps dedicated to chillers and heat exchangers in Zone 3 and Zone 4 are constant speed pumps. The configuration of the water piping system of this building is the reverse-return system.

Most of air-conditioning terminals are air-handling units (AHUs) except that some fan coil units are used in the block building. For each floor of the tower building, two AHUs located in the core are used to handle the mixture of the fresh air and recycled air from offices. The fresh air is delivered to each AHU through the shaft in the core by primary air units (PAUs), which are located on mechanical floors. The PAUs handle the outdoor air to 16.5°C (design condition). All fans in AHUs and PAUs are equipped with VFDs allowing the energy efficiency.

The major specifications of main HVAC equipment, such as chillers, cooling towers, water pumps, AHU fans and PAU fans, are summarized in Table 3.1. The design total power load of the main equipment in this air-conditioning system is 18,497.2 kW. Chillers are the largest electricity consumer in this air-conditioning system, which occupy 43.66% of the design total power load. The second largest electricity consumer is the fans of AHUs and PAUs contributing 27.64% of the design total power load. The design power loads of the pumps and cooling tower fans are 3,796.2 kW and 1,512 kW respectively, and they contribute about 20.52% and 8.17% of the design total power load in this air-conditioning system, respectively. From Table 3.1, it also can be observed that the design total power load of the central chilling system takes about 72.5% of the design total power load of the overall air-conditioning

system. Therefore, the central chilling system should be controlled properly to achieve reliable and energy efficient operation.

Table 3.1 Specifications of main equipment in the air-conditioning system

Chillers	N*	$M_{w,ev}$ (L/s)	$M_{w,cd}$ (L/s)	CAP (kW)	W (kW)	W_{tot} (kW)
WCC-06-01 to 06	6	345.0	410.1	7,230	1,346	8,076
Cooling Towers	N	M_w (L/s)	M_a (m^3/s)	Q_{rej} (kW)	W (kW)	W_{tot} (kW)
CTA-06-01 to 06	6	250.0	157.2	5,234	152	912
CTB-06-01 to 05	5	194.0	127.0	4,061	120	600
Pumps	N	M_w (L/s)	$Head$ (m)	η (%)	W (kW)	W_{tot} (kW)
CDWP-06-01 to 06	6	410.1	41.60	83.6	202	1,212
PCHWP-06-01 to 06	6	345.0	31.60	84.5	126	756
SCHWP-06-01 to 02	1(1)	345.0	24.60	82.2	101	101
SCHWP-06-03 to 05	2(1)	345.0	41.40	85.7	163	326
SCHWP-06-06 to 08	2(1)	345.0	30.30	84.2	122	244
SCHWP-06-09 to 11	2(1)	155.0	39.90	78.8	76.9	153.8
PCHWP-42-01 to 07	7	149.0	26.00	84.9	44.7	312.9
SCHWP-42-01 to 03	2(1)	294.0	36.50	87.8	120	240
SCHWP-42-04 to 06	2(1)	227.0	26.20	84.3	69.1	138.2
PCHWP-78-01 to 03	3	151.0	20.60	84.3	36.1	108.3
SCHWP-78-01 to 03	2(1)	227.0	39.20	85.8	102	204
Air-side PAU fan	29	/	/	/	/	513
Air-side AHU fan	152	/	/	/	/	4,600
Design total power load	Chillers		**8,076** kW		**43.66%**	
	Cooling towers		**1,512** kW		**8.17%**	
	Pumps		**3796.2 kW**		**20.52%**	
	AHU and PAU fans		**5,113** kW		**27.64%**	
	Total		**18,497.2** kW		---	

*Value in parentheses indicates number of stand by pumps

The nomenclature in Table 3.1 is defined as follows. N is the number of components, M is the flow rate, CAP is the chiller capacity, Q is the heat transfer rate, η is the efficiency, W is the power consumption, and subscripts w, a, ev, cd, rej and tot indicate water, air, evaporator, condenser, rejection and total, respectively.

3.2 Development of The Dynamic Simulation Platform

3.2.1 Outline of the Dynamic Simulation Platform

A simulation platform based on the complex chilling system mentioned before is developed based on TRNSYS, which is a complete and extensible simulation environment for the transient simulation of systems, including multi-zone buildings. It is used by engineers and particularly researchers to validate new energy concepts, from simple domestic hot water systems to the design and simulation of buildings and their equipment, including control strategies, occupant behavior, alternative energy systems (wind, solar, photovoltaic, hydrogen systems), etc.

One of the key factors in TRNSYS' is its open, modular structure. The source code of the kernel as well as the component models is delivered to the end users. This simplifies extending existing models to make them fit the user's specific needs. The DLL-based architecture allows users and third-party developers to easily add custom component models, using all common programming languages (C, C++, PASCAL, FORTRAN, etc.). In addition, TRNSYS can be easily connected to many other applications, for pre- or post-processing or through interactive calls during the simulation (e.g. Microsoft Excel, Matlab, COMIS, etc.). TRNSYS applications include:

- *Solar systems (solar thermal and PV)*
- *Low energy buildings and HVAC systems with advanced design features*

(natural ventilation, slab heating/cooling, double facade, etc.)

- *Renewable energy systems*
- *Cogeneration, fuel cells*
- *Anything that requires dynamic simulation*

The simulation platform representing the complex chilling system under study is constructed using detailed physical models of components, such as chillers, cooling towers, pumps, heat exchangers, air handling units (AHU), controllers, etc. The system structure and interactions of each component in the simulation platform are the same with the complex chilling system under study shown in Figure 3.2. The multi-zone building model of TRNSYS 16 is employed to simulate the thermal behavior of the building. The heat load from the occupants, equipment and lighting system and weather data are considered in the simulation as an input files. The weather condition used is the data of the typical year in Hong Kong. The air flow rates and AHU inlet air dry-bulb temperatures of each individual zone are simulated according to the whether data and cooling loads of each zone provided together with certain reasonable assumptions. The assumptions used are presented as follows: (1) a minimum ratio of the fresh air to supply air is assumed as 20%; (2) the room design air dry-bulb temperature is 23°C (actually controlled value) for summer and autumn cases, and 21°C for winter and spring cases with a 50% humidity ratio; (3) the air dry-bulb temperature leaving AHUs is controlled at the given set-point which can be different from season to season with a 95% humidity ratio. The major component

models used to construct this complex dynamic simulation platform are summarized in the following briefly.

3.2.2 Models of the Water Network and Major Components

3.2.2.1 Chillers

The chiller model used in this simulation is to simulate the chiller dynamic performance under various working conditions, which is based on the model of Wang et al. (2000). It is based on the physical parameters of chillers, such as the impeller tip speed (u_2), impeller exhaust area (A), impeller blades angle (β) and other coefficients/constants. The compressor is modeled on the basis of mass conservation, Euler turbo-machine equation and energy balance equation. The Euler equation is modified by considering the impeller exit radial velocity (c_{r2}) distribution and derived as in Equation (3.1). Energy balance equations are applied to the compressor control volume and impeller control volume resulting in Equations (3.2) and (3.3), respectively. The hydrodynamic losses ($h_{hyd,com}$ and $h_{hyd,imp}$) in the two control volumes are considered to be composed of three elements, i.e., flow friction losses, inlet losses and incidence losses, as shown in Equations (3.4) and (3.5), respectively.

$$h_{th} = u_2\left[u_2 - \left(\frac{\pi^2}{8}\right)^2 c_{r2}\left(ctg\beta + B\frac{\upsilon_1}{\upsilon_i}tg\theta\right)\right] \tag{3.1}$$

$$h_{th} = h_{pol.com} + h_{hyd.com} \tag{3.2}$$

$$h_{th} = h_{pol.imp} + h_{hyd.imp} + \frac{c_i^2}{2} \tag{3.3}$$

$$h_{hyd.com} = \zeta\left[1 + \psi_1\left(\frac{\upsilon_1}{\upsilon_i}\frac{1}{\cos\theta}\right)^2 + \psi_2\left(\frac{\upsilon_1}{\upsilon_i}\mathrm{tg}\theta\right)^2\right]c_{r2}^2 \tag{3.4}$$

$$h_{hyd.imp} = \zeta\left[\chi + \psi_1\left(\frac{\upsilon_1}{\upsilon_i}\frac{1}{\cos\theta}\right)^2 + \psi_2\left(\frac{\upsilon_1}{\upsilon_i}\mathrm{tg}\theta\right)^2\right]{c_{r2}}^2 \tag{3.5}$$

where h_{th} is the compressor theoretical head, h_{hyd} is the hydrodynamic losses, h_{pol} is the polytrophic compression work, B is the ratio of the impeller channel depth at the intake to that at exhaust, υ_1 and υ_i are the specific volumes at the impeller intake and exhaust, respectively, c_i is the vapor velocity at the impeller exhaust, θ is the inlet guide vane angle, ζ, ψ_1, ψ_2, χ are the introduced constants, and subscripts *com* and *imp* indicate compressor and impeller, respectively.

The evaporator and condenser are simulated using the classical heat exchanger efficiency method. The chiller power consumption (W) is calculated on the basis of the internal compression power (W_{inter}), as shown in Equation (3.6), which consists of three elements, i.e., internal compression power, a variable part of the losses proportional to the internal compression power and a constant part of the losses (W_l). Two thermal storage units (one at the cooling water inlet of the condenser and the other at the chilled water inlet of the evaporator) are used to represent the dynamic responses of the chiller to the changes of working conditions (inlet temperatures) and the dynamic effects of the working condition changes on the compressor load. They

are mathematically represented by two first-order differential equations as shown in Equations (3.7) and (3.8), respectively.

$$W = \alpha W_{\text{int}er} + W_l \tag{3.6}$$

$$C_{ev} \frac{dT'_{ev,in}}{d\tau} = c_{p,w} M_{w,ev} (T_{ev,in} - T'_{ev,in}) \tag{3.7}$$

$$C_{cd} \frac{dT'_{cd,in}}{d\tau} = c_{p,w} M_{w,cd} (T_{cd,in} - T'_{cd,in}) \tag{3.8}$$

Where α is a coefficient, T is the temperature, T' is the temperature after introducing dynamic effects, and the subscript *in* indicates inlet.

3.2.2.2 Cooling Tower

The cooling tower model simulates the states of the outlet air and outlet water of the cooling tower, which is based on Braun's effectiveness model (1989c). The effectiveness model utilizes the effectiveness relationship developed for sensible heat exchangers by introducing an air saturation specific heat and a modified definition of the number of heat transfer units. Based on the steady-state energy and mass balances on an incremental volume, the differential equations as shown in Equations (3.9)-(3.11) can be derived. The effectiveness of the cooling tower (ε_a) is used to simulate heat and mass transfer processes in the cooling tower and the actual heat transfer is then calculated in terms of this effectiveness as in Equation (3.12). The outlet air state and water state are computed through the overall energy balances as

in Equations (3.13)-(3.15). The number of transfer units (NTU) is calculated using Equation (3.16). Empirical formulas as shown in Equations (3.17) and (3.18) are used to predict the required air flow rate (M_a) and power consumption of the cooling tower (W_{ct}), respectively.

$$\frac{d\omega_a}{dV} = -\frac{NTU}{V_T}\left(\omega_a - \omega_{s,w}\right) \tag{3.9}$$

$$\frac{dh_a}{dV} = -Le\frac{NTU}{V_T}\left[\left(h_a - h_{s,w}\right) + \left(\omega_a - \omega_{s,w}\right)\left(1/Le - 1\right)h_{g,w}\right] \tag{3.10}$$

$$\frac{dT_w}{dV} = \frac{dh_a/dV - c_{p,w}\left(T_w - T_{ref}\right)d\omega_a/dV}{\left[M_{w,i}/M_a - \left(\omega_{a,o} - \omega_a\right)\right]c_{p,w}} \tag{3.11}$$

$$Q = \varepsilon_a M_a\left(h_{s,w,i} - h_{a,i}\right) \tag{3.12}$$

$$h_{a,o} = h_{a,i} + \varepsilon_a\left(h_{s,w,i} - h_{a,i}\right) \tag{3.13}$$

$$\omega_{a,o} = \omega_{s,w,e} + \left(\omega_{a,i} - \omega_{s,w,e}\right)\exp(-NTU) \tag{3.14}$$

$$T_{w,o} = T_{ref} + \frac{M_{w,i}\left(T_{w,i} - T_{ref}\right)c_{p,w} - M_a\left(h_{a,o} - h_{a,i}\right)}{M_{w,o}c_{p,w}} \tag{3.15}$$

$$NTU = c\left[\frac{M_w}{M_a}\right]^{1+n} \tag{3.16}$$

$$M_a = M_{a,des}\left[c_{01} + c_{02}\left(\frac{Freq}{Freq_{des}}\right) + c_{03}\left(\frac{Freq}{Freq_{des}}\right)^2\right] \tag{3.17}$$

$$W_{ct} = W_{ct,des}\left[c_{11} + c_{12}\left(\frac{Freq}{Freq_{des}}\right) + c_{13}\left(\frac{Freq}{Freq_{des}}\right)^2\right] \tag{3.18}$$

where ω_a is the air humidity ratio, $\omega_{s,w}$ and $\omega_{s,w,e}$ are the saturation air humidity ratio and effective saturation air humidity ratio with respect to the temperature of the water surface, respectively, V_T is the total volume, Le is the Lewis number, T_w is the temperature of water, T_{ref} is the reference temperature for zero enthalpy of liquid water, h_a is the enthalpy of the moist air per mass of dry air, $h_{s,w}$ is the saturation air enthalpy with respect to the temperature of the water surface, $h_{g,w}$ is the enthalpy of water above the reference state for liquid water at T_{ref}, M_w and M_a are the mass flow rates of water and dry air, respectively, $W_{ct,des}$ and $M_{a,des}$ are the power consumption and air flow rate of the cooling tower at the design condition, $Freq$ is the fan operating frequency, and c_{01}-a_{03} and c_{11}-c_{13} are coefficients.

3.2.2.3 Pumps

The variable speed pump is simulated by a steady-state pump, a steady-state frequency inverter and a dynamic actuator of the inverter (Wang 1998). The frequency at the outlet of the inverter is linear to the input signal from the actuator. The efficiency of the inverter is included within the model of the pump energy performance. The energy performance and pump characteristics at various speeds are simulated using fourth-order polynomial functions as shown in Equations (3.19) and (3.20), respectively. The coefficients in the equations can be determined by regression using the performance data from the manufacturer's catalogues.

$$W_{pu}(Freq, M_{pu}) = \sum_{i=0}^{m} \sum_{j=0}^{n} G_{ij} Freq^{i} M_{pu}^{j} \tag{3.19}$$

$$P_{pu}(Freq, M_{pu}) = \sum_{i=0}^{m} \sum_{j=0}^{n} E_{ij} Freq^{i} M_{pu}^{j} \quad (3.20)$$

where W_{pu} *and* P_{pu} are the pump power consumption and pressure head, respectively, *Freq* is the frequency input to the pump, M_{pu} is the water flow rate through a pump, *G* and *E* are coefficients.

3.2.2.4 AHU/PAU Coils

The AHU and PAU coil model is simulates the outlet water and outlet air states. In this study, the physical model developed by Wang (1998) is used. The AHU coil is modeled using a dynamic approach. A first-order differential equation, as shown in Equation (3.21), is used to represent the dynamics of a coil with lumped thermal mass. The dynamic equation based on the energy balance ensures that the energy is conserved. The outlet air and water temperatures ($t_{a,out}$, $t_{w,out}$) are computed using Equations (3.22) and (3.23) respectively, by the heat balances of both sides. The heat transfer calculation applies the classical number of transfer units (NTU) and heat transfer effectiveness methods. The classical method to calculate the effect of the fins in the air side on the thermal resistance is used.

$$C_c \frac{dt_c}{d\tau} = \frac{t_{a,in} - t_c}{R_1} - \frac{t_c - t_{w,in}}{R_2} \quad (3.21)$$

$$t_{a,out} = t_{a,in} - \frac{SHR(t_{a,in} - t_c)}{R_1 C_a} \quad (3.22)$$

$$t_{w,out} = t_{w,in} - \frac{t_c - t_{w,in}}{R_2 C_w} \tag{3.23}$$

where t_c is the mean temperature of the coil, $t_{a,in}$ and $t_{w,in}$ are the inlet air and water temperatures, C_c is the overall thermal capacity of the coil, C_a and C_w are the capacity flow rates of air and water, R_1 and R_2 are the overall heat transfer resistances at air and water sides, *SHR* is the sensible heat ratio.

3.2.2.5 Heat Exchangers

The dynamic performance of a heat exchanger is represented by a classical steady-state heat transfer model and a simple dynamic model (Wang 1998). The heat transfer model computes the number of transfer units and heat transfer efficiency (ε) using Equation (3.24) for a counter flow heat exchanger and Equation (3.25) for a crossover flow heat exchanger. The dynamic models, similar to that represented in Equations (3.7) and (3.8), are used to represent the thermal storage characteristics of the heat exchanger and then to simulate its dynamic response.

$$\varepsilon = \frac{1 - \exp[-NTU(1-\omega)]}{1 - \omega\exp[-NTU(1-\omega)]} \tag{3.24}$$

$$\varepsilon = \frac{1 - \exp[-\omega(1-\exp(NTU))]}{\omega} \tag{3.25}$$

where ω is the capacity flow rate ratio, ε is the number of transfer units and heat transfer efficiency, and NTU is the number of transfer units.

3.2.3 Parameter identification

The parameters and coefficients in the above component models are constants when their size and type are determined. In this study, these parameters are identified using regression method based on numerous field operation data of each component.

3.3 Summary

This chapter introduces the super high-rise building and its complex central chilling system concerned in this research. Referring to this complex central chilling system, a dynamic simulation platform was constructed using detailed physical models of components. The developed robust and optimal control strategies for HVAC system in this thesis will be tested and evaluated in this simulation platform in terms of operation robustness and energy performance. The developed fault detection and diagnosis (FDD) strategies will be validated on this simulation platform as well.

CHAPTER 4 IN-SITU DIAGNOSIS OF THE LOW DELTA-T SYNDROME IN THE CHILLED WATER SYSTEM: A CASE STUDY

A case study that diagnoses the low deltas-T syndrome in the studied chilled water system is presented in this chapter. The associated experiment validation is provided as well.

Section 4.1 presents the operation problem in the central chilling system of the super high-rise building under study. Section 4.2 outlines the proposed diagnosis methodology for identifying the exact faults. In Section 4.3, the detailed diagnosis results are presented via in-situ operation data analysis and experimental validation. Suggestions for correcting the faults and improving the operation performance are provided as well. A summary of this chapter is given in Section 4.4.

4.1 Operation Problems

Over the last two decades, primary-secondary chilled water systems have been widely employed to offer comfortable indoor environment in commercial buildings, especially in large buildings, due to its higher energy efficiency than the traditional constant flow system [Wang 2010]. While in real applications, most of the primary-secondary systems, from time to time, do not work as efficient as expected because of the excess secondary flow demand, which causes deficit flow problem

(i.e. the required flow rate of secondary loop exceeds that of the primary loop). When the deficit flow problem exists, the temperature difference produced by the terminal units will be much lower than its design values, which is known as the low delta-T syndrome [Kirsner et al. 1994, Waltz 2000, Kirsner 1998, Avery 1998]. Kirsner [1994] pointed out that the low delta-T chilled water plant syndrome existed in almost all large distributed chilled water systems. For practical applications, it is essential to find the causes before adopting proper corrections. However, the detailed study for detection and diagnosis of the low delta-T syndrome and deficit flow problem, particularly in real applications, is still insufficient.

This chapter offers a practical approach and some useful experiences for researchers as well as engineers and operators to find causes of the low delta-T syndrome effectively and enhance the energy performance of chilled water systems. In this study, the history operation data were analyzed and experiments were designed and conducted to diagnose and determine the causes for low delta-T syndrome in a complex central chilled water system of a super high-rise building in Hong Kong.

The detailed description of the central chilling system of the super high-rise building under study has been introduced earlier in Chapter 3. This central chilled water plant frequently suffered from the deficit flow problem and low chilled water temperature difference disease after its first use at it early operating stage (since the middle of 2008). Figure 4.1 presents the measured water flow rate in the bypass line and the measured chilled water temperature difference of the main supply and

return pipes (i.e., namely the system temperature difference) in five consecutive summer days respectively in 2009. It is obvious that the average system temperature difference during the five days was very low, only about 3.5 K. It is also noted the deficit flow (negative value for water flow rate in the bypass line means the deficit flow) existed in nearly half of the period and the average duration was about 12 hours a day. When the deficit flow occurred, the system delta-T became much lower, which indicates that the deficit flow and the low delta-T syndrome in this system seemed to be highly correlated. Since the cooling coils are selected to produce a temperature rise at full load that is equal to the differential temperature selected for the chillers (i.e., 5 K in this case), the flow rate of secondary loop should be therefore equal to that of the primary loop under full load condition and should be less than that of primary loop under part load condition. However, when the deficit flow problem exists, the excessive water flow rate of secondary loop will greatly reduce the temperature difference produced by the terminal units, which is known as low delta-T syndrome. Therefore, the low delta-T syndrome existing in this chilled water system was mainly due to the occurrence of the deficit flow problem. In order to raise the system chilled water temperature difference, it is necessary to find the exact faults that caused the deficit flow problem, solve the low delta-T syndrome, and accordingly enhance the energy performance of the overall chilled water system.

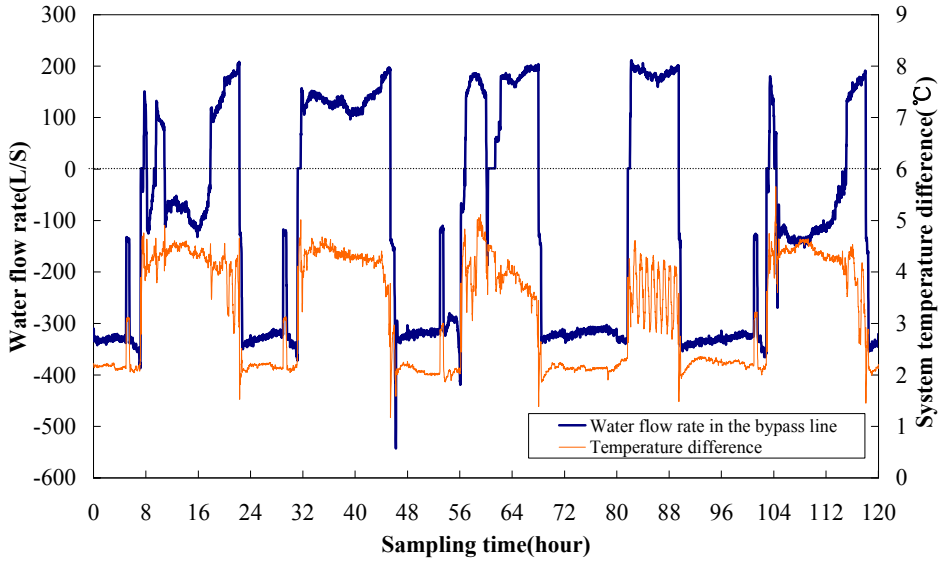

Figure 4.1 Measured water flow rate in the by-pass line and temperature difference in secondary system in five summer days

4.2 Outline of the in-situ diagnosis methodology

There are a lot of faults that can result in the deficit flow and the low delta-T syndrome. The faults mainly include improper set-points or poor control calibration, the use of three-way valves, improper coil and control valve selection, no control valve interlock, and uncontrolled process load, reduced coil effectiveness, outdoor air economizers and 100% outdoor air systems, and so on. The chilled water system under study was new-built and was properly designed, installed and well commissioned. The following faults were excluded according to the analysis and site investigations, such as coil fouling, improper sensor calibration, the use of three-way valves and the improper selection of components. Therefore, possible faults considered finally are within the category of control faults.

A practical diagnosis process is developed in this study to diagnose the deficit flow

problem and low delta-T syndrome resulted from improper controls in this complex chilled water system, which mainly includes faults detection and diagnosis, and validation of the FDD results as well as evaluation of the energy impacts, as shown in Figure 4.2. To detect faults, the water flow rate in the bypass line and the differential temperature of the entire system are selected as the indicators to detect whether the low delta-T syndrome existed in the chilled water system. If the water flow rate in the bypass line is negative and the measured differential temperature of the main supply and return pipes are much lower than the predefined threshold (i.e., 3 K in this study), the chilled water system can be determined to suffer from deficit flow problem and low delta-T syndrome.

Faults identification scheme is implemented to identify the exact faults that cause the deficit flow problem. As there are several sub-systems in a complex chilled water system, the fault location will be firstly determined by comparing the differential temperature of different sub-systems. Then, the history operation data will be analyzed to observe whether the set-point used for controlling secondary pumps speed can be achieved when the deficit flow occurred. If the occurrence of the deficit flow is closely correlated to the set-point for controlling secondary pumps speed, it can be preliminarily considered that the deficit flow problem is mainly resulted from the improper set-point. At last, selected relative operation parameters will be analyzed to identify the faults according to the control strategy used in the system, such as valve openings, pumps frequency, pumps sequence, and heat exchangers sequence.

An experimental validation test is conducted to further validate and confirm the fault detection/identification results. In this test, the specific faults identified preliminarily will be introduced artificially in the chilled water system. If the deficit flow phenomenon is triggered as soon as the faults are introduced and is eliminated when faults are released, the previous faults detection/identification results is validated and confirmed. Meanwhile, the energy impacts caused by the faults are also evaluated by comparing the energy consumption of the system with deficit flow to that of the system without deficit flow in the experiments.

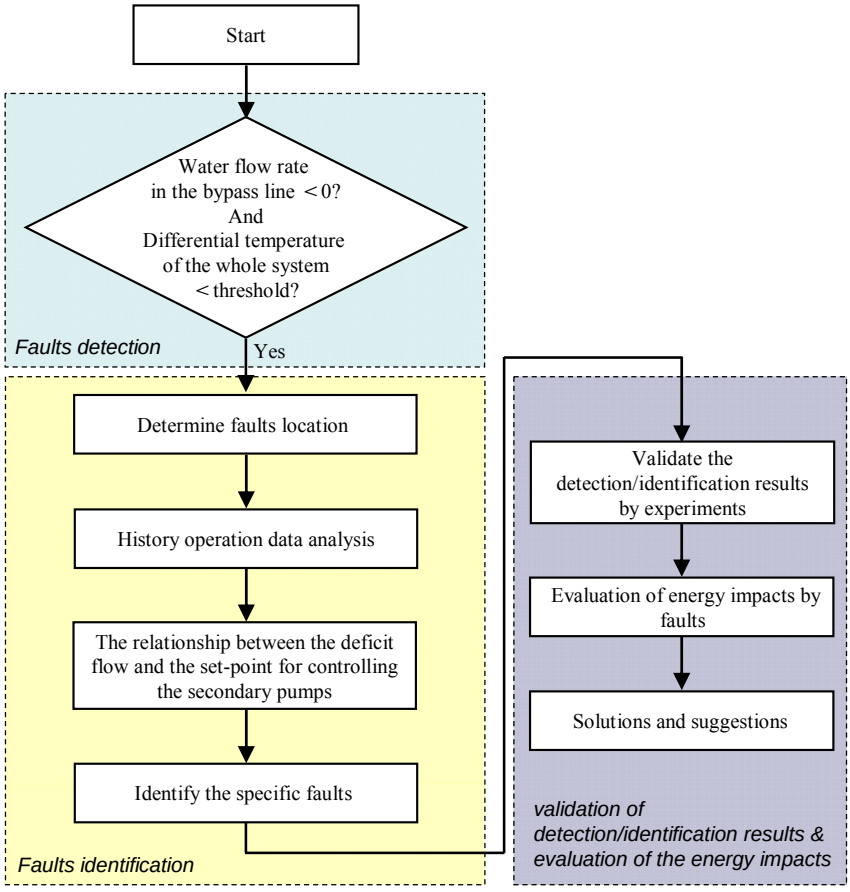

Figure 4.2 Schematic of the in-situ diagnosis process

4.3 Diagnosis result and discussions

An advanced building management system (BMS) is installed in this building and the operation data of the chilled water system are collected and stored in the database. The database consists of the main operation data of the HVAC system, such as temperatures, flow rates, air and water pressures at some key points as well as energy consumptions of chillers, pumps, cooling towers, and AHUs. The history operation data are essential to analyze the operation performance of the chilled water system.

The deficit flow problem and the low delta-T syndrome have been detected in this system under study mentioned earlier, as shown in Figure 4.1. In the following sections, the fault location and identification by using the proposed FDD method are presented. Validation of the FDD method and evaluation of the energy impacts are also addressed.

4.3.1 Faults identification by analyzing operation data

Since the temperature difference is a key indicator to evaluate the operation performance of a chilled water system, temperature difference of each sub-system was analyzed first through history operation data to find at which sub-system the faults located. Figure 4.3 shows the temperature difference of each sub-system in five summer days (i.e., the same period as mentioned in Figure 4.1) when the system suffered from low delta-T syndrome. It can be observed that only differential temperature of the riser serving Zone 2 maintained over 4 K most of time, which is

normally accepted in most of systems. The temperature differences of the risers serving Zone 1 and Zone 3&4 were much lower. Particularly, during the occurrence of the deficit flow, the temperature differences of these two risers were only about 1 K. It indicates that the low delta-T syndrome was very serious in these two zones. Comparing the temperature differences of the three risers, it was found that the low delta-T syndrome was mainly contributed by the riser serving Zone 1 and the riser serving Zone 3&4. Because the pump configurations and the pump control strategies in the two risers are very similar, Zone 3&4 is selected as the example to be analyzed and diagnosed in the followings.

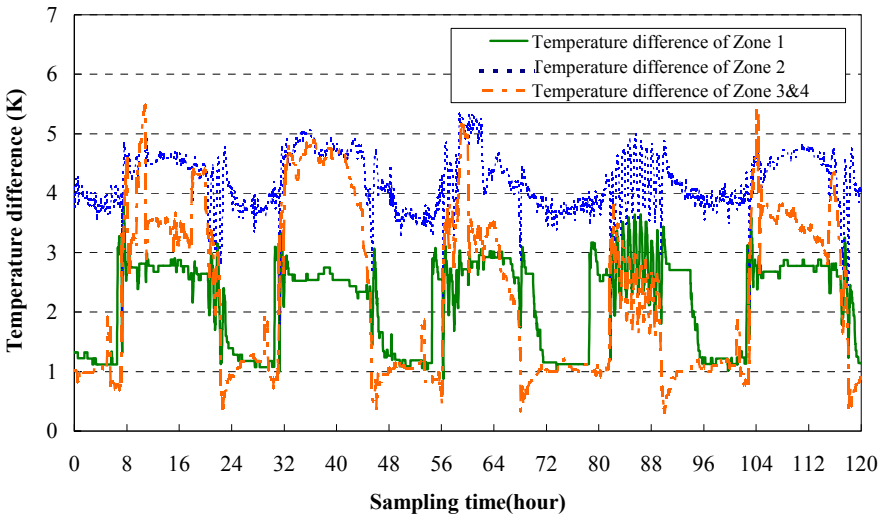

Figure 4.3 Temperature difference of individual riser in five summer days

In order to further determine the exact faults of the controls that cause the deficit flow problem in Zone 3&4, the history operation data of two typical summer days were selected for comparison and analysis, in which one day experienced significant deficit flow problem during daytime and the other day experienced significant deficit

flow during night. Figure 4.4 shows the operation data of the day when significant deficit flow occurred during daytime, including water flow rate in the bypass line, the operating number of heat exchangers and pumps before heat exchangers (i.e., on the primary side of heat exchangers), the outlet water temperature ($T_{out,ahx}$) after heat exchangers (i.e., on the secondary side of heat exchangers), and the set-point of the outlet water temperature after heat exchangers. It is obvious that the deficit flow began to occur at about 4:00am and lasted nearly the entire daytime. While in another summer day as shown in Figure 4.5, the deficit flow only occurred during the night and disappeared during the daytime. An interesting fact is that the set-point of $T_{out,ahx}$ was closely correlated to the occurrence of deficit flow. When the deficit flow existed, the measured $T_{out,ahx}$ was significantly higher than the set-point of $T_{out,ahx}$. In contrast, when there was no deficit flow, the measured $T_{out,ahx}$ basically was not higher than the set-point of $T_{out,ahx}$. It is worthy noticing that when the water flow rate of the bypass line changed from the positive flow to deficit flow, the measured $T_{out,ahx}$ accordingly varied from below its set-point to above its set-point. Therefore, a preliminary conclusion can be drawn that the deficit flow might be easily triggered when $T_{out,ahx}$ cannot be maintained at its set-point, and the deficit flow will be eliminated when $T_{out,ahx}$ can be maintained at its set-point. Another fact shown in Figure 4.4 and Figure 4.5 is that the operating numbers of heat exchangers and pumps before heat exchangers were significantly increased when the deficit flow occurred. The more deficit flow occurred, the more heat exchangers and pumps before heat exchangers were activated.

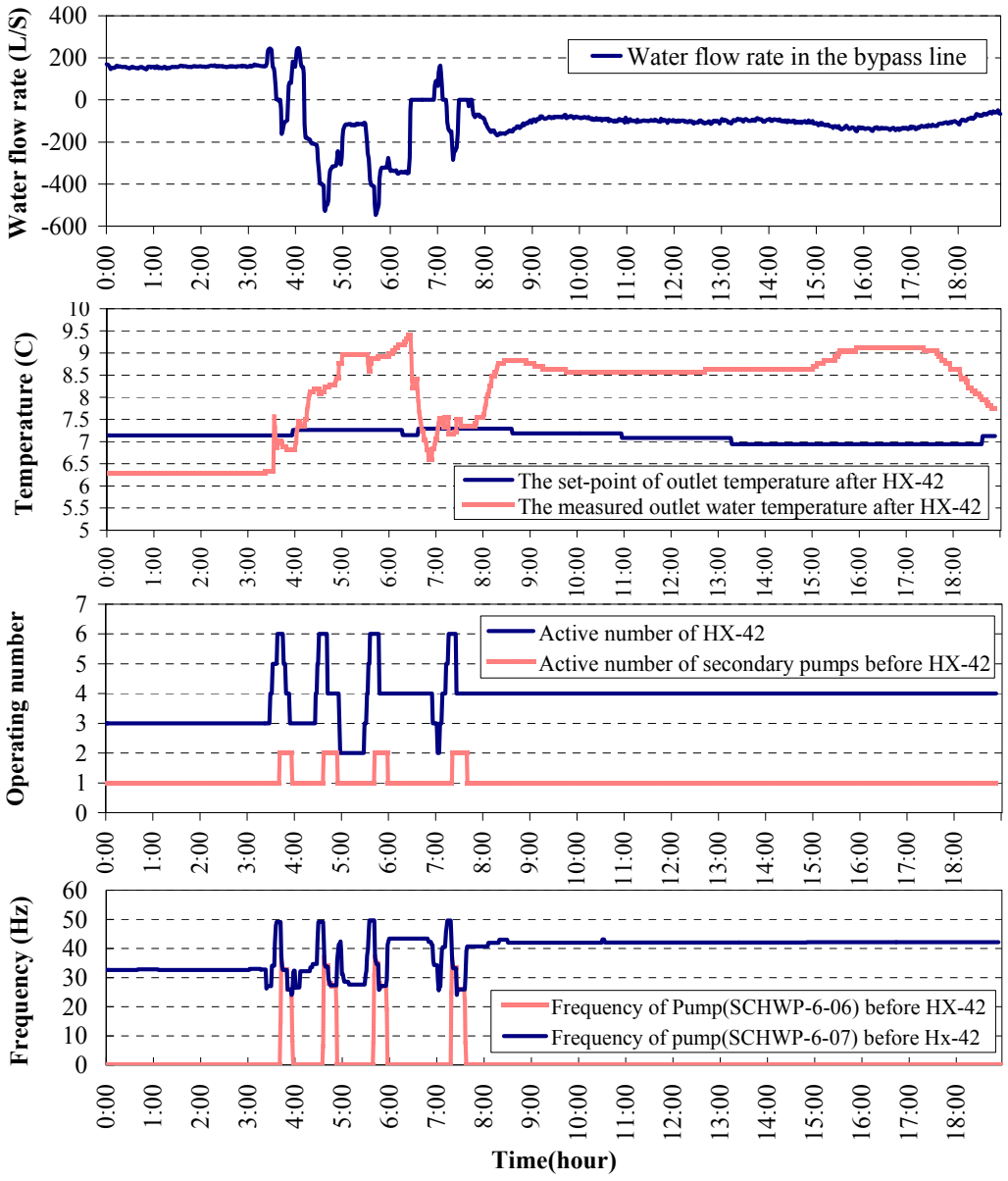

Figure 4.4 The operation data in the typical day when deficit flow existed during daytime

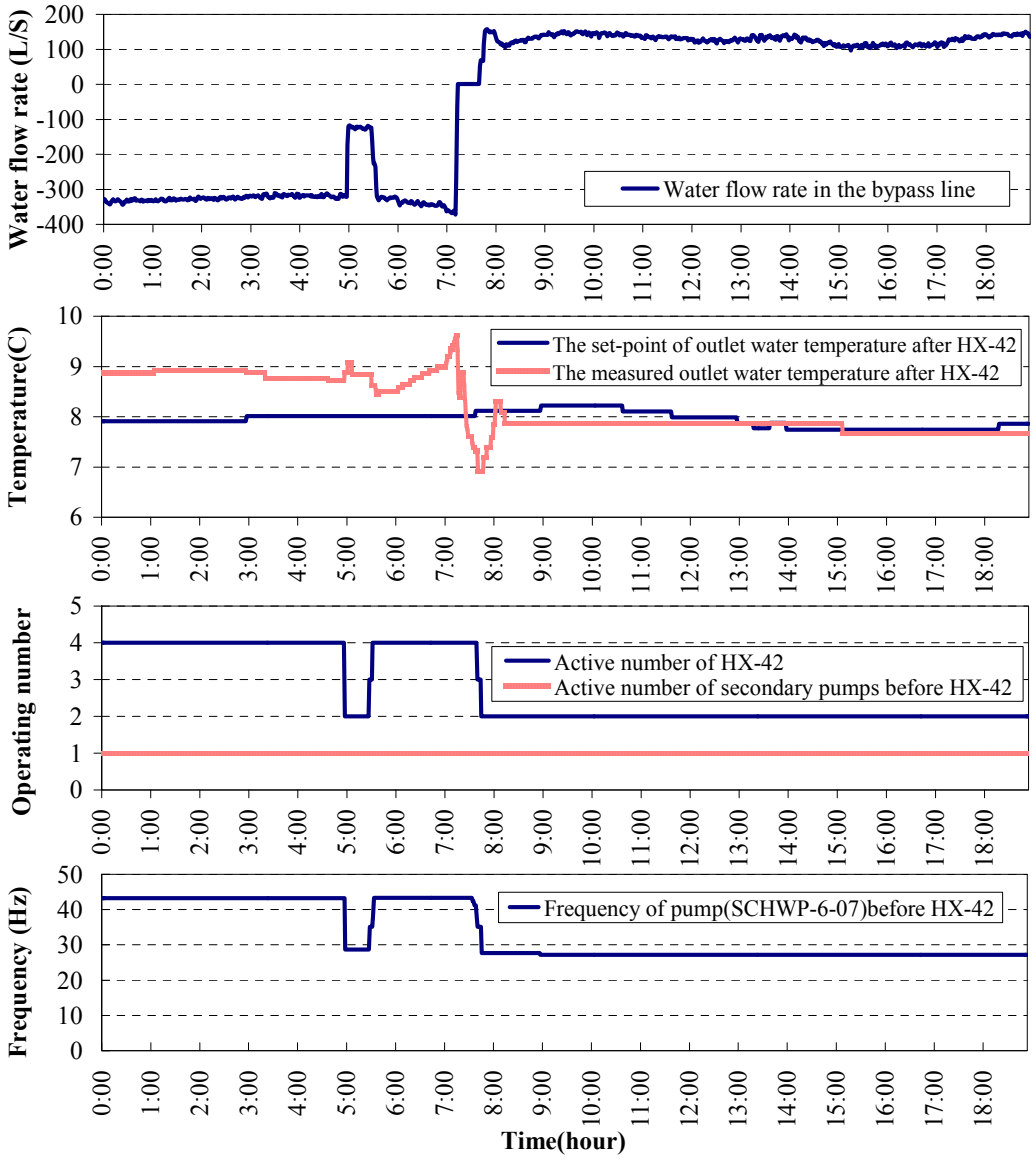

Figure 4.5 Operation data in the typical day when deficit flow occurred during night

The above phenomenon observed can be interpreted according to the control strategies for pumps and heat exchangers currently used in this system, as shown in Figure 4.6. The variable speed pumps before heat exchangers distribute the chilled water from the chillers to the heat exchangers. The pumps speed is controlled to maintain the measured differential pressure between the main supply and return water pipes before the heat exchanger group at its set-point. A temperature controller

is used to keep the outlet temperature ($T_{out,ahx}$) after heat exchangers at its set-point by modulating the openings of the valves before heat exchangers. In the control strategy, the differential pressure set-point is a constant, while the temperature set-point after heat exchanger keeps a fixed temperature difference (i.e., 0.8 K) above the chiller supply water temperature that varies based on the outdoor dry-bulb temperature, as shown in Figure 4.7. When $T_{out,ahx}$ is higher than its set-point, the modulating valves before heat exchangers will widely open to demand more chilled water before heat exchangers.

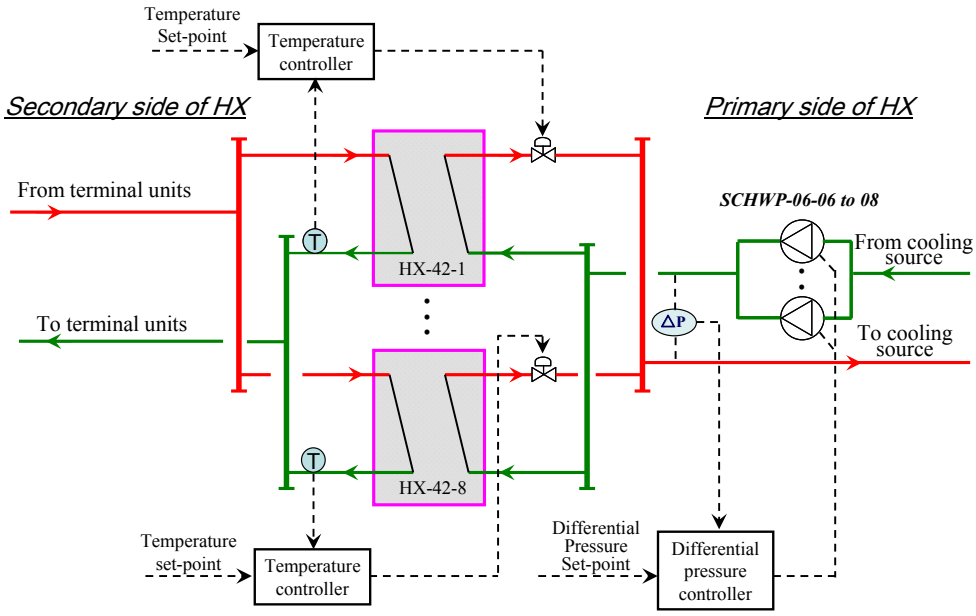

Figure 4.6 Speed control for pumps before HX serving zone3&4

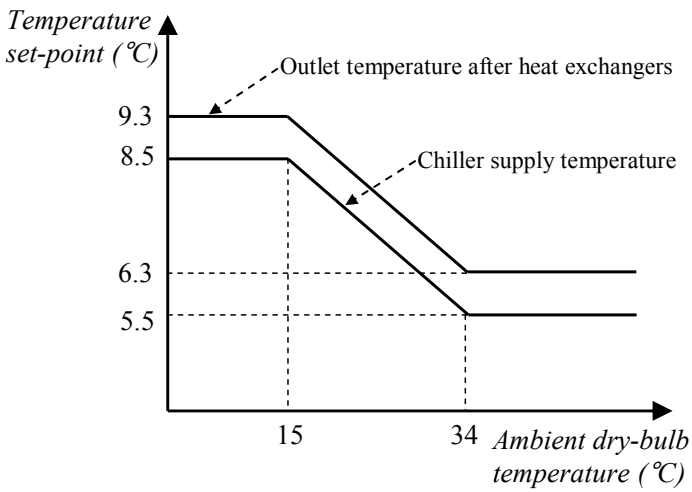

Figure 4.7 The original scheme for determining the set-point of outlet water after heat exchangers

Moreover, according to the sequence control strategy used in this case, if one of the valves reach its maximum position and $T_{out,ahx}$ still cannot reach its set-point, the additional heat exchanger will be switched on to enhance the heat transfer effect. As the heat exchangers are connected in parallel, more operating heat exchangers and more widely opened valves will significantly decrease the overall water resistance at the primary side of heat exchangers. When the overall water flow resistance was reduced, the pumps speed before heat exchangers would be continually increased to maintain the measured differential pressure across of the heat exchangers at its set-point until the set-point was reached or the pumps reach their full speeds. The over-speeded pumps distributed more chilled water than necessary, which caused the deficit flow in the bypass line and in turn led to the low delta-T syndrome. These analyses are based on Figure 4.4 and Figure 4.5, which can be summarized in Figure 4.8.

Based on the above analysis, the preliminary conclusion can be drawn that the too

low outlet water temperature set-point after heat exchangers that cannot be reached led to the deficit flow problem and the low delta-T syndrome in the system investigated.

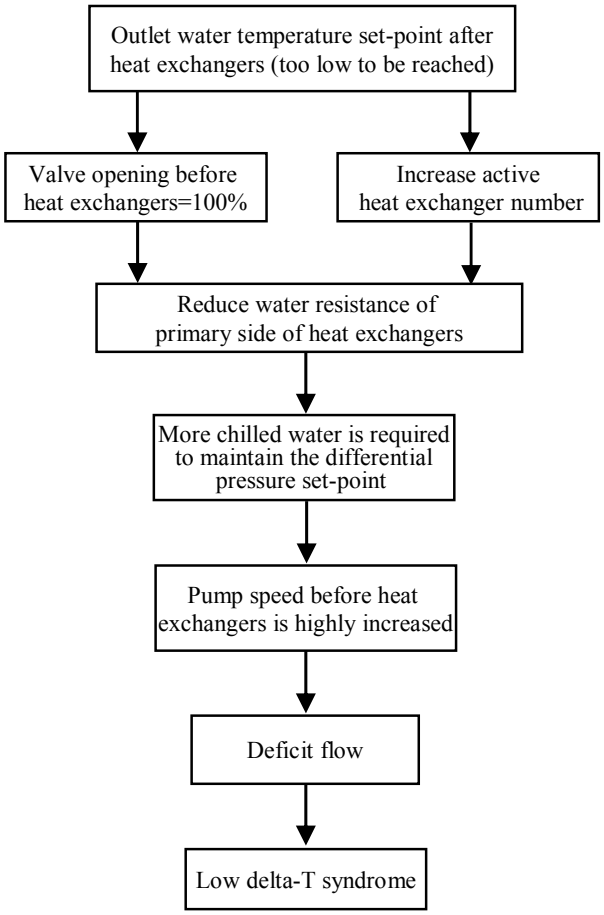

Figure 4.8 Flow chart for low delta-T syndrome diagnosis

4.3.2 Validation of FDD method and evaluation of energy impacts

In order to validate the FDD method in above analysis, two repeated field tests were conducted to verify the cause of the deficit flow in the bypass line by varying the set-point of the outlet water temperature ($T_{out,ahx}$) after heat exchangers in two separate days. The results of the two tests show the consistent conclusions and the results presented as follows came from the latest test in the autumn of 2010. In this

test, the set-point of $T_{out,ahx}$ was firstly changed from 8.2°C (while no deficit flow occurred) to 6.8°C, and 6°C respectively. Then, the set-point was increased back to 7.4°C and 8.2°C respectively. During the whole test period, the chiller supply water temperature was fixed at 5.5°C, and the operating number of chillers as well as the primary water flow rate remained unchanged.

Figure 4.9(a) and 4.9(b) show the water flow rates in the bypass line and the relationship between $T_{out,ahx}$ and its set-point. It can be observed that, before changing the set-point of $T_{out,ahx}$, the deficit flow did not occur and $T_{out,ahx}$ basically could be maintained at its set-point before 11:10am. When the set-point of $T_{out,ahx}$ was reduced to 6.8°C, and 6°C respectively, the water flow rate of the bypass line dropped rapidly from about 170 l/s to negative (-25 l/s), which means the deficit flow occurred. Meanwhile, $T_{out,ahx}$ experienced a gradual dropping process but could not be low enough to reach its set-point. On the other hand, when the set-point of $T_{out,ahx}$ was increased again to 7.4°C and 8.2°C respectively, the deficit flow was eliminated and $T_{out,ahx}$ also returned to be controlled approximately at its set-point. The test results indicate that the deficit flow would most likely occur if the set-point of $T_{out,ahx}$ is too low to be reached. The deficit flow can be eliminated if the correct control of $T_{out,ahx}$ is resumed, which confirms the preliminary conclusion in Section 4.1.

It is also worthy pointing out that, in Figure 4.9(a) and 4.9(b), the actual measured outlet water temperature after heat exchangers was not significantly decreased and

basically maintained stable at about 7.2°C although the set-point of $T_{out,ahx}$ changed from 6.8°C to 6°C. The reason is that the inlet water temperature on the primary side of heat exchangers was significantly increased because of the deficit flow. The more supplied chilled water with higher temperature failed to improve the overall cooling effect of the heat exchangers when the deficit flow occurred.

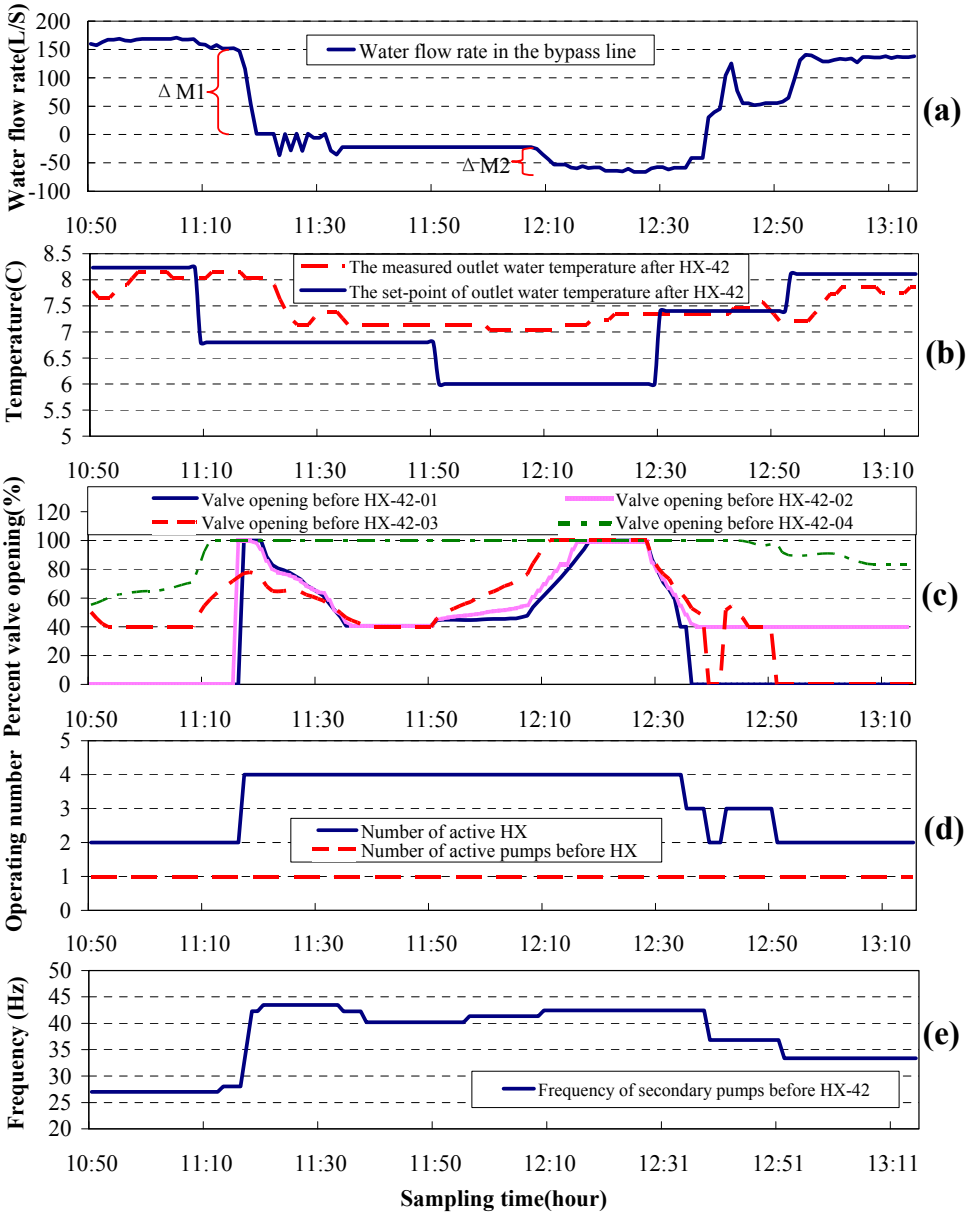

Figure 4.9 The operation data during the test period

Figure 4.9(c) and 4.9(d) present the openings of modulating valves before heat

exchangers and the operating number of heat exchangers during the test period. It can be observed that the openings of modulating valves were closely related to $T_{out,ahx}$ and its set-point. Once the set-point of $T_{out,ahx}$ was lower than $T_{out,ahx}$, the modulating valves opened rapidly. When one of the modulating valves fully opened, additional heat exchangers were switched on by the control logic used in this case. When the set-point increased from 6°C to 7.4°C and further to 8.2°C respectively, the modulating valves closed down until reaching the minimum position and the operating number of heat exchangers also was reduced from four to two eventually. The valve openings and the operating number of heat exchangers greatly affected the controlled speed of pumps at the primary side of heat exchangers, as shown in Figure 4.9(e). It can be found that the speed (frequency) of the pumps before heat exchangers significantly increased when either the valves were widely opened or extra heat exchangers were switched on. On the other hand, when both the valve openings and operating number of heat exchangers were reduced, the speed of pumps before heat exchangers dropped again. Both wider valve openings and more operating heat exchangers mean a lower overall water resistance of the heat exchanger group at primary side. Therefore, the pump speed had to be increased to transfer more water to meet the predetermined pressure differential set-point. It is worth noticing that the variation of overall water resistance of heat exchanger group was more sensitive to the operating number of heat exchangers compared with the valve openings. As indicated in Figure 4.9(a), water flow variation (i.e., ΔM2) in the bypass line resulted from valve openings was far less than that (i.e., ΔM1) resulted

from changing heat exchanger operating number.

Figure 4.10 depicts the dynamic energy consumption of pumps on both sides of heat exchangers during the test period. Clearly, the total energy of the pumps significantly increased when the set-point of Tout,ahx was greatly reduced and deficit flow occurred. Compared to that before test, 87.67 kW (72.37%) of the averaged power of all pumps on both sides of the heat exchangers was wasted during the test. It was also found that the energy consumption of the three kinds of pumps associated to heat exchangers varied in different ways when the set-point of $T_{out,ahx}$ decreased. The secondary pumps before heat exchangers and the primary pumps after heat exchangers consumed more energy while the secondary pumps after heat exchangers consumed less energy. But the energy wasted by the first two was far more than that saved by the third. The results demonstrated that a too low set-point of $T_{out,ahx}$ badly degraded the energy performance the chilled water system although the building cooling load still can be satisfied.

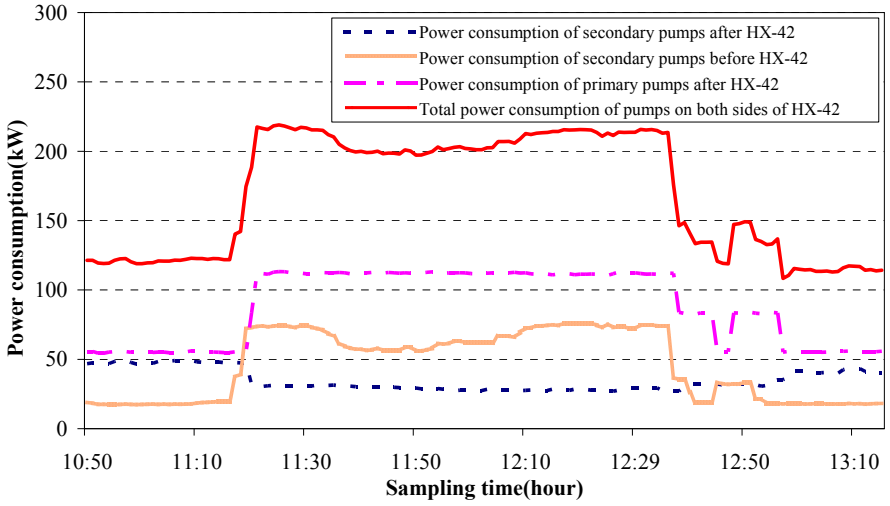

Figure 4.10 Power consumption of pumps on both sides of heat exchangers

The above test results confirmed the conclusion of the analysis in Section 4.1. It demonstrated that the deficit flow and the low delta-T syndrome in the chilled water system under study were mainly resulted from the improperly low set-point of the outlet water temperature after heat exchangers.

4.3.3 Discussion and suggestions

The in-situ operations and experiments have demonstrated that it is not robust and is unreliable to reset the set-point of outlet water temperature after heat exchangers ($T_{out,ahx}$) using a fixed differential temperature difference above the chiller supply water temperature, particularly when the differential temperature is relatively small. It is because that the inlet water temperature before heat exchangers is not always equal to the chiller supply water temperature due to the deficit flow problem in practical applications. Once the inlet water temperature before heat exchangers is higher than the chiller supply water temperature, the actual temperature difference between the inlet water temperature before heat exchangers and the set-point of $T_{out,ahx}$ will be reduced. When such phenomenon occurs, more chilled water before heat exchangers will be provided by the control, which makes the deficit flow worse. Particularly in the summer days when the cooling is relatively high, $T_{out,ahx}$ is more easily affected by some uncertainties and disturbances, such as sudden cooling load increasing or temporarily high inlet water temperature before heat exchangers. This also interprets the reason why the deficit flow more easily occurred in summer season than in the spring season, as observed through field investigations and history

operation data.

Simulation tests on the system under study were conducted to study the impact of the temperature set-point of chilled water after heat exchangers on the operation and energy performances of pumps. Figure 4.11 shows the test results under a fixed cooling load (i.e., 60% of design cooling load of Zone 3) when the chiller supply water temperature was fixed at 5.5°C. It can be observed that the overall power of pumps associated with heat exchangers gradually increased while the set-point of $T_{out,ahx}$ increased from 6.3°C to 8°C. When the set-point of $T_{out,ahx}$ reduced below 6.2°C, the power of pumps increased dramatically and all the pumps at primary side were at maximum speed. The reason is that the deficit flow occurred when the set-point of $T_{out,ahx}$ (i.e., temperature difference of water before and after heat exchangers) was lowered, which cannot be reached under this working condition. The results indicates that the set-point of $T_{out,ahx}$ (around 6.3°C) currently used sometimes was at risk of causing deficit flow although it was the design value and was thought to be safe for the studied chilled water plant under the design working condition. Therefore, a higher temperature difference above chiller supply water temperature is recommended for resetting the set-point of $T_{out,ahx}$ in this system to ensure the system to be maintained at healthy operation condition. It also can be found in Figure 4.11 that proper increase of the set-point of $T_{out,ahx}$ had minor effect on the overall pump power. Compared with the overall pump power (207.8kW) using the current set-point at 6.3°C (i.e., 0.8 K of temperature difference), the increase was about 0.86kW only (0.5% of the total pumps energy) when the system

worked under the set-point of $T_{out,ahx}$ at 6.7°C (i.e., 1.2 K of temperature difference). Obviously, a higher set-point of $T_{out,ahx}$ can allow the operation and control more robust and reliable while the overall pump power was almost unchanged. The reset scheme for set-point of outlet water temperature after heat exchangers ($T_{set,out,ahx}$) is therefore proposed for the studied chilled water system as expressed by Equation (4.1).

$$T_{max} \geq T_{set,out,ahx} = \max\left(T_{ch,sup} + 1.2, T_{meas,in,bhx} + 0.8\right) \quad (4.1)$$

where, $T_{ch,sup}$ is the chiller supply water temperature, $T_{meas,in,bhx}$ is the measured inlet water temperature before heat exchangers. The proposed scheme for resetting $T_{set,out,ahx}$ adopts double security. One is to ensure that $T_{set,out,ahx}$ is 0.8 K higher than the actual inlet water temperature before heat exchangers at least. This ensures the outlet water temperature after heat exchangers be reached easily because 0.8 K is temperature difference used for selecting heat exchangers at design stage. The other insurance is that the temperature difference between $T_{ch,sup}$ and $T_{set,out,ahx}$ is increased from 0.8 K to 1.2 K. This is because that the use of a higher $T_{set,out,ahx}$ results in less probability of deficit flow while the overall pump energy consumption is not increased obviously. The revised set-point resetting scheme provides better chance for the system to resume itself to healthy mode (surplus flow in bypass line) when possible. A high limit (T_{max}) is set for the set-point of $T_{out,ahx}$ to guarantee the temperature of chilled water supplied to clients within the guaranteed range and proper for humidity control in occupied zones. It is noted that the actual coefficients

in Equation (4.1) are only suitable for the studied chilled water plant and different values may be needed for other plants.

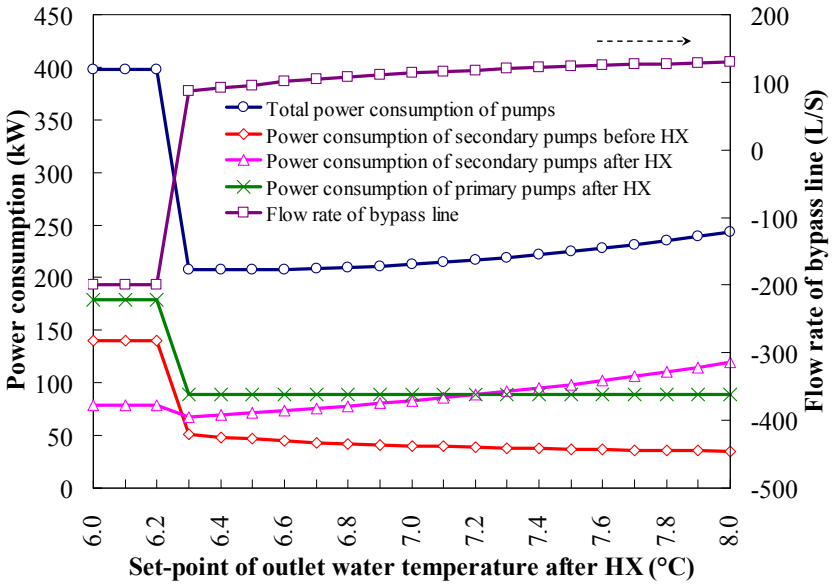

Figure 4.11 Power consumption of pumps and flow rate of bypass line under different set-point of $T_{out,ahx}$ under a fixed cooling load

4.4 Summary

This chapter presented a method and a case study to diagnose the low delta-T syndrome and deficit flow problem in a real chilled water system of a super high-rise building. The improper set-point reset of the outlet water temperature at the secondary sides of heat exchangers was found to be the actual fault that caused the deficit flow problem in the system. The analysis results show that a too low set-point of outlet water temperature at the secondary side of heat exchangers would lead to more pumps to be activated with higher speed on the primary side of heat exchangers, which easily caused deficit flow. Deficit flow could be eliminated when this set-point was reset reasonably and slightly higher.

Results of an in-situ test confirmed the fault detection/identification results. In the meanwhile, a proper set-point of outlet water temperature on the secondary side of heat exchangers achieved an average power saving of 87.67 kW (72.37%) of pumps on primary and secondary sides of heat exchangers.

It is also suggested to set the temperature difference between the set-point of outlet water temperature and the supply chilled water temperature at sufficiently high level in real applications.

CHAPTER 5 ONLINE ADAPTIVE OPTIMAL CONTROL STRATEGY FOR THE CHILLED WATER SYSTEM INVOLVING INTERMEDIATE HEAT EXCHANGERS

The complex building chilled water system involving intermediate heat exchangers as the medium to transfer the cooling energy is more complicated than the typical primary-secondary system. This chapter presents an optimal control strategy for online control of complex chilled water systems involving heat exchangers to enhance the system operation and energy performances. This optimal control strategy determines the optimal settings of the outlet water temperature after heat exchangers and the required operating number of heat exchangers and pumps in order to minimize the total energy consumption of pumps under varying working conditions. The control robustness and reliability in eliminating deficit flow is also considered.

Section 5.1 presents an overview on the existing control methods for the building chilled water system. Section 5.2 presents the formulation of the proposed optimal control strategy for complex chilled water systems involving heat exchangers. Simplified models are proposed to predict the system performance, and adaptive methods are used to accurately update key parameters online. Section 5.3 describes the set up of the simulation platform for validating and evaluating the performance

of the proposed strategy. In Section 5.4, the energy performance and control robustness of the proposed optimal control strategy are evaluated. A summary of this chapter is given in Section 5.5.

5.1 An overview on control methods for chilled water systems

During the last two decades, a number of studies have been made to enhance the reliability and energy efficiency of chilled water systems using various improved control methods. Some studies [Moor et al. 2003, Ma and Wang 2009, Wang and Ma 2010, Rishel 1991, Rishel 2003, Tillack et al. 1998] focused on the energy efficient control for variable speed pumps in the chilled water system. Among the existing studies, Moore and Fisher [2003] stated that the speed of pumps could be controlled to maintain at least one chilled water valve of cooling coils 90% open to save pumps energy consumption under part cooling load conditions. Ma and Wang [2009] presented optimal control strategies for variable speed pumps with different configurations in complex building air-conditioning systems to enhance their energy efficiencies, in which an optimal pump sequence control strategy is developed to determine the optimal number of pumps in operation. Wang and Ma [2010] also developed a control strategy for variable speed pumps distributing chilled water to the heat exchangers in super high-rise buildings. A cascade control method is employed to generate a variable water flow set-point for pump speed control. The results showed that up to 16.01% of the pumps can be saved using this control strategy.

Some other researchers [Braun et al. 1989, Lu et al. 2005, Ma and Wang 2009, Austin 1993, Hydeman et al. 2007, Fong et al. 2006, Jin et al. 2007, Ma 2000] paid more attention to the global optimization of the whole chilled water systems. Braun [1989] presented two methods for optimal control of chilled water systems without storage. One is a component-based nonlinear optimization algorithm that is a simulation tool for investigating optimal system performance. The other is a simpler system-based method for near optimal control that is simple enough for online implementation. Lu et al. [2005] presented a model-based global optimization for overall HVAC systems, which is formulated based on mathematical models of chillers, pumps, and fans. A modified genetic algorithm is used to find the optimal control settings, such as chilled water supply water temperature, operating number of equipments, differential pressure set-point, and etc. Simulations results show that the energy usage could be substantially reduced compared with the conventional methods. An optimal control strategy for complex building central chilled water system was developed by Ma and Wang [2009] for real-time online applications. This optimal control strategy can determine the optimal chiller supply water temperature and optimal differential pressure set-point to minimize the total operating cost of the chillers and chilled water pumps. 1.28-2.63% of the total energy in the studied system can be saved.

The above studies demonstrate the potential energy savings associated with the optimal control in the typical chilled water systems. However, most of the control strategies are suitable only for typical chilled water systems with simple

configurations, and fail to investigate the real-time applications in the complex chilled water systems. For instance, in a complex chilled water system using intermediate heat exchangers to transfer cooling energy from the low zones to high zones of a high-rise building, the heat exchanger outlet water temperature (hot side) and the operating number of heat exchangers could not be optimized in the above studies. In such complex systems, the existing control strategies could not ensure the robust control for variable speed pumps to avoid deficit flow problem (i.e., the chilled water delivered to buildings exceeds the total flow of the chillers) that frequently occurred in primary–secondary systems [Wang et al. 2010] when certain faults or disturbances occurred, such as sudden rise of heat exchanger inlet water temperature (cold side).

In this chapter, an online adaptive optimal control strategy for the complex chilled water systems involving heat exchangers is proposed to enhance their energy performance. Simplified models are proposed to predict the pumps energy consumption under various working conditions. Adaptive methods are utilized to online update parameters of models to achieve accurate predictions. The optimal control settings of the heat exchanger outlet water temperature (hot side) and operating number of heat exchangers are determined by using the exhaustive searching method to minimize the total energy consumption of pumps associated to heat exchanger group. The proposed strategy is tested and evaluated on a simulated virtual platform representing an actual complex chilled water system.

5.2 Formulation of the optimal control strategy

5.2.1 Outline of the optimal control strategy

The optimal control strategy aims to optimize the operation of complex building chilled water systems using model-based prediction control algorithm. As shown in Figure 5.1, the optimal strategy mainly consists of model-based performance predictors of components, cost estimation, optimization algorithm, and local control strategies. The overall energy consumptions of chilled water systems, including variable speed pumps and constant speed pumps on both sides (i.e. hot side and cold side) of heat exchangers, are minimized under all working conditions by optimizing the settings of the set-point ($T_{set,out,ahx}$) of the outlet water temperature after heat exchangers, the operating number of heat exchangers (N_{hx}), the operating number ($N_{pu,bhx}$) of pumps before heat exchangers, and the operating number of pumps after heat exchangers ($N_{pu,ahx}$).

Simplified adaptive models are adopted in this strategy to predict the energy consumption pumps under varying system working conditions. The exhaustive search method is implemented to search for the optimal $T_{set,out,ahx}$ and the required operating number of heat exchangers. In order to achieve energy efficient and robust operation, local control strategies for pumps and heat exchangers are also included in this strategy. The descriptions of the problem formulation, the models of components, the operating constraints, and the local control strategies are presented as below as well as the detailed optimization procedures for applications.

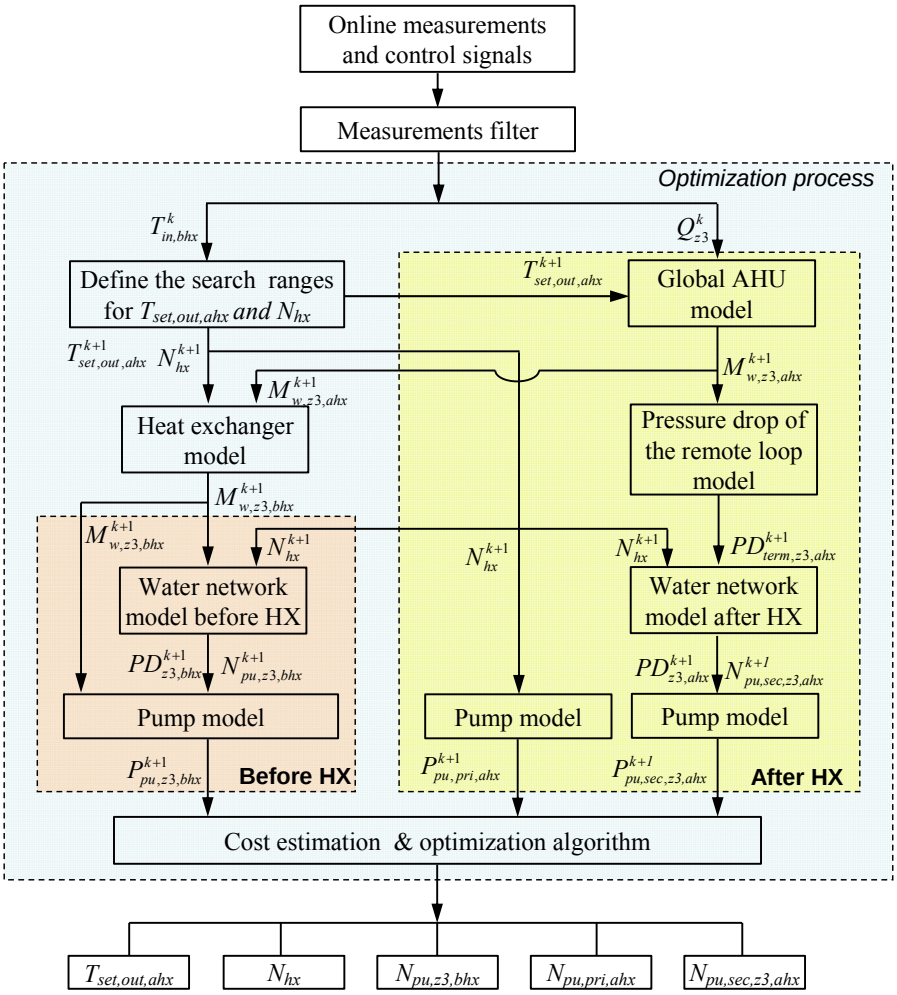

Figure 5.1 Illustration of optimization procedure of the optimal control strategy

5.2.2 Problem formulation

In practical applications, the chilled water system usually worked under part-load conditions with lower energy efficiency than under design conditions, which provides opportunities to enhance the overall energy performance by updating the real time operating settings. In fact, the set-point ($T_{set,out,ahx}$) of the outlet water temperature after heat exchangers significantly affects the energy consumption of secondary chilled water pumps on both sides of heat exchangers. A lower $T_{set,out,ahx}$ allows supplying less chilled water to the terminal units of the occupied zones,

which can save energy of secondary pumps after heat exchangers. Meanwhile, a lower $T_{set,out,ahx}$ also demands more water before heat exchangers, which will consume more energy of secondary pumps before heat exchangers. On the other hand, more operating number of heat exchangers is beneficial for improving the heat transfer effect of heat exchangers while increasing energy consumption of primary constant pumps, and vice versa.

Therefore, this proposed optimal control strategy aims to minimize the total energy (P_{tot}) of the pumps associated with heat exchangers, including secondary pumps before heat exchangers ($P_{pu,sec,bhx}$), primary pumps after heat exchangers ($P_{pu,pri,ahx}$), and secondary pumps after heat exchangers ($P_{pu,sec,bhx}$). Optimal control settings will be determined over the entire operating range in terms of $T_{set,out,ahx}$ and the required operating number of heat exchangers and pumps. The objective function of the system under study can be expressed as Equation (5.1).

$$J = \min_{T_{out,ahx}\,\&\,N_{hx}} (P_{tot}) = \sum_{i=1}^{N_{pu,\mathrm{sec},bhx}} P_{pu,\mathrm{sec},bhx,i} + \sum_{j=1}^{N_{pu,pri,ahx}} P_{pu,pri,ahx,j} + \sum_{n=1}^{N_{pu,\mathrm{sec},ahx}} P_{pu,\mathrm{sec},ahx,n} \tag{5.1}$$

5.2.3 Operating constraints

Some operation constrains are considered in this optimal control strategy, such as energy and mass balance, mechanical limitations. The cooling energy generated by chillers is assumed to equal the cooling energy provided to the buildings. Since the chillers, pumps, and heat exchangers are installed in parallel, water is assumed to be distributed to the active ones evenly. Because a too high water temperature for

terminal units cannot satisfy the indoor humidity requirement, the set-point of outlet water temperature after heat exchangers is bounded as Equation (5.2) based on the inlet water temperature ($T_{in,bhx}$) before heat exchangers. The inlet water temperature of condensers is assumed to be constant (i.e. 30°C) in this study. Since a too low frequency will result in unstable operation of pumps, the low limit of operating frequency for variable speed pumps is set to 20 Hz. This optimal strategy also considered the elimination of the deficit flow problem. This optimal strategy also considered the deficit flow problem. The settings that could cause the occurrence of deficit flow will be discarded. The minimum water flow rate through any side of the individual heat exchanger is set to be 20% of its design condition to avoid laminar flow.

$$T_{in,bhx} + 0.1°C \le T_{set,out,ahx} \le 9°C \tag{5.2}$$

5.2.4 Component models

A few simplified models of components are developed in this study and used by the control strategy to predict their operation performances under varying working conditions. These simplified models predict the system response accurately in a short time step because the system operation has no noticeable change in a time step. Some key parameters in the models are identified and updated online using adaptive methods to ensure the model accuracy at varying operating conditions.

Adaptive model of global AHU

The global AHU model is developed to predict the required chilled water flow of all the AHUs in the occupied zone under different cooling load conditions under given AHU inlet water temperatures. It is known that the required water flow rate of an individual AHU to satisfy a given cooling load is highly influenced by the AHU inlet water temperature, AHU inlet air temperature, air flow rate through this AHU, and the cooling load of the associated zone. In this studied HVAC system, the variable air volume (VAV) system is used to maintain the AHU outlet air temperature at a constant set-point. For an individual AHU in the VAV system with constant outlet air temperature, the required air flow rate through AHU is proportional to the cooling load of the occupied zone. In addition, the AHU inlet air temperature is equal to the indoor air temperature, which is also controlled to be maintained at a constant set-point (i.e. 23°C in the studied building). Therefore, the required water of an individual AHU in this study can be determined using cooling load of the occupied zone and AHU inlet water temperature as the variables under the fixed indoor air temperature (i.e. 23°C), as shown in Equation (5.3). According to the actual configurations of the chilled water system under study, all the AHUs in the sub-zone are identical and connected in parallel. The total required water flow of the subsystem can be described as Equation (5.4). If Q_{tot} is used to represent the total cooling load of the subsystem at a given time step, Equation (5.4) can be then re-written as Equation (5.5). The last term in Equation (5.5) represents the cooling load distribution profile for individual AHUs, which varies with time because every individual AHU changes its instantaneous cooling load with time. Replacing the last

term of Equation (5.5) with a variable factor β, Equation (5.5) then can be finally expressed as Equation (5.6).

$$M_{w,indi} = a_0 \cdot (\frac{T_{w,in}}{T_{w,des}})^{a_1} \cdot (\frac{Q_{indi}}{Q_{des}})^{a_2} \tag{5.3}$$

$$M_{w,tot} = \sum_{i=1}^{n} M_{w,indi,i} = a_0 \cdot (\frac{T_{w,in}}{T_{w,des}})^{a_1} \cdot \left[(\frac{Q_{indi,1}}{Q_{des}})^{a_2} + (\frac{Q_{indi,2}}{Q_{des}})^{a_2} + \cdots (\frac{Q_{indi,n}}{Q_{des}})^{a_2} \right] \tag{5.4}$$

$$M_{w,tot} = a_0 \cdot (\frac{T_{w,in}}{T_{w,des}})^{a_1} \cdot (\frac{Q_{tot}}{Q_{des}})^{a_2} \cdot \left[(\frac{Q_{indi,1}}{Q_{tot}})^{a_2} + (\frac{Q_{indi,2}}{Q_{tot}})^{a_2} + \cdots (\frac{Q_{indi,n}}{Q_{tot}})^{a_2} \right] \tag{5.5}$$

$$M_{w,tot} = \beta \cdot a_0 \cdot (\frac{T_{w,in}}{T_{w,des}})^{a_1} \cdot (\frac{Q_{tot}}{Q_{des}})^{a_2} \tag{5.6}$$

Since β is a variable that is associated with the cooling load distribution of each AHU, an adaptive method is utilized to predict the required total water flow rate at the next time step. At current time k, the operating parameters of the subsystem can be measured or calculated online, including the total water flow rate of the subsystem ($M_{w,tot}$), the inlet water temperature for the AHUs ($T_{w,in}$), and the total cooling load of the subsystem (Q_{tot}). The time-varying factor β at time k can be calculated using Equation (5.6). It is assumed that the cooling load distribution of each AHU keeps unchanged during short period. Therefore, the factor β calculated at time k can be used as a constant for calculating the required total water flow rate in next time step $k+1$, as shown in Figure 5.2. For online applications, three parameters (a_0, a_1, $a2$) in this model need be identified in advance by regressing the measured total water flow rate of the subsystem, the measured inlet water temperature for each

AHU, and the calculated cooling load of the subsystem.

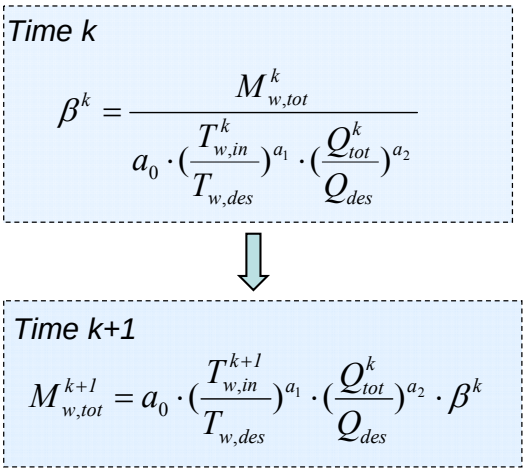

Figure 5.2 Adaptive method for calculating required water flow rate

Adaptive hydraulic model of water network after heat exchangers

The model is developed for calculating the water network pressure drop after heat exchangers. The water network after heat exchangers is used to deliver chilled water from the heat exchangers to the terminal units, including heat exchangers, pumps distributing water to the terminal units, AHUs, and the associated water pipe lines. Since different structures and configurations of the subsystem can result in different models, this model is developed according to the Zone 3 of the chilled water system under study.

Figure 5.3 shows the simplified structure of the chilled water network representing the subsystem of Zone 3 in the real system under study. It is a typical reverse return structure and each loop theoretically has the same pressure drop. The loop through the remote terminal AHU is selected to establish the predictive model. The total

pressure drop across this subsystem (i.e., the required secondary pumps head in this loop) includes the pressure drop on the fittings around pumps (i.e., pressure drop between points E and F), the pressure drop on main supply and return pipelines (including the pipeline sections of D-E, F-A_1, and B_n-C), the pressure drop on the sub-branches (i.e., A_1-A_n), and the pressure drop on the remotely terminal loop (i.e., A_n-B_n), as can be expressed as in Equation (5.7). The pressure drop of the overall heat exchanger group is overcome by the primary constant speed pumps after heat exchangers, which is not included in this model.

$$PD_{tot,ahx} = PD_{pf,tot,ahx} + PD_{pipe,tot,ahx} + PD_{term} \tag{5.7}$$

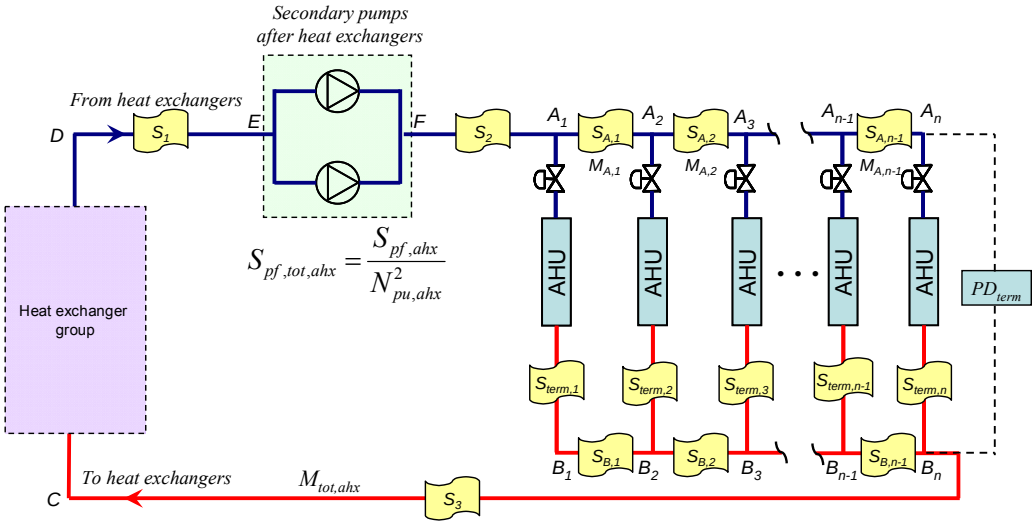

Figure 5.3 Illustration of the hydraulic model of water network after heat exchangers

The pressure drop on the fittings around pumps can be calculated using Equation (5.8), which is proportional to the water resistance and the square of water flow rate and is inversely proportional to operating number squared. The pressure drop on the pipelines (including pipeline sections of D-E, F-A_1, B_n-C, and A_1-A_n) can be

mathematically described as in Equation (5.9), which can be further re-written as Equation (5.10) by transferring the water flow rate in each branches into the function of the total subsystem water flow rate ($M_{,tot,ahx}$). The first item on the right-hand side of Equation (5.10) can be considered as a single factor ($S_{pipe,tot,ahx}$) shown in Equation (5.11), which represents the fictitious total water resistance of all the pipelines of the loop under study. Obviously, $S_{pipe,tot,ahx}$ is a variable that reflects the dynamic water flow distribution of each AHU. It will change when the water flow rate of any individual AHU varies. But in a relatively short period, it can be assumed that the cooling load handled by each AHU keeps unchanged, which means that the ratio of required water flow rate of each AHU to the total subsystem water flow rate approximately maintains unchanged. Therefore, an adaptive method can be utilized to determine the factor $S_{pipe,tot,ahx}$ at current time *k,* which is used for predicting the pressure drop on the all pipelines at next time *k+1*, as shown in Figure 5.4. At current time *k*, the factor $S_{pipe,tot,ahx}$ can be calculated using the measured total water flow rate of the subsystem and the calculated total pressure drop of all the pipelines in the loop, which is equal to the difference between the measured pump head and the sum of the calculated pressure drops of pump fittings and the measured pressure drop of the terminal loop. The factor $S_{pipe,tot,ahx}$ determined at time k is then used for predicting the pressure drop across all the pipelines in the loop at time *k+1*.

$$PD_{pf,tot,ahx} = \frac{S_{pf,ahx}}{N^2_{pu,\mathrm{sec},ahx}} M^2_{tot,ahx} \tag{5.8}$$

$$PD_{pipe,tot,ahx} = (S_1 + S_2 + S_3) M^2_{tot,ahx} + S_{A,1} M^2_{A,1} + S_{A,2} M^2_{A,2} + \cdots + S_{A,n-1} M^2_{A,n-1} \tag{5.9}$$

$$PD_{pipe,tot,ahx} = (S_1 + S_2 + S_3 + S_{A,1}\frac{M_{A,1}^2}{M_{tot,ahx}^2} + S_{A,2}\frac{M_{A,2}^2}{M_{tot,ahx}^2} + \cdots + S_{A,n-1}\frac{M_{A,n-1}^2}{M_{tot,ahx}^2})M_{tot,ahx}^2 \quad (5.10)$$

$$S_{pipe,tot,ahx} = S_1 + S_2 + S_3 + S_{A,1}\frac{M_{A,1}^2}{M_{tot,ahx}^2} + S_{A,2}\frac{M_{A,2}^2}{M_{tot,ahx}^2} + \cdots + S_{A,n-1}\frac{M_{A,n-1}^2}{M_{tot,ahx}^2} \quad (5.11)$$

Time k

$$S_{pipe,tot}^k = \frac{H_{pu,sec,ahx}^k - \frac{S_{pf,ahx}}{N_{pu,sec,ahx}^2}(M_{tot,ahx}^k)^2}{(M_{tot,ahx}^k)^2}$$

⇩

Time k+1

$$PD_{pipe,tot}^{k+1} = S_{pipe,tot}^k (M_{tot,ahx}^{k+1})^2$$

Figure 5.4 Adaptive method for calculating pressure drop of all pipelines in the network

For online applications, there are only one parameter (i.e., $S_{pf,ahx}$) which needs to be identified in this model. $S_{pf,ahx}$ can be considered as a constant that can be determined by measuring the pressure drop on single secondary pump after heat exchangers (i.e., pressure drop between points E and F in Figure 5.3) and its water flow rate. The fictitious water resistance across the overall pipelines in the loop ($S_{pipe,tot,ahx}$) needs not to be identified in advance because it is a variable and varies under different working conditions. Instead, $S_{pipe,tot,ahx}$ can be automatically calculated in the model at every time step.

Adaptive model of pressure drop on the remote terminal loop

The model of pressure drop on the remote terminal loop is proposed to predict the pressure drop on the remote AHU loop under different AHU inlet water temperature.

In this study, the pump speed is controlled to maintain the pressure drop (PD_{term}) of the remote terminal loop at a variable set-point to keep its valve always nearly fully open. PD_{term} (i.e. the pressure drop on A_n-B_n in Figure 5.3) is determined by the water resistance of this loop and the water flow rate through AHU, as shown in Equation (5.12). Equation (5.12) can be re-written as Equation (5.13) by introducing the total subsystem water flow rate. The water resistance of the remote terminal loop (i.e. S_{term}) consists of the water resistance of the cooling coil, the modulating valve, and the associated pipeline. S_{term} can be considered as a constant over a short period because the valve of this loop basically keeps nearly fully open in the variable pressure drop pump control scheme. Similarly, the ratio of the water flow rate through the AHU of this loop (M_{term}) to the total water flow rate ($M_{tot,ahx}$) also can be considered as a constant over a short period because the cooling load handled by each AHU over a short period can be assumed approximately unchanged. The two items in the bracket of Equation (5.13) can be integrated into one factor ($S_{term,fic}$) that represents the fictitious water resistance of the remote terminal loop. $S_{term,fic}$ is a variable for a long time period, and can be considered as a constant over a short period. An adaptive method is used to calculate $S_{term,fic}$ at current time k and use it to predict the pressure drop on the remote terminal loop at next time step $k+1$, as described in Figure 5.5. At time k, $S_{term,fic}$ can be determined using the measured pressure drop of the remote terminal loop by a pressure meter and the measured total subsystem water flow rate. The pressure drop at time $k+1$ then can be determined when the total subsystem water flow rate is known.

$$PD_{term} = S_{term} M_{term}^2 \tag{5.12}$$

$$PD_{term} = (S_{term} \frac{M_{term}^2}{M_{tot,ahx}^2}) M_{tot,ahx}^2 = S_{term,fic} M_{tot,ahx}^2 \tag{5.13}$$

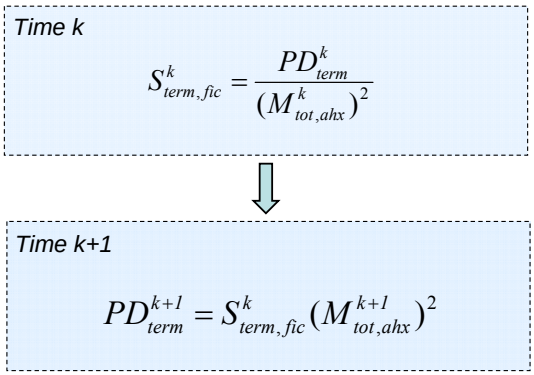

Figure 5.5 Adaptive method for calculating pressure drop of the remote terminal loop

Hydraulic model of water network before heat exchangers

The hydraulic model of water network before heat exchangers is proposed to predict the pressure drop of the whole water loop before heat exchangers when the total water flow rate before heat exchangers is given. The water networks before heat exchangers deliver chilled water from the cooling source to the heat exchangers, including pumps distributing water to heat exchangers, heat exchangers, and the associated water pipelines, are illustrated in Figure 5.6. Obviously, the structure of the water network before heat exchangers can be regarded as the simplification of that after heat exchangers presented earlier. Therefore, the model for predicting the water pressure drop before heat exchangers is similar to the model after heat exchangers.

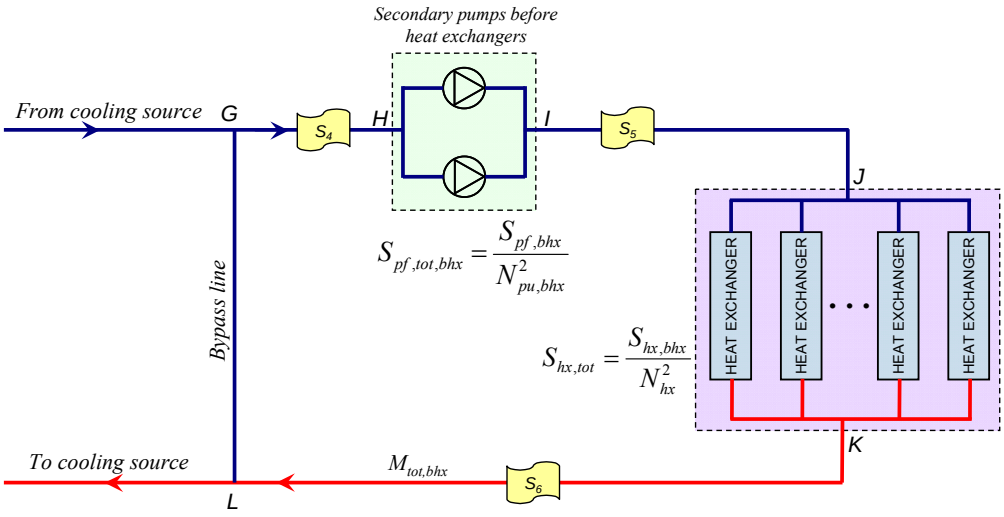

Figure 5.6 Illustration of the hydraulic model of water network before heat exchangers

As shown in Figure 5.6, the total pressure drop of the water network before heat exchangers consists of the pressure drop of the fittings associated to pumps (i.e., the pressure drop between points H and I), the pressure drop of heat exchangers (i.e., the pressure drop between points J and K), and the pressure drop of the associated pipelines (i.e., the pipelines of GH, IJ, and KL), which is mathematically described in Equation (5.14). The pressure drop of the heat exchangers, pump fittings and pipelines can be described as in Equation (5.15), Equation (5.16), and Equation (5.17) respectively. Equation (5.17) can be re-written in Equation (5.18) when considering the sum of water resistance of each pipeline as a single fictitious parameter (i.e., $S_{pipe,fic,bhx}$).

$$PD_{tot,bhx} = PD_{hx,tot,bhx} + PD_{pf,tot,bhx} + PD_{pipe,tot,bhx} \tag{5.14}$$

$$PD_{hx,tot,bhx} = \frac{S_{hx,bhx}}{N_{hx}^2} M_{tot,bhx}^2 \tag{5.15}$$

$$PD_{pf,tot,bhx} = \frac{S_{pf,bhx}}{N^2_{pu,\sec,bhx}} M^2_{tot,bhx} \tag{5.16}$$

$$PD_{pipe,tot,ahx} = (S_4 + S_5 + S_6) M^2_{tot,bhx} \tag{5.17}$$

$$PD_{pipe,to,ahx} = S_{pipe,fic,bhx} M^2_{tot,bhx} \tag{5.18}$$

For online applications, there are three parameters (i.e., $S_{hx,bhx}$, $S_{pf,tot,bhx}$, and $S_{pipe,fic,bhx}$) required to be identified in this model. The three parameters basically are considered as constants that can be determined based on commissioning.

Simplified model of pumps

The model of pumps is used to predict the power of pumps when the total water flow rate through pumps is known, which is modified based on existing studies [Bahnfleth et al. 2001 and 2006]. Some polynomial approximations are employed to mathematically describe the pumps performance based on the performance data provided by manufacturers. Equation (5.19) describes the pumps head (H_{pu}) as a function of the water flow rate (M_w) and the operating frequency (*Fre*), which can be used to determine the operating frequency of pumps if pumps head and water flow rate are given. Equation (5.20) is used to calculate the power input to a pump-motor-VFD set with given pumps efficiency (η_{pu}), motor efficiency (η_m), and variable frequency drive efficiency (η_v). The efficiencies of pump, motor and VFD can be described as in Equation (5.21), Equation (5.22), and Equation (5.23) respectively. For online applications, the coefficients in the models (b_0–b_2, c_0–c_2,

d_0–d_1, e_0–e_3) can be identified based on the pump performance data or curves and efficiency curves of pump, motor and VFD provided by the manufactures.

$$H_{pu} = b_0 M_w^2 + b_1 M_w Fre + b_2 Fre^2 \tag{5.19}$$

$$P_{pu} = \frac{M_w H_{pu} SG}{102 \eta_{pu} \eta_{vfd} \eta_m} \tag{5.20}$$

$$\eta_{pu} = c_0 + c_1 M_w Fre + c_2 M_w^2 Fre^2 \tag{5.21}$$

$$\eta_m = d_0 (1 - e^{d_1 Fre}) \tag{5.22}$$

$$\eta_{vfd} = e_0 + e_1 Fre + e_2 Fre^2 + e_3 Fre^3 \tag{5.23}$$

Simplified model of heat exchangers

The model of heat exchangers is proposed to predict the required water flow rate before heat exchangers (M_c) in this study when the water flow rate after heat exchangers (M_h) is given, which uses the *ε-NTU* method based on the basic principle of thermodynamics. This model will firstly guess an initial value for the water flow rate before heat exchangers to calculate the overall heat transfer coefficient (UA) using Equation (5.24). The overall number of transfer units (NTU) is then defined using Equation (5.25). The heat transfer effectiveness (ε) for the counter flow heat exchanger can be expressed as in Equation (5.26). The inlet water temperature before heat exchangers is calculated based on the previously guessed water flow rate before heat exchangers using Equation (5.27), which will be compared with the measured one until the difference between the two values within the predefined tolerance. The

required water flow rate before heat exchangers is thus determined when the cooling load of the subsystem, the inlet water temperature after heat exchangers and the water flow rate after heat exchangers are given. For online applications, two parameters (i.e., *m, n*) in Equation (5.24) need to be identified by regression method.

$$UA = UA_{des} \cdot (\frac{M_c}{M_{c,des}})^m \cdot (\frac{M_h}{M_{h,des}})^n \tag{5.24}$$

$$NTU = \frac{UA}{C_{\min}} \tag{5.25}$$

$$\varepsilon = \frac{1 - \exp(-NTU(1 - \frac{C_{\min}}{C_{\max}}))}{1 - \frac{C_{\min}}{C_{\max}} \exp(-NTU(1 - \frac{C_{\min}}{C_{\max}})} \tag{5.26}$$

$$T_{c,w,in} = T_{h,w,in} - \frac{Q}{\varepsilon \cdot C_{\min}} \tag{5.27}$$

5.2.5 Local control strategies

The local control strategies utilized in the optimal strategy mainly consist of the sequence control and the speed control for chilled water pumps associated with heat exchangers.

Sequence control for pumps

The sequence control strategy determines the operating number of pumps on both sides of heat exchangers. For secondary variable speed pumps, a conventional strategy is utilized. Using this strategy, an additional pump is switched on when the

frequencies of operating pumps exceed 90% (corresponding to 45Hz) of their full capacity. One of the operating pumps is switched off when the frequencies of the operating pumps are lower than 60% (corresponding to 30Hz) of the full capacity. For primary constant speed pumps after heat exchangers, their operating number is the same as the operating number of the heat exchangers.

Speed control for pumps before heat exchangers

The secondary variable speed pumps before heat exchangers distribute the chilled water from the cooling source to the heat exchangers. The pumps speed is controlled to maintain the average outlet water temperature after heat exchangers at its set-point. A modified cascade control is employed that involves two loops: inner loop and outer loop, as shown in Figure 5.7. In the outer loop, a temperature controller is utilized to generate a differential pressure set-point for the inner loop by comparing the measured water temperature after heat exchangers with the predefined temperature set-point. In the inner loop, a differential pressure controller is employed to control the pump speed before heat exchangers by comparing the measured differential pressure between the main supply and return water pipe before the heat exchanger group with its set-point produced in the outer loop. The temperature set-point after heat exchangers will be optimized in this study to achieve energy efficient operation, while the differential pressure set-point before heat exchangers is a variable in the process.

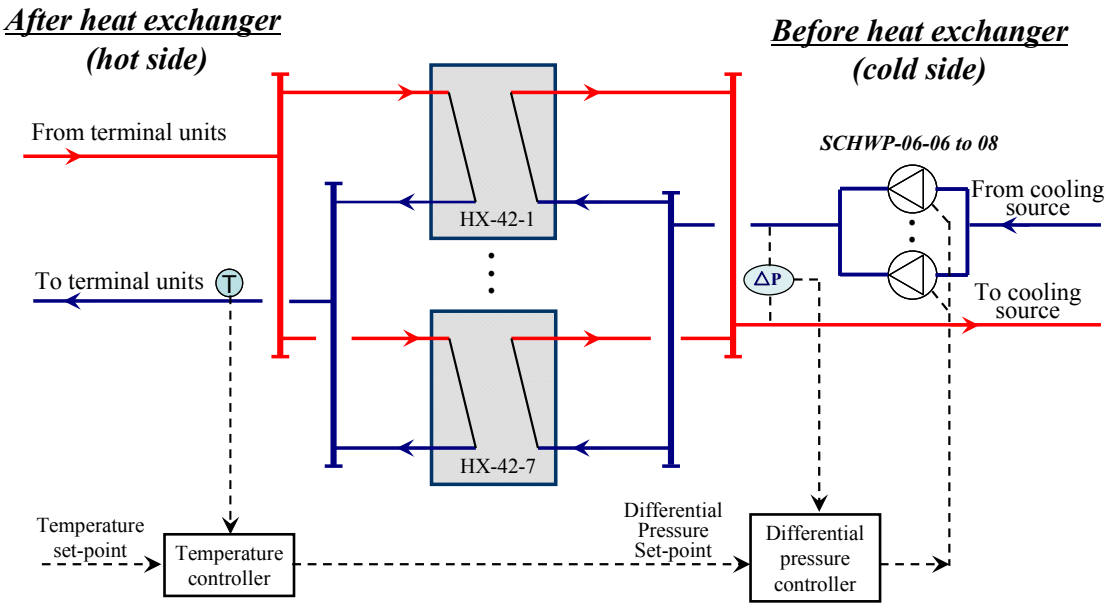

Figure 5.7 The optimal speed control strategy for pumps before heat exchangers

Speed control for pumps after heat exchangers

The secondary variable speed pumps after heat exchangers distribute the chilled water from the heat exchangers to the terminal units. The pump speed is controlled to maintain the differential pressure of the critical loop at its set-point. This pressure set-point is a variable, which is reset to keep the modulating valve of the critical loop nearly fully open to reduce the required pump head while still satisfying the needs of critical zones for having the water flow rate required.

5.2.6 The application procedures

For online applications, the proposed optimal control strategy is to search the optimal control settings including the optimal set-point of outlet water temperature after heat exchangers, the required operating number of heat exchangers and pumps. The detailed optimization procedures can be described as follows (also illustrated

earlier in Figure 5.1).

(1) Check the control signals and measurements using a filter;

(2) Define the search range for the set-point of outlet water temperature after heat exchangers ($T_{set,out,ahx}$) based on the given inlet water temperature before heat exchangers, and define the search range for the required operating number of heat exchangers;

(3) Compute the required total chilled water of all the terminal units after heat exchangers using the global AHU model under the given $T_{set,out,ahx}$;

(4) Compute the pressure drop of the remote loop after heat exchangers and predict the total pressure drop of the water network and the required operating number of pumps after heat exchangers based on the given total chilled water flow rate after heat exchangers. Compute the power consumption of secondary variable speed pumps after heat exchangers using the pumps model;

(5) Compute the required water flow rate before heat exchangers using heat exchanger model at the given total water flow rate and the outlet water temperature after heat exchangers. Compute the total pressure drop of the water network and the required operating number of pumps before heat exchangers, and the power consumption of secondary variable speed pumps before heat exchangers;

(6) Compute the power consumption of primary constant speed pumps before heat exchangers using the pump model;

(7) Determine the optimal settings (i.e. $T_{set,out,ahx}$) and the operating number of heat

exchangers and pumps) that can minimize the total power consumption of the pumps on both sides of heat exchangers by using the cost estimation and the optimization algorithms.

5.3 Test platform

A simulation platform representing the complex chilled water system is developed to validate and evaluate the proposed optimal control strategy. Only Zone 3 and two chillers of the super high-rise building under study are included in the simulation platform as shown in Figure 5.8. This is a typical primary-secondary chilled water system, in which two water cooled centrifugal chillers with rated cooling capacity of 7230 kW are installed to generate the chilled water of 5.5°C under design condition. Each chiller is associated with a constant speed primary pump. In the secondary loop, heat exchangers are used to transfer the cooling energy from the chillers to the terminal units. After each heat exchanger, a primary constant speed pump is installed to ensure the constant flow through each heat exchanger. The secondary pumps in this platform are divided in to two groups. One group has three identical secondary pumps distributing chilled water from the chillers to the heat exchangers (i.e., before heat exchangers). The other group also has three pumps distributing chilled water from the heat exchangers to the terminal units (i.e., after heat exchangers). All the secondary pumps are equipped with VFDs. AHUs are implemented in the air-conditioning system to provide cooled air for indoor thermal comfortable control. The valves of AHUs are controlled to maintain the supply air temperature at its

set-point (i.e., 13°C). The AHU fans are also equipped with VFDs to vary supply air flow rate and the VAV boxes are used to maintain the indoor air temperature at a fixed set-point (i.e., 23°C). The models of chillers, cooling towers, pumps, and cooling coils are all detailed physical models that can represent the real chilled water system. The entire simulation platform is developed on TRNSYS 16. The weather condition used is the data of the typical year in Hong Kong.

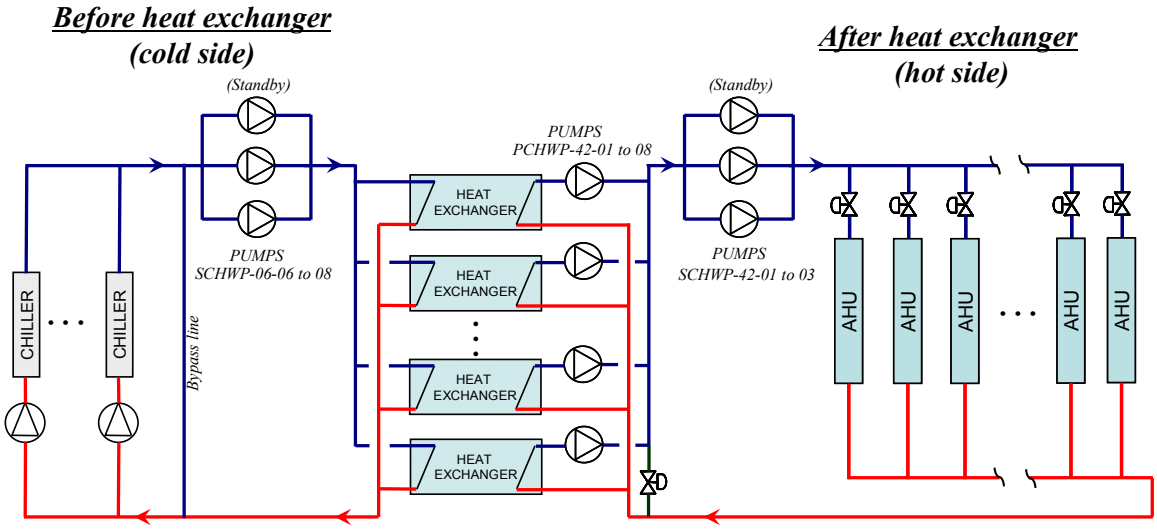

Figure 5.8 The simplified schematic of chilled water system of the simulation platform

5.4 Performance tests and evaluation of the optimal control strategy

5.4.1 Accuracy of the optimal control strategy

The accuracy of the proposed component models directly affects the reliability and accuracy of the entire optimal control strategy. This section validates each proposed model in the developed simulation platform first. The operational performance of the optimal control strategy is then tested to verify whether it can find the optimal

settings under different working conditions.

The online adaptive models of components

The "measured" data from the tests on the simulated virtual platform were used to train the models. Figures 5.9 - 5.13 show the results by comparing the "measured" values collected from the simulated virtual platform with those predicted by the online models. The solid points represent the "measured" values under the current working condition, while the hollow points are the predicted values under the same condition when using different set-points ($T_{set,out,ahx}$) of outlet water temperature after heat exchangers. It can be observed that the relative differences between the "measured" values and model outputs in most cases are less than 10%, showing that the online adaptive models have acceptable accuracy in online application. It is noted that the predicted results will be more accurate when the predicted value is approaching the optimal value. It is due to the fact that the optimization is done progressively and continuously, and the optimal value at the new condition will be not far from the optimal value at the previous condition.

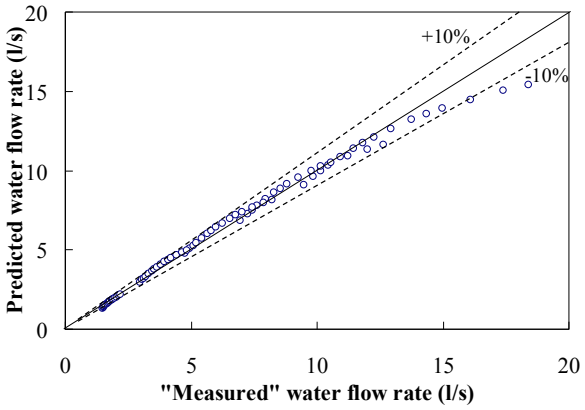

Figure 5.9 Validation results of the individual AHU model

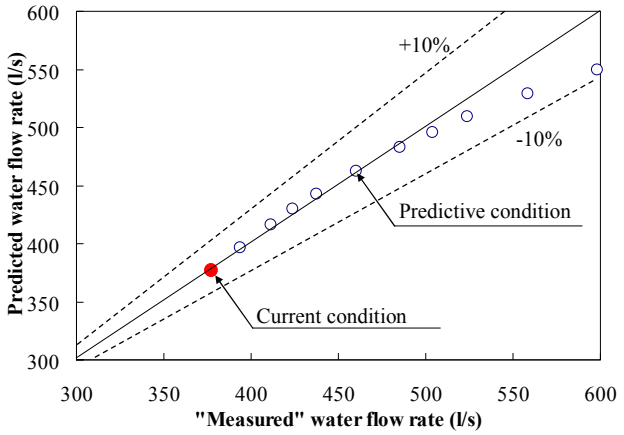

Figure 5.10 Validation results of the global AHU model

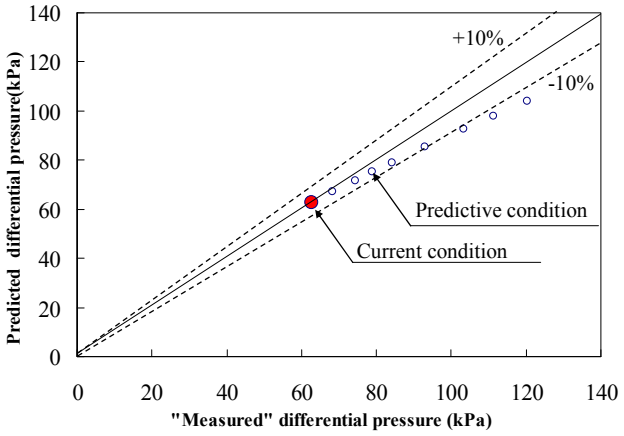

Figure 5.11 Validation results of the model of pressure drop on the remote terminal loop

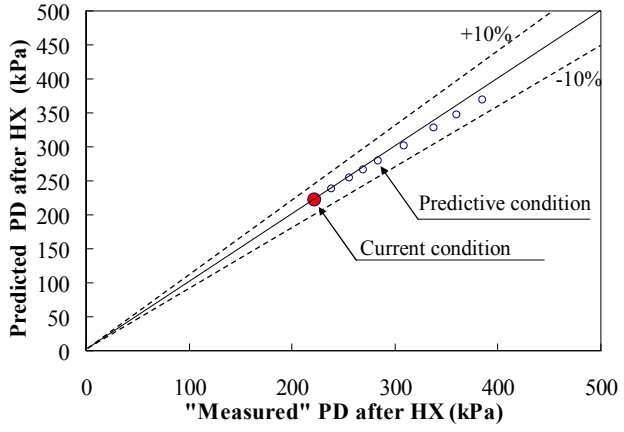

Figure 5.12 Validation results of the model of water network after heat exchangers

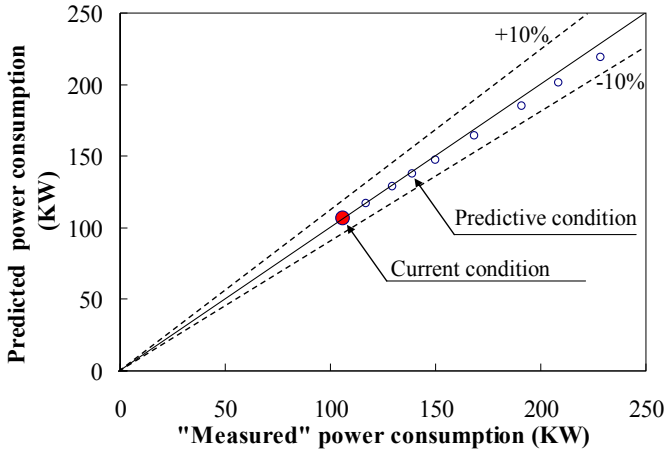

Figure 5.13 Validation results of pumps model

The optimal control strategy

In order to validate the accuracy of the proposed optimal control strategy, tests in ideal conditions were conducted on the simulation platform by resetting different $T_{set,out,ahx}$ under the same cooling load condition. The set-point associated with the least power consumption of pumps on both sides of heat exchangers was selected as the ideal test result, which is used as the benchmark for comparison with the predicted result by the proposed strategy. Three typical working conditions were selected to represent the chilled water system working under Spring, Mild-Summer and Sunny-Summer days. The increment of resetting $T_{set,out,ahx}$ used in the two methods was 0.1°C and the chiller supply water temperature was fixed at 5.5°C.

Table 5.1 shows the test conditions of the three typical days and the optimization results resulted from the proposed method (predicted values) and the ideal values ("measured" values) respectively. Obviously, the proposed optimal control strategy

can find the same optimal values of $T_{set,out,ahx}$ as those generated by the ideal tests. The maximum relative difference of the total pump power consumptions between the two methods was about 0.18% only. The operating number of pumps and heat exchangers determined by the proposed method also agreed well with those of the ideal tests.

Table 5.1 Comparison between results using the proposed method and the ideal approach

Items	Seasons					
	Spring		Mild-Summer		Sunny-Summer	
Typical working conditions						
Cooling load (kW)	4938.09		7825.85		10180.13	
Chiller operating number	1.00		2.00		2.00	
Chiller supply water temperature (°C)	5.50		5.50		5.50	
Items	Methods					
	Proposed (predicted)	Ideal tests ("measured")	Proposed (predicted)	Ideal tests ("measured")	Proposed (predicted)	Ideal tests ("measured")
Optimization results						
Optimal $T_{out,ahx}$	6.90	6.90	6.60	6.60	6.60	6.60
$P_{pu,sec,bhx}$	35.54	35.87	57.13	57.67	93.42	94.62
$P_{pu,sec,ahx}$	55.09	54.51	97.95	97.62	180.37	179.76
$P_{pu,pri,bhx}$	44.70	44.70	89.40	89.40	134.10	134.10
$P_{pu,sec,bhx}$+ $P_{pu,sec,ahx}$ + $P_{pu,pri,bhx}$	135.33	135.09	244.48	244.69	407.89	408.48
$N_{pu,sec,bhx}$	1	1	2	2	2	2
$N_{pu,sec,ahx}$	1	1	2	2	2	4
$N_{pu,pri,bhx}$	1	1	2	2	3	3
N_{hx}	1	1	2	2	3	3

Figure 5.14 presents the details in determining $T_{set,out,ahx}$ using the proposed method in the Mild-Summer day when the operating number of heat exchangers remained unchanged. It can be found that the power of secondary pumps after heat exchangers increased with the increase of the outlet water temperature after heat exchangers. On

the contrary, the lower the outlet water temperature after heat exchangers was, the more energy the secondary pumps before heat exchangers was consumed. It also can be observed that the power of the primary pumps after heat exchangers remained unchanged because the operating number of heat exchangers was fixed in this case. Therefore, the minimum total power of pumps occurred at the point where the rate of energy decrease in the secondary pumps before heat exchangers was equal to the rate of energy increase in the secondary pumps after heat exchangers. The set-point with the minimum total pumps energy consumption was selected as the optimal set-point, which varied with working condition.

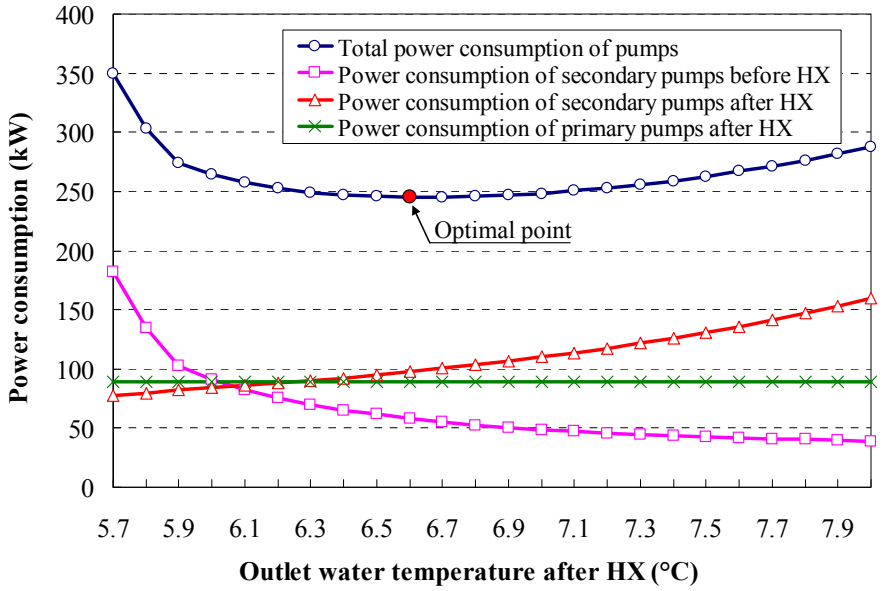

Figure 5.14 The optimal set-point of the outlet water temperature after heat exchangers in the Mild-Summer case

For a given outlet water temperature ($T_{out,ahx}$) after heat exchangers, there is a required minimum operating number of heat exchangers that can provide adequate transfer heat areas to ensure $T_{out,ahx}$ to be controlled at the set-point. The operating

number of heat exchangers that is larger than this minimum value also satisfies the requirements, but different operating number of heat exchangers will result in different pumps energy consumptions although $T_{out,ahx}$ remains unchanged. Table 5.2 shows the searching process of the best operating number of the heat exchangers for a given $T_{out,ahx}$ (i.e. 6.6°C) in the mild-summer case. In this case, although the operation of more heat exchangers can reduce the energy consumption of secondary pumps before heat exchangers, more heat exchangers also require more primary constant speed pumps after heat exchangers that consumed additional energy that exceeds the energy saving of the pumps before heat exchangers. The proposed optimal control strategy successfully searched the best operating number of the heat exchangers that resulted in the minimal total energy consumptions of pumps associated with the heat exchangers.

Table 5.2 The operating number of heat exchangers under a given outlet water temperature after heat exchangers ($T_{out,ahx}$=6.6°C)

N_{hx}	$P_{pu,sec,bhx}$(kW)	$P_{pu,pri,ahx}$(kW)	$P_{pu,sec,ahx}$(kW)	Total(kW)
2	57.67	89.40	97.62	244.69
3	32.39	134.10	97.62	264.12
4	24.81	178.80	97.62	301.23
5	21.45	223.50	97.62	342.58

5.4.2 Optimal control strategy energy performance tests

The proposed optimal control strategy (Strategy #3) was evaluated in energy performance by comparing it with two conventional control strategies (Strategy #1, #2) separately in the same simulated virtual platform shown in Section 5.3. The detailed description of the control strategies are listed in Table 5.3. It is noted that the

set-point ($T_{set,out,ahx}$) used by both Strategy #1 and Strategy #2 was reset with a fixed temperature approach (i.e., 0.8°C) above the chiller supply water temperature, and the required operating number of heat exchangers was reset to be twice as many as the operating number of secondary pumps after heat exchangers when using the fixed approach set-point. Strategy #1 employs a conventional speed control strategy of pumps before heat exchangers to maintain a fixed differential pressure set-point before the entire heat exchangers group by adjusting the openings of modulating valves before heat exchangers, as shown in Figure 5.15. If $T_{set,out,ahx}$ cannot be achieved while the valves fully open, an additional heat exchangers will be switched on. Strategy #2 and #3 adopted the optimized varying differential pressure set-point generated by the proposed optimal control strategy to maintain the modulating valves before heat exchangers nearly fully open, as described in Section 5.2.5. When using the three control strategies, the chiller supply water temperature was fixed at 5.5°C. Detailed description on the sequence control strategies of secondary pumps is given in Section 5.2.5. Three typical days (working period between 8:00am and 18:00pm) were selected to test this system in typical Spring, Mild-Summer and Sunny-Summer conditions under the control of the three strategies respectively. The system energy performance by using Strategy #1 is used as the benchmark for comparison. It is worthy of noticing that the energy consumption of chillers were identical at each test case using the three control strategies.

Table 5.3 Description of the pump control strategies

No.	Strategies	Description
1	Strategy #1	Using the fixed temperature approach for resetting $T_{set,out,ahx}$ and the fixed differential pressure set-point for speed control of pumps before heat exchangers
2	Strategy #2	Using the fixed temperature approach for resetting $T_{set,out,ahx}$ and the optimal differential pressure set-point for speed control of pumps before heat exchangers
3	Strategy #3	Using the proposed optimal $T_{set,out,ahx}$ and the optimal differential pressure set-point for speed control of pumps before heat exchangers

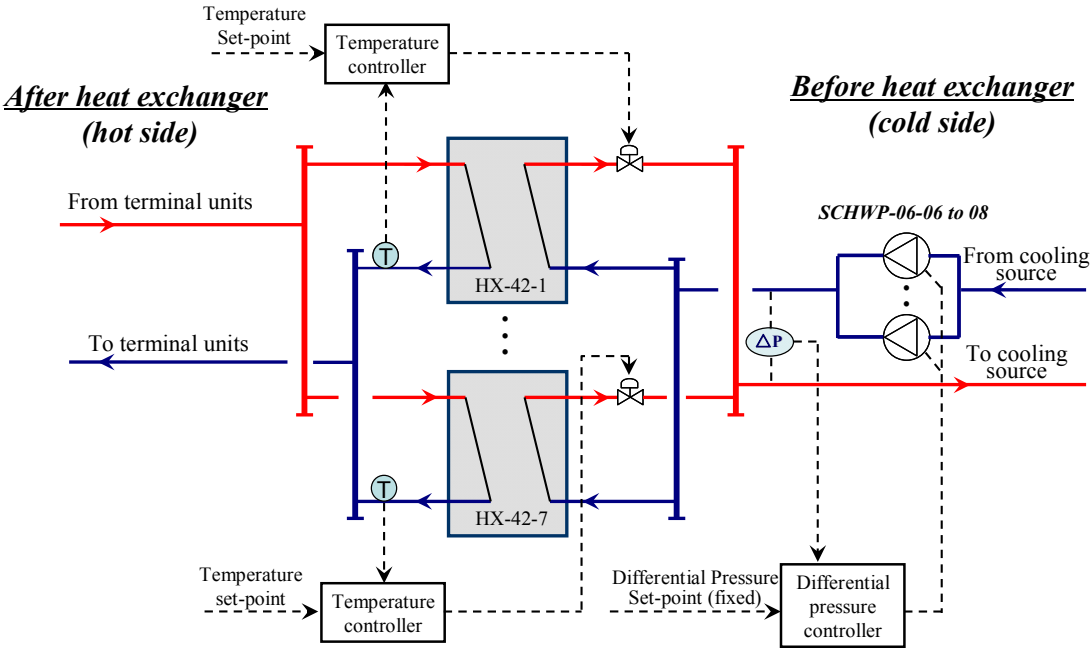

Figure 5.15 The conventional speed control strategy for pumps before heat exchangers

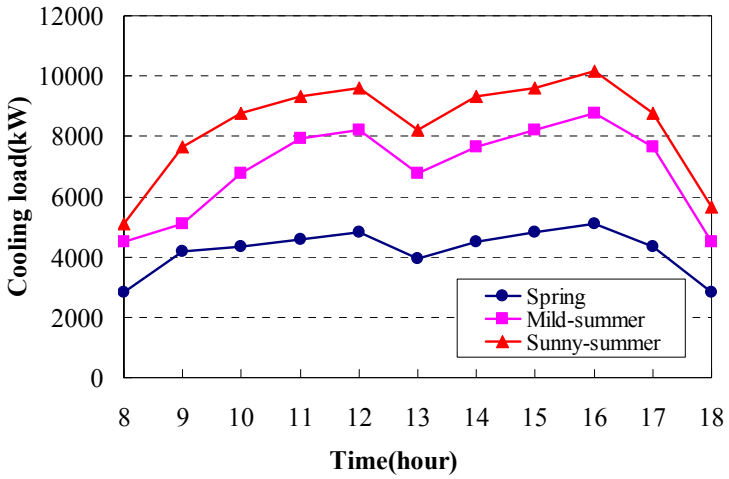

Figure 5.16 Cooling load profiles in three typical days

Figure 5.17–5.19 show the total energy consumption of pumps on both sides of the heat exchangers when using three control strategies in the typical Spring day, Mild-Summer day and Sunny-Summer day, including the secondary pumps before heat exchangers, the primary pumps and secondary pumps after heat exchangers. It is obvious that significant energy of pumps was saved when using the proposed optimal control strategy (Strategy #3). The maximum hourly energy savings by using Strategy #3 were about 39.50kW, 85.46kW, and 42.98kW respectively in the typical Spring, Mild-Summer and Sunny-Summer days when compared with that using the Strategy #1. It also can be observed that the total energy consumptions of pumps under some working conditions were very similar when using the three control strategies. The reason was that the three control strategies used the similar $T_{set,out,ahx}$ and the operating number of heat exchangers under these working conditions.

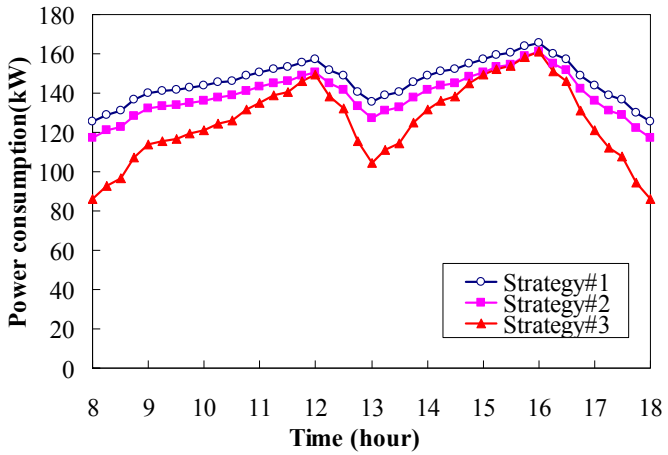

Figure 5.17 Power consumptions of secondary pumps in Spring test case

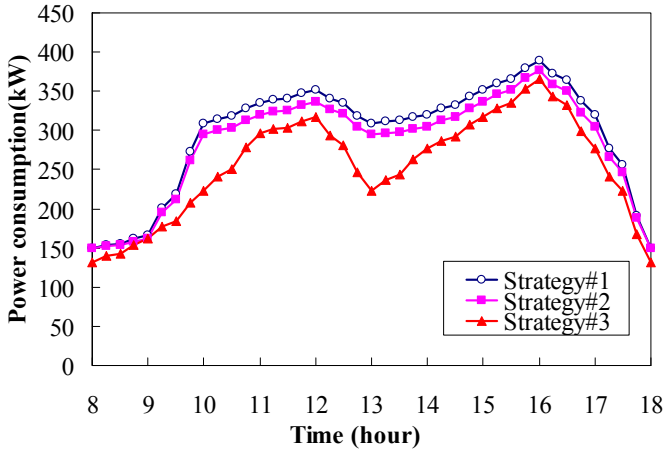

Figure 5.18 Power consumptions of secondary pumps in Mild-Summer test case

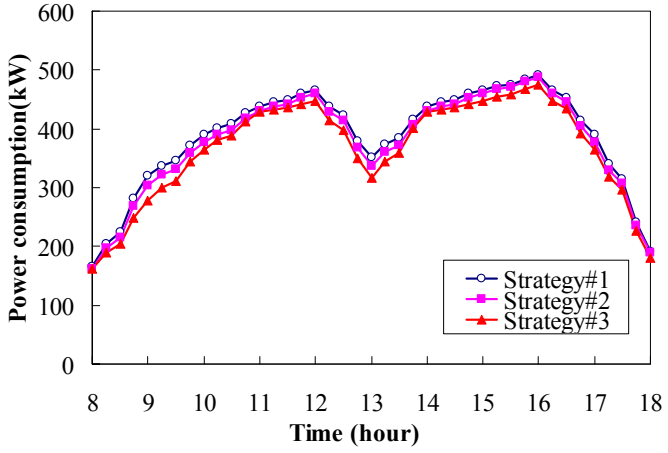

Figure 5.19 Power consumptions of secondary pumps in Sunny-Summer test case

Table 5.4 summaries the daily energy consumption of pumps associated with heat exchangers using three different control strategies in the three typical days. Compared to Strategy #1 (fixed temperature approach set-point/fixed differential pressure set-point), the proposed optimal control strategy (Strategy #3) saved about 234kWh (14.69%), 427.48kWh (13.58%), and 216.18kWh (5.26%) of the pumps energy for the typical spring day, mild-summer day and sunny-summer day respectively. The energy savings were mainly contributed by using the optimal outlet water temperature set-point and the optimized variable differential pressure set-point.

It can be found in Table 5.4 that Strategy #2 (using the optimized variable differential pressure set-point for pumps control) saved significant energy of pumps when compared with Strategy #1 (using the fixed differential pressure set-point). About 79.98kWh (5.02%), 119.98kWh (3.81%) and 94.68kWh (2.30%) of the total energy of pumps were saved by using Strategy #2 when compared with Strategy #1 in the three typical days respectively. The energy savings by Strategy #2 were mainly contributed from the implementation of the optimal differential pressure set-point that helps in reducing the energy consumption of secondary pumps before heat exchangers. The energy consumptions of primary pumps and secondary pumps after heat exchangers using Strategy #2 were almost the same as that using Strategy #1.

Table 5.4 Daily energy consumptions of pumps in three typical days

Strategies	$P_{pu,sec,bhx}$	$P_{pu,pri,ahx}$	$P_{pu,sec,ahx}$	Total	$P_{pu,sec,bhx}$ saving		$P_{pu,pri,ahx}$ saving		$P_{pu,sec,ahx}$ saving		Total saving	
	(kWh)	(kWh)	(kWh)	(kWh)	(kWh)	(%)	(kWh)	(%)	(kWh)	(%)	(kWh)	(%)
Spring												
Strategy #1	248.29	983.40	361.70	1593.39	-	-	-	-	-	-	-	-
Strategy #2	166.49	983.40	363.52	1513.41	81.80	32.95	0.0	0.00	-1.83	-0.50	79.98	5.02
Strategy #3	319.08	536.40	503.91	1359.39	-70.79	-28.51	447.0	45.45	-142.21	-39.32	234.00	14.69
Mild-summer												
Strategy #1	582.70	1698.60	865.76	3147.06	-	-	-	-	-	-	-	-
Strategy #2	461.04	1698.60	867.44	3027.08	121.65	20.88	0.0	0.00	-1.68	-0.19	119.98	3.81
Strategy #3	561.02	1162.20	996.36	2719.58	21.68	3.72	536.4	31.58	-130.59	-15.08	427.48	13.58
Sunny-summer												
Strategy #1	891.21	1788.00	1429.56	4108.77	-	-	-	-	-	-	-	-
Strategy #2	795.17	1788.00	1430.92	4014.09	96.04	10.78	0.0	0.00	-1.36	-0.10	94.68	2.30
Strategy #3	866.00	1430.40	1596.19	3892.59	25.21	2.83	357.6	20.00	-166.63	-11.66	216.18	5.26

Compared with Strategy #2, the proposed optimal strategy (Strategy #3) saved around 154.02kWh (9.67%), 307.5kWh (9.77%) and 121.5kWh (2.96%) of the total pumps energy in the three typical days respectively. The energy savings were obtained from applying the optimal $T_{set,out,ahx}$ and the operating number of heat exchangers. Figure 5.20 presents the energy savings of different pump groups using Strategy #3 when compared with Strategy #2. It is obvious that the energy savings by using Strategy #3 over Strategy #2 mainly obtained from the energy reduction of the primary pumps after heat exchangers. On the contrary, the secondary pumps before and after heat exchangers using Strategy #3 consumed a little more energy than Strategy #2. This was due to that the proposed optimal strategy used a higher $T_{set,out,ahx}$ and less operating number of heat exchangers under some working conditions to minimize the total energy consumptions of all the pumps on both sides of heat exchangers. Table 5.5 presents the detailed hourly $T_{set,out,ahx}$ and the operating number of heat exchangers of Strategy #2 and #3 in the typical Mild-Summer day. It demonstrates that a higher $T_{set,out,ahx}$ along with less operating heat exchangers could be more energy efficient while still satisfying the indoor thermal comfort requirements.

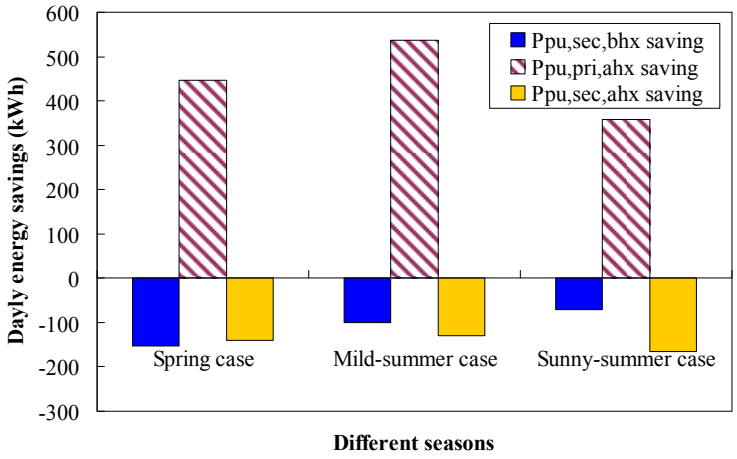

Figure 5.20 Daily energy savings of three pump groups when using Strategy #3 (Compared with that when using Strategy #2)

Table 5.5 Set-points of outlet water temperature after heat exchangers and operating number of heat exchangers in the typical Mild-Summer day

Time (hour)	8	9	10	11	12	13	14	15	16	17	18
$T_{out,ahx}$ (Strategy#2)	6.3	6.3	6.3	6.3	6.3	6.3	6.3	6.3	6.3	6.3	6.3
$T_{out,ahx}$ (Strategy#3)	6.9	6.3	6.5	6.4	6.4	6.5	6.3	6.4	6.5	6.3	6.9
N_{hx} (Strategy#2)	2	2	4	4	4	4	4	4	4	4	2
N_{hx} (Strategy#3)	1	2	2	3	3	2	3	3	3	3	1

In Table 5.4, it can also be observed that more energy of pumps can be saved when using the proposed optimal strategy (Strategy #3) over the conventional strategy (Strategy #1) in the Spring case compared with that in the other two typical days. The reason was that the use of Strategy #1 resulted in lower valve openings of AHUs and more operating number of primary constant pumps after heat exchangers when the cooling load was low in the typical Spring day.

It is worth noticing that the above optimization results using Strategy #3 was achieved under a constant chiller supply water temperature (i.e., 5.5°C). The optimizations results using Strategy #3 under different chiller supply water

temperature were also presented in this chapter under two selected certain cooling load conditions (i.e., 45% and 70% of the design load condition). Figure 5.21 and Figure 5.22 show the total energy consumption of chillers and pumps under different chiller supply water temperatures when using the proposed optimal control strategy (Strategy #3). The two figures indicate that a small increase in the total power consumptions of chillers and pumps when increasing the chiller supply water temperature from 5.5°C to 7.5°C in this complex chilled water system. That means that the energy savings of chillers with a high chiller supply water temperature exceeded the energy wasting of the overall pumps in this particular chilled water system. The reason is that the energy consumption of the total pumps account for a higher percentage in this complex system than that in conventional systems with simple configuration. The effect of chiller supply water temperature on the pumps is even more significant than that on the chillers. Therefore, the chiller supply water temperature was not optimized in the study presented in this chapter.

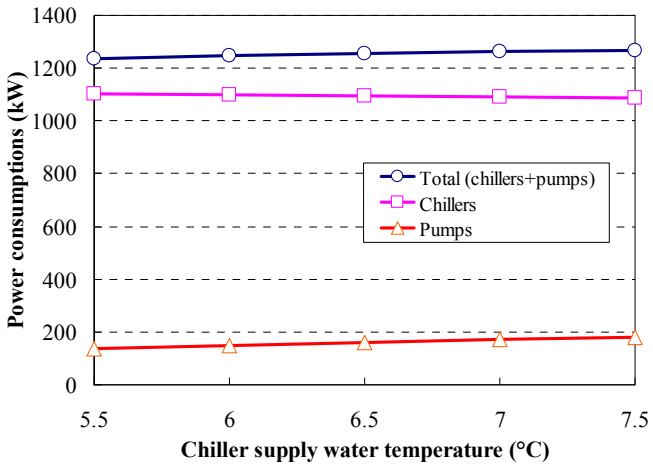

Figure 5.21 Power consumption using the optimal control strategy (45% of design cooling load)

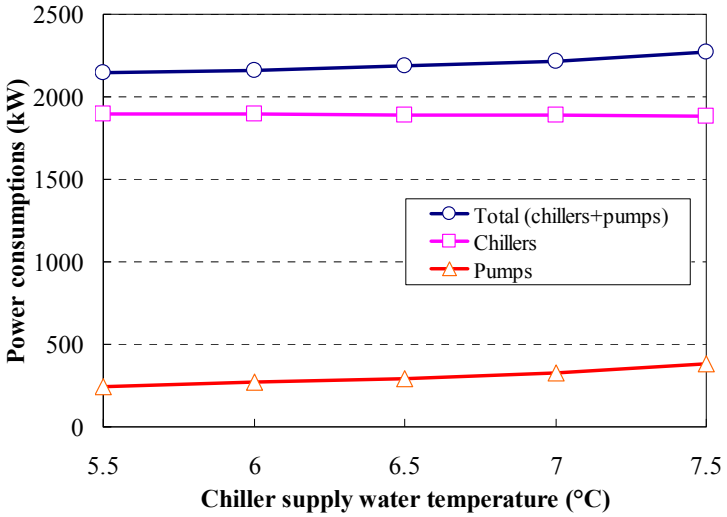

Figure 5.22 Power consumptions using the proposed optimal control strategy (70% of design cooling load)

Based on the above energy performance tests, it can be concluded that the proposed optimal control strategy can save significant pump energy when compared with the conventional control strategies. The saving was achieved by adopting the optimal set-point of outlet water temperature after heat exchangers and the optimized variable differential pressure set-point. It should be pointed out that the above case study showed the application of the proposed optimal strategy in the complex chilled water system in which the primary constant pumps are installed after each heat exchanger. Actually, the proposed optimal strategy is also applicable to the chilled water system without the primary constant speed pumps after each heat exchanger.

5.4.3 Evaluation of control robustness to avoid the deficit flow

Since the chilled water system under study was frequently suffered from the low temperature difference syndrome and the deficit flow problem in actual operation

when using the conventional control strategies, the control robustness to avoid the deficit flow of the proposed optimal control strategy (i.e. Strategy #3 in the Section 5.4.2) was evaluated when compared to the conventional control strategy (i.e. Strategy#1 in the Section 5.4.2) in the simulation platform. The chiller supply water temperature was maintained at 5.5°C under the two control strategies and its operating number was simply determined by the "measured" cooling load. When the "measured" cooling load was larger than 90% of its nominal cooling capacity, additional chiller was switched on.

A disturbance was introduced in the chilled water system at 13:00 by increasing the inlet water temperature before heat exchangers by a constant value of 0.3°C. This phenomenon could occur in real complex chilled water systems involving several subsystems. When one of the subsystems delivered much more water than that required, the additional return water with high temperature would mix with the supply water from chillers resulting in increased temperature of the main supply water to other individual subsystems. In order to check effect of the disturbance on the system operation performance, the cooling load during the whole tests maintained unchanged.

Figure 5.23 presents the variation of the water flow rate in the bypass line using the two control strategies respectively. It is obvious that the chilled water system using the conventional control strategy (Strategy #1) suffered from serious deficit flow in the bypass line right after 13:00pm when the disturbance was introduced. The

maximum deficit flow even reached near -200l /s (negative value means deficit flow), which indicates that water delivered by the pumps before heat exchanger group was about 300 l/s more than that required. The reason for the deficit flow when using Strategy #1 was that the actual outlet water temperature after heat exchangers could not be maintained at the fixed set-point (6.3°C) after 13:00pm, as shown in Figure 5.24. When the outlet water temperature after heat exchangers could not be maintained at its set-point, the modulating valves fully opened and additional heat exchangers were switched on. Both of the reasons resulted in reducing the overall water resistance before the heat exchanger group. The speed of secondary pumps before heat exchangers would therefore increase continually until reached the maximum value.

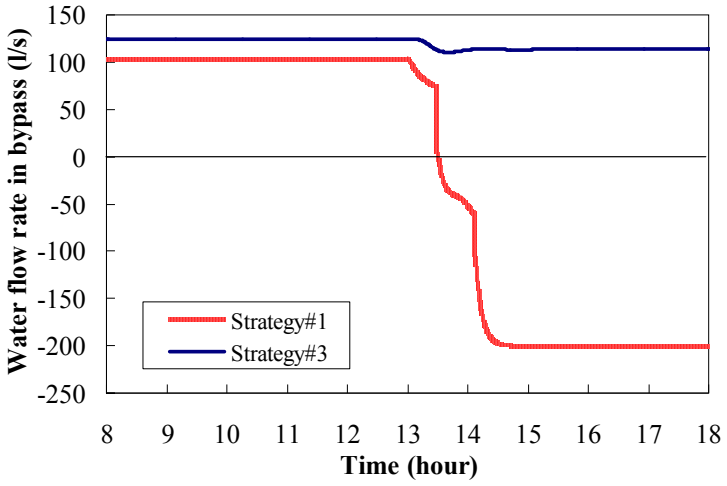

Figure 5.23 Water flow rate in the bypass line using different control strategies

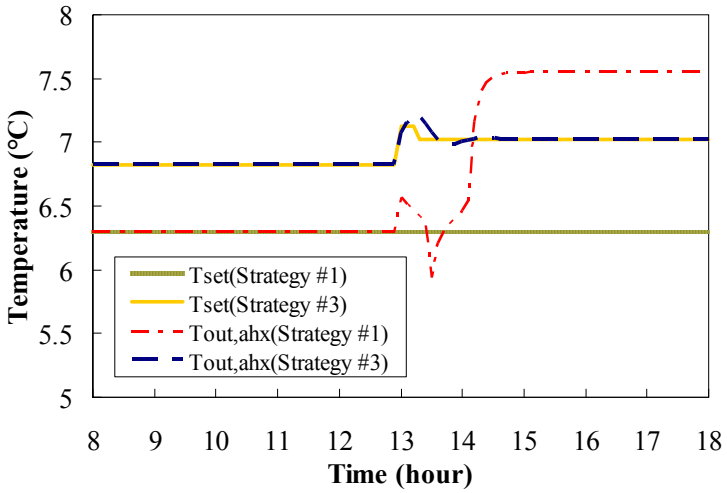

Figure 5.24 The relationship between the set-point and the measured $T_{out,ahx}$ using different control strategies

When using the proposed optimal control strategy (Strategy #3), the flow rate in the bypass line only experienced a small reduction and there was far from the risk of deficit flow after 13:00pm. Figure 5.24 shows that the outlet water temperature after heat exchangers could be basically maintained at its set-point after the disturbance occurred. The reason was that the use of the proposed strategy resulted in increased set-point after heat exchangers when the inlet water temperature before heat exchangers rose after 13:00pm.

Figure 25–26 present the energy consumption of each pump group when using two control strategies. It can be seen in Figure 25 that significant pump energy was wasted when using Strategy #1 after 13:00pm after the disturbance was introduced. The energy waste when using Strategy #1 was mainly from the secondary pumps before heat exchangers and the primary constant speed pumps after heat exchangers. The power consumption of secondary pumps before heat exchangers increased

significantly because the set-point of outlet water temperature after heat exchangers could not be reached. The power consumption of primary constant speed pumps also increased significantly because their operating number increased along with more operating heat exchangers (i.e. from 2 to 4). When using Strategy #3, there were only small increases in the power consumption of secondary pumps before and after heat exchangers after the disturbance was introduced. The power consumption of primary pumps after heat exchangers basically kept unchanged because their operating number did not change.

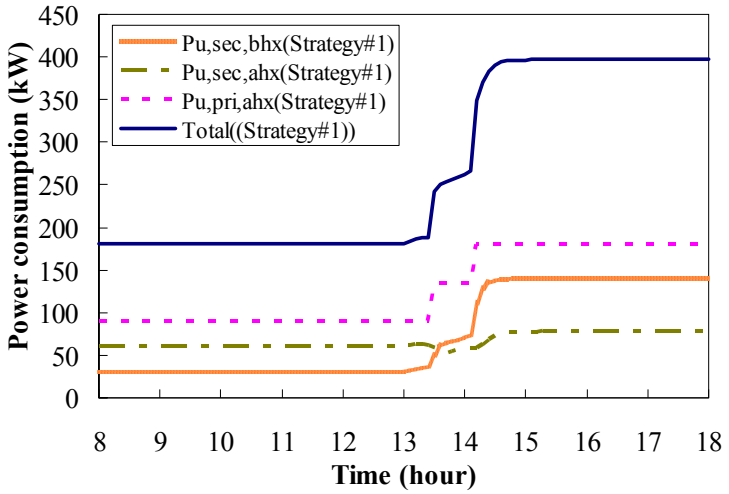

Figure 5.25 Power consumptions of pumps when using Strategy #1

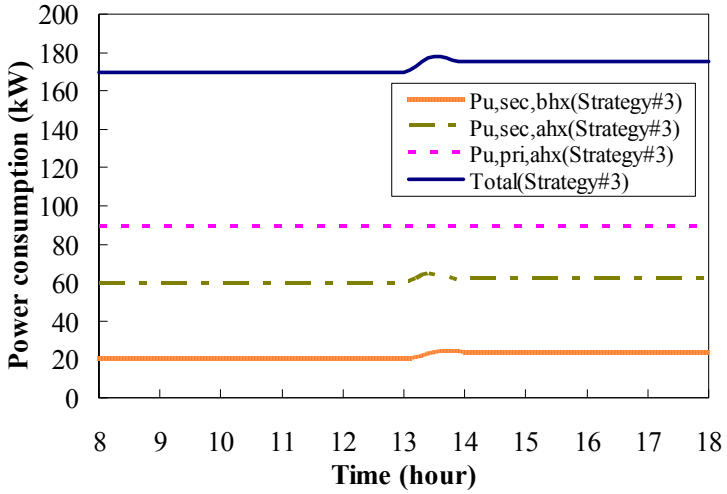

Figure 5.26 Power consumptions of pumps when using Strategy #3

Table 5.6 shows the details of the power consumption of pumps before and after 13:00pm using two control strategies. The power consumption of pumps in the morning (8:00am-13:00pm in this study) was regarded as the benchmark for comparison. Using Strategy #1, about 889.16kWh (96.50%) of the total energy consumption of pumps was wasted due to the disturbance in the afternoon (13:00am-18:00pm in this study) when compared to that in the morning. About half of the energy waste was contributed by the secondary pumps before heat exchangers. Their energy consumption in the afternoon was about 374.37% of that in the morning. When using Strategy #3, only 28.14 kWh (3.25%) of the total energy consumption of pumps was wasted. The energy waste when using Strategy #3 was mainly from the secondary pumps before and after heat exchangers.

It also can compare the total energy consumptions of pumps when using the two control strategies in Table 5.6. The total pump energy when using Strategy #1 was slightly higher than that when using Strategy #3 in the morning because a fixed

differential pressure set-point was used in Strategy #1. In the afternoon, the proposed optimal control strategy (Strategy #3) saved about 915.97 kWh (50.59%) of the total energy consumption of pumps when compared to that using the conventional control strategy (Strategy #1). The energy savings were mainly contributed by the fact that the deficit flow was eliminated due to the better control robustness and reliability of Strategy #3. The detailed comparison between the total hourly pump energy when using the two strategies in the whole day is presented in Figure 5.27.

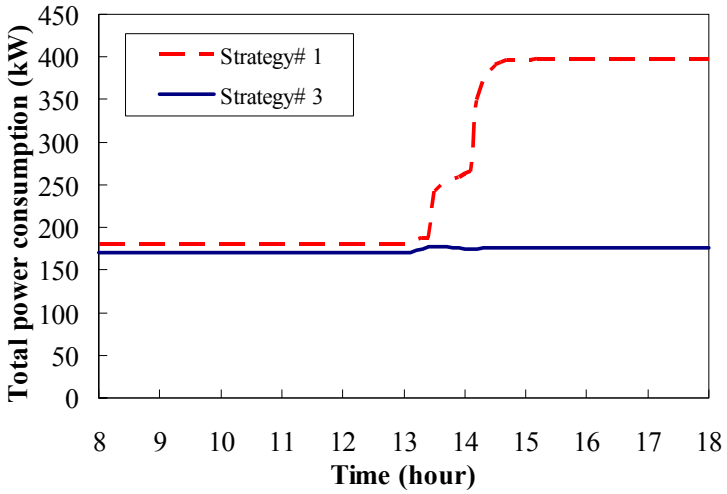

Figure 5.27 Total pump power consumptions using two strategies

From the above comparisons, it can be concluded that the proposed optimal control strategies has good control robustness and reliability when facing the disturbance (increasing the inlet water temperature before heat exchangers). When using the conventional control strategy, performance of the same system was significantly affected by the disturbance and the system operation significantly deviated from the healthy operation state. Significant energy saving of pumps therefore was achieved using the proposed optimal control strategy.

Table 5.6 Power consumptions of pumps using two control strategies

Strategies	$P_{pu,sec,bhx}$	$P_{pu,pri,ahx}$	$P_{pu,sec,ahx}$	Total	$P_{pu,sec,bhx}$	saving	$P_{pu,pri,ahx}$	saving	$P_{pu,sec,ahx}$	saving	Total saving	
	(kWh)	(kWh)	(kWh)	(kWh)	(kWh)	(%)	(kWh)	(%)	(kWh)	(%)	(kWh)	(%)
Strategy #1												
8:00-13:00	161.86	455.94	303.58	921.38	-	-	-	-	-	-	-	-
13:00-18:00	605.95	835.89	368.70	1810.54	-444.09	-274.37	-380.0	-83.33	-65.12	-21.45	-889.16	-96.50
Strategy #3												
8:00-13:00	107.82	455.94	302.67	866.43	-	-	-	-	-	-	-	-
13:00-18:00	121.67	455.94	316.96	894.57	-13.85	-12.85	0.0	0.00	-14.29	-4.72	-28.14	-3.25

5.5 Summary

An online adaptive optimal control strategy for complex building chilled water systems involving intermediate heat exchangers is proposed in this chapter. This strategy determines the optimal settings which minimize the energy consumption of chilled water pumps. This strategy adopts simplified adaptive models allowing the simple strategy can be accurate and effective under various working conditions.

The validation results show that the simplified adaptive models agree well with the "measured" operation data. The proposed optimal control strategy was proven to be able to accurately determine the optimal settings of the outlet water temperature after heat exchangers and the operating number of heat exchangers. The results of the energy performance evaluation tests show that 5.26%-14.69% of the pump energy could be saved when using the proposed optimal control strategy in normal operation as compared with conventional strategies.

The test results also demonstrate that the proposed optimal control strategy has enhanced control robustness and reliability in eliminating deficit flow in the system when facing disturbances, such as a sudden increase of inlet water temperature before heat exchangers. In the cases having deficit flow, up to 50.59% of the chilled pump energy could be saved when using the proposed strategy, which eliminated the deficit flow, as compared with that using the conventional control strategy.

CHAPTER 6 FAULT-TOLERANT CONTROL STRATEGY FOR PRIMARY-SECONDARY CHILLED WATER SYSTEM

This chapter presents a fault-tolerant and energy efficient control strategy for secondary chilled water pump systems to solve this operation and control problem and therefore to enhance the operation performance and energy efficiency of chilled water systems. The strategy employs the flow-limiting technique that can ensure the water flow of secondary loop not exceed that of the primary loop while still maintaining highest possible delivery capacity of cooling to terminals. The strategy is also integrated with differential pressure set-point optimizer to determine the optimal set-point online.

Section 6.1 presents the formulation of the fault-tolerant control strategy for the primary-secondary chilled water system. The strategy employs the flow-limiting technique that can ensure the water flow of secondary loop not exceed that of the primary loop while still maintaining highest possible delivery capacity of cooling to terminals. Section 6.2 briefly introduces the setup of simulation platform which is used for validating the proposed control strategy. The performance of this proposed control strategy is validated in Section 6.3. A summary of this chapter is given in Section 6.4.

6.1 Formulation of the fault-tolerant control strategy

In actual applications, most of the primary-secondary systems, from time to time, cannot work as efficient as expected due to low delta-T syndrome and deficit flow problem. The deficit flow may cause a series of operational problems, such as the high supply water temperature, the over-supplied chilled water, and the increased energy consumption of the secondary pumps. The existing studies demonstrate that low delta-T syndrome and deficit flow problem widely exist in the primary-secondary chilled water system and the elimination of this problem can improve the energy efficiency of the chilled water system. However, most of the studies pay more attention on analyzing the possible causes and solutions of this problem from the view of design and commissioning. In practice, although the HVAC systems were properly designed and well commissioned, deficit flow still cannot be completely avoided in the operation period due to some disturbances, e.g. improper control. There are no reliable, robust and secure solutions that can eliminate deficit flow in real applications.

The research associated with proper control of secondary pumps to eliminate deficit flow and low delta-T syndrome for real applications is missing. In the existing studies, a number of researchers have paid great efforts on the energy efficient control and operation of variable speed pumps to enhance their energy efficiencies [Jin et al. 2007, MA 2000, Wang et al. 2010, Bahnfleth et al. 2001 and 2006, Ma et al. 2008, Jack et al. 1991, Chase et al. 1993, Powell et al. 1994, McCormick et al.

2003, Ma et al. 2009]. However, when the deficit flow occurs, these control strategies cannot handle such problem, resulting in that the chilled water system is hard to be controlled as the anticipation with high robustness and energy efficiency in real applications.

Further more, many of the proposed solutions from the viewpoint of design might be only feasible to be adopted in new systems, while solutions from the viewpoint of operation and control are practical and preferable for the large number of existing systems suffering from the deficit flow and low delta-T syndrome. The developed fault-tolerant control strategy for secondary pumps is to avoid deficit flow in the bypass line and improve the low delta-T syndrome while taking the energy saving of the secondary pumps into consideration at the same time.

6.1.1 Outline of the fault-tolerant control strategy

The fault-tolerant control strategy for secondary pumps is developed not only to eliminate the deficit flow problem but also to enhance the energy efficiency of the chilled water distribution systems. It provides a method based on flow-limiting technique that can ensure the flow rate in the bypass line is positive (a negative value means deficit flow). Figure 6.1 illustrates this control strategy, which consists of a set-point reset control of differential pressure at remote (*DP2*), a flow-limiting controller, a differential pressure reset controller at supply (*DP1*), and a pump controller.

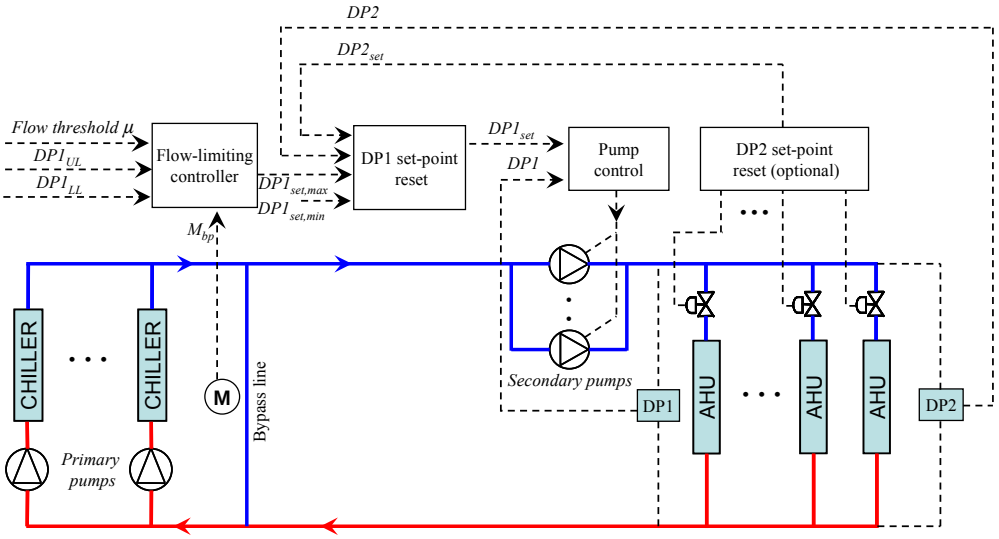

Figure 6.1 Outline of the fault-tolerant control strategy

In this strategy, the secondary pumps are controlled to achieve two objectives: one is to eliminate the deficit flow in the bypass line and the other is to maintain a lowest pump head while still satisfying the cooling demands of all AHUs. The working principle of this control strategy is illustrated in Figure 6.2. A modified cascade control is employed to achieve a balance of stable control and fast response which involves two loops. In the outer loop, the DP1 set-point reset controller determines the differential pressure set-point ($DP1_{set}$) at the main supply by comparing the measured differential pressure of at remote ($DP2$) with the set-point ($DP2_{set}$). In the inner loop, $DP1$ is compared with the differential pressure set-point at supply ($DP1_{set}$) in by the pump controller to control the speed of the pumps. $DP1_{set,max}$ is introduced as the maximum value of $DP1_{set}$ in the outer loop, which is determined by the flow-limiting controller. The function of introducing $DP1_{set,max}$ is to eliminate the deficit flow, which is reset according to the measured flow rate (M_{by}) in the bypass line. When deficit flow occurs, $DP1_{set,max}$ will be reduced gradually by feedback

control until the deficit flow disappears. The *DP2* set-point reset controller might be eliminated in practical applications to simplify the application of the strategy or the valve opening information is not available. It is worthy noticing that, to simplify the control strategy in implementation, resetting of the differential pressure at the supply ($DP1_{set}$) can be achieved by maintaining a differential pressure at remote (*DP2*) at certain level without using the valve opening information or by using directly the valve opening information without using the differential pressure at remote (*DP2*).

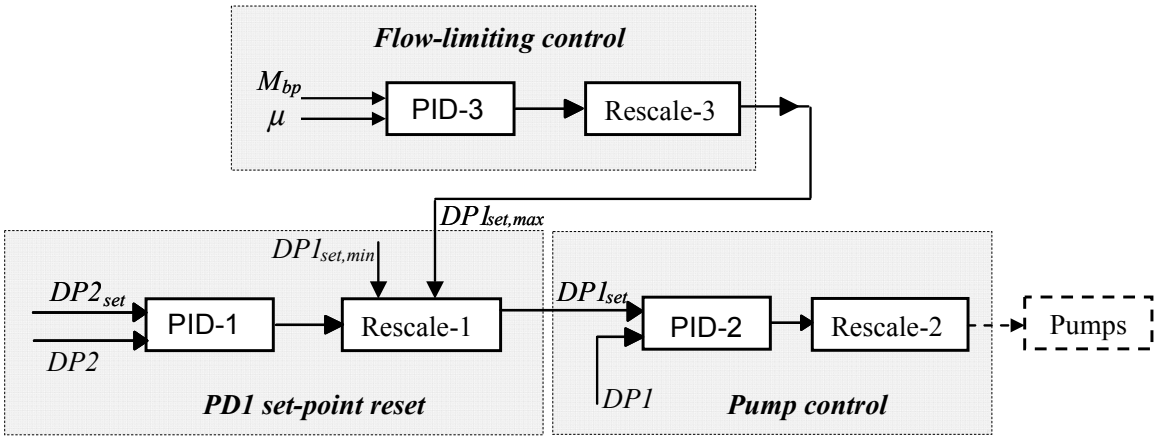

Figure 6.2 Principle of pump and flow limiting controls

6.1.2 Control of secondary pumps

Flow-limiting controller

The flow-limiting controller is employed to limit the water flow rate of the secondary loop not larger than that of the primary loop (i.e. to avoid deficit flow in the bypass line), as shown in Figure 6.2. This strategy utilizes a feedback control using the measured water flow rate in the bypass line. A threshold μ, which represents the expected minimal and positive (negative means deficit flow) flow rate

in the bypass line, is set by the users. $\boldsymbol{\mu}$ can be determined according to the system design or practical requirements. If $\boldsymbol{\mu}$ is set to zero exactly, the water flow rate is possible to be negative because of the fluctuations of the control process resulting lower control stability. Therefore, it is better to set $\boldsymbol{\mu}$ to a small but positive value in order to avoid deficit flow in the bypass line for stable control. In this study, μ is set to be about 3% of the design water flow rate of a single chiller. A PID controller compares the measured water flow rate (M_{by}) in the bypass line with the predefined threshold μ to generate a control signal $\boldsymbol{\alpha}$ (between 0 and 1). $\boldsymbol{\alpha}$ is rescaled to generate $DP1_{set,max}$, the maximum value (upper limit) for the differential pressure set-point $DP1_{set}$ of the $DP1$ set-point reset controller by using Equation (6.1).

$$DP1_{set,\max} = DP1_{LL} + \alpha(DP1_{UL} - DP1_{LL}), \alpha \in (0,1) \tag{6.1}$$

where, $\boldsymbol{\alpha}$ is the output of the PID control (PID-1), $DP1_{LL}$ and $DP1_{UL}$ are the lower and upper limits for the $DP1_{set,max}$ respectively. They can be determined based on the practical chilled water system design data considering the operation safety and stability.

$DP1_{set,max}$ is a variable that is used as the maximum value for the differential pressure set-point ($DP1_{set}$) to control the speed (and number) of secondary pumps to ensure the water flow rate in the bypass line is not less than the predefined threshold $\boldsymbol{\mu}$. $DP1_{set,max}$ is reset according to the measured flow rate in the bypass line. When M_{by} is larger than the predefined threshold $\boldsymbol{\mu}$, $DP1_{set,max}$ will increase gradually (to release the limit for supply flow control) until reaching its upper limit $DP1_{UL}$. On the

contrary, when M_{by} is less than the predefined threshold $\boldsymbol{\mu}$, $DP1_{set,max}$ will decrease gradually (to limit the supply flow) until reaching the lower limit DP_{LL}. The reduction of $DP1_{set\ ,max}$ will consequently lower the $DP1_{set}$ that will decrease the speed of the secondary pumps and therefore limit the flow supplied to building to avoid deficit flow in the bypass line.

Set-point reset of differential pressure at supply (DP1)

The *DP1* set-point reset controller is utilized to generate the differential pressure set-point at the supply ($DP1_{set}$) as shown in Figure 6.2. In this process, the *PID-1* generates the control signal by comparing the measured differential pressure (*DP2*) at remote with its set-point ($DP2_{set}$). The control signal is rescaled to generate the set-point of the differential pressure at supply ($DP1_{set}$) for the pump control. Figure 6.3 shows rescale function for determining $DP1_{set}$ using a linear relationship between $DP1_{set}$ and the output of *PID-1*. When the output of *PID-1* increases, which means more chilled water is required, $DP1_{set}$ will increase accordingly. $DP1_{set,min}$ is the lower limit of the controlled differential pressure at supply side, which is a constant determined by operators based on system design or practical requirements. Selecting $DP_{set,\ min}$ should consider the stability of the pumps operation. $DP1_{set,max}$ is the upper limit for $DP1_{set}$, which is a variable generated by the flow-limiting controller.

When the flow demands of AHUs increase, the AHU valves will open more and the $DP1_{set}$ will increase consequently. When deficit flow occurs, the higher temperature of the supply water to AHUs will result in more flow demand and consequently

higher $DP2_{set}$. When the AHU outlet air temperatures cannot reach their set-points, $DP2_{set}$ will increase to its maximum value rapidly. Consequently, the output of PID-1 in the *DP1* set-point reset controller will increase to a very high value. If such $DP1_{set}$ is used directly for pump control without applying proper constraints, the pump might work at full speed and the deficit flow will be further deteriorated. In this strategy, $DP1_{set,max}$ determined by the flow-limiting controller performs the role of limiting the flow in the secondary loop when deficit flow occurs as shown in Figure 6.3. Although deficit flow results in the increase of $DP2_{set}$, $DP1_{set,max}$ will be reduced simultaneously by the flow limit controller. The set-point of *DP1* will eventually drop resulting in reduced pump speed until the deficit flow disappears. Note, the reduced total chilled water flow supplied to terminal units (AHUs) (for eliminating the deficit flow in case it occurs) will not reduce the supplied total cooling capacity to the terminal units. It will be further discussed later in this chapter.

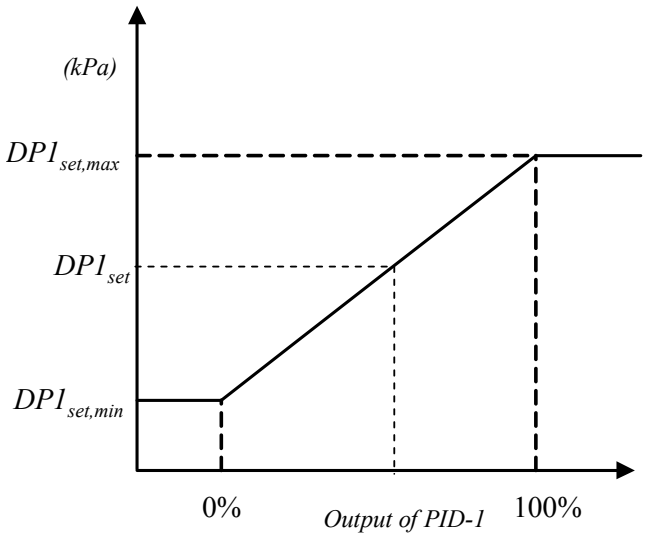

Figure 6.3 The working principle of the determination of DP_{set}

Set-point reset of differential pressure at remote (DP2)

This set-point reset control is used to produce an optimal differential pressure set-point ($DP2_{set}$) at remote, as shown in Figure 6.4. This strategy is developed to search the optimal differential pressure set-point that can make the secondary pumps provide the enough and just enough differential pressure to the hydraulically critical loops at all times. This objective can be achieved by increasing or reducing the differential pressure set-point to keep only one valve nearly fully open and to ensure this AHU can satisfy the cooling demand. As shown in Figure 6.4, at time k, the strategy will firstly check whether the maximum valve opening (OS_{max}) of all AHUs reached 100% or not. Then, the number of the valves with 100% opening will be counted. Last, the supply air temperature ($T_{a,sup}$) of the AHU with nearly fully open valve will be checked whether it has reached the set-point ($T_{a,set}$) or not. By judging the three these conditions, the strategy modulates the differential pressure set-point ($DP2_{set,k}$) based on the previous setting ($DP2_{set,k-1}$) by increasing or decreasing a predefined incremental (ΔP). The predefined pressure incremental is different in various practical systems, which is determined to keep the control process stable and flexible. In this study, ΔP is equal to 1.5% of the required pressure drop of the remote loop under full load condition.

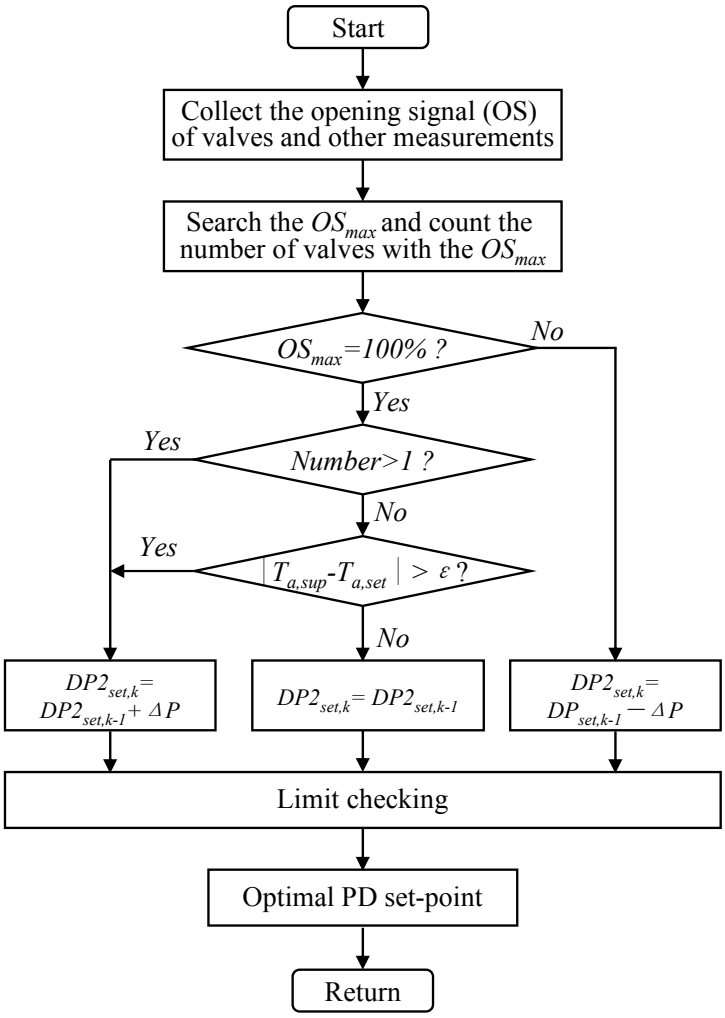

Figure 6.4 Control logic flow chat of set-point reset of differential pressure at remote (*DP2*)

For a given water network with air-handling units whose valves opening are controlled using feedback control to maintain the outlet air temperatures at their set-points , the secondary pumps should provide enough chilled water to all the terminal units to satisfy the cooling demands. If one of the AHUs cannot reach its supply air temperature set-point, its valve will fully open to allow the highest possible water flow. If the supply air temperature of an AHU is lower than its set-point, its valve will be closed down to decrease water flow rate. When only one of all those valves fully opens, it indicates that this AHU is the critical loop

hydraulically. Therefore, providing enough and just enough chilled water to the hydraulically critical loop to satisfy the cooling demand and minimizing its water resistance by fully opening its valve can minimize the pressure drop of secondary pumps.

Pump speed and sequence control

The pump controller generates the speed signal for the secondary pumps. It compares the measured differential pressure at the supply side (*DP1*) with its set-point ($DP1_{set}$) given by DP1 set-point reset controller to output a control signal. PID feedback control is used to modulate the speed of the pumps.

The sequence control strategy for secondary pumps determines the operating number of pumps. In this study, a conventional strategy is utilized. Using this strategy, an additional pump is switched on when the frequencies of operating pumps exceed 90% (corresponding to 45Hz) of their nominal capacity). One of the operating pumps is switched off when the frequencies of the operating pumps are lower than 60% (corresponding to 30Hz) of the nominal capacity. In addition, in order to ensure the reliability and stability of the chilled water distribution system, a minimal time interval is set when changing the operating number of pumps.

6.1.3 The detailed application procedure

A flow meter is installed on the bypass line, which can monitor the quantity and direction of water flow rate in the bypass line. The proposed fault-tolerant control

strategy for secondary pumps works as the following steps as illustrated in Figure 6.5.

(1) Check the valve control signals and bypass flow measurement using a filter;

(2) Determine the maximum value ($DP1_{set,max}$) for the differential pressure set-point (DP1set) by comparing the measured water flow rate (M_{bp}) in the bypass line with the predefined threshold by the flow-limiting controller;

(3) Determine the optimal differential pressure set-point at remote ($DP2_{set}$);

(4) Determine the differential pressure set-point at supply ($DP1_{set}$) for secondary pumps control by DP1 set-point reset controller according to Figure 6.3;

(5) Determine the operating number for the secondary pumps using pump sequence controller;

(6) The final decision will be made by the control supervisor after checking control constraints.

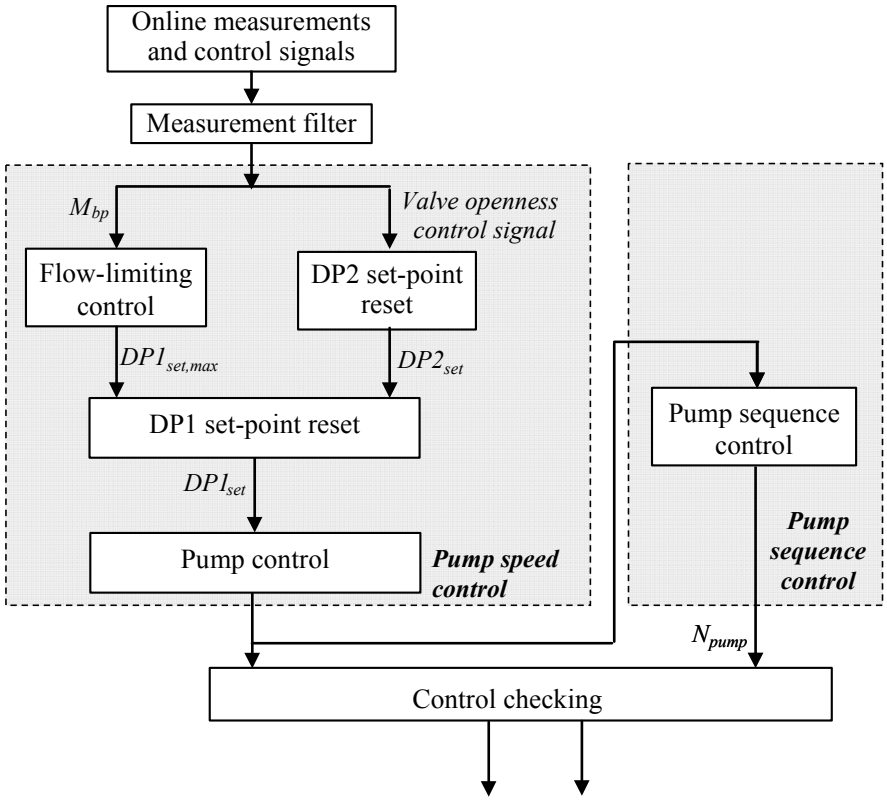

Figure 6.5 The flow chart of the detailed control procedures

6.2 Setup of the tests

It is hard to compare various control strategies in real air-conditioning systems due to its extreme complexity. The proposed fault-tolerant control strategy was validated and evaluated using a dynamic simulation platform representing a typical chilled water system for a building, as shown in Figure 6.6. This is a typical primary-secondary chilled water system, in which two water cooled centrifugal chillers with rated cooling capacity of 7230 kW are installed to generate the chilled water of 7°C at design condition. Each chiller is associated with a constant speed primary pump. In the secondary loop, there are three identical secondary pumps distribute chilled water to the terminals, one of which is a standby pump. All the

secondary pumps are equipped with VFDs to control the pump speed according to the terminal cooling demand. The detailed parameters for chillers and pumps are listed in Table 6.1. AHUs are implemented in the air-conditioning system to provide cooled air for indoor thermal comfortable control. The valves of AHUs are controlled to maintain the supply air temperature at its set-point (i.e., 13°C in this study). The AHU fans are also equipped with VFDs to vary supply air flow rate and the VAV boxes are used to maintain the indoor air temperature at a fixed set-point (i.e., 23°C in this study). The models of chillers, cooling towers, pumps, and cooling coils are all detailed physical models that can simulate the real chilled water system.

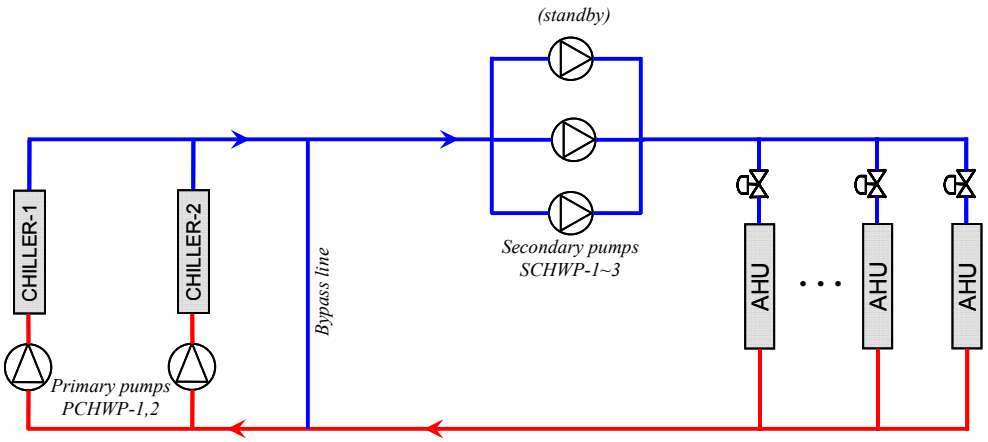

Figure 6.6 Schematic of the chilled water system

Table 6.1 Design specifications of chillers and pumps in the chilled water system

Chillers	Number	Cooling capacity (kW)	$M_{w,ev}$ (L/s)	$M_{w,cd}$ (L/s)	W (kW)	W_{tot} (kW)
Chiller-1,2	2	7,230	345	410.1	1,346	2792
Pumps	Number	M_w (L/s)	Head (m)	η (%)	W (kW)	W_{tot} (kW)
PCHWP-1,2	2	345	31.6	84.5	126	256
SCHWP-1~3	3	345	41.4	85.7	163	323

The multi-zone building model (TYPE 56) of TRNSYS 16 is employed to simulate a building with 75 floors. The ratio of widow to wall is 0.5. The heat load from the occupants, equipment and lighting system and weather data are considered in the simulation as an input file. The weather condition used is the data of the typical year in Hong Kong.

6.3 Performance tests and evaluation of the fault-tolerant control strategy

In order to compare the control performance and energy efficiency of the chilled water system before and after the utilization of this proposed fault-tolerant control strategy (Strategy #3), two conventional control strategies are used for comparison, as shown in Table 6.2. In the first conventional control strategy (Strategy #1), secondary pumps are controlled to maintain a fixed differential pressure of the remote loop, which is the upper limit of the differential pressure set-point constrains under the full load condition in the Strategy #3. The second conventional strategy (Strategy #2) uses an optimal differential pressure set-point that can ensure one of the valves associated with the heavily loaded terminal unit fully open at all times.

Table 6.2 Description of the control strategies

No.	Strategies	Description
1	Strategy #1	Using a fixed set-point for differential pressure at remote
2	Strategy #2	Using the optimal set-point for differential pressure at remote
3	Strategy #3	Using the optimal set-point for differential pressure at remote and flow-limiting control

The chiller sequence control strategies used in the simulations are as follows according to the conventional operation of a real system in Hong Kong. Chillers are sequenced only based on the cooling load of the terminals. When the measured cooling load exceeds the nominal cooling capacity of the chiller for ten minutes, another chiller is switched on. When the remaining chiller can handle the cooling load, one of the chillers is switched off.

Two case studies are conducted to test and validate the operation and energy performance of the chilled water system using the fault-tolerant strategy. One case is to evaluate the strategy in a chilled water system without faults, the other one is in a system with faults that will cause deficit flow. Both morning start period and normal operating period are studied.

A typical air-conditioning system usually experiences two typical working modes, namely (morning) start period and normal operating period. In the start period, the chilling system is switched on before occupation to cool down the indoor air temperature to the comfortable level. In normal operating period, the indoor thermal comfort condition has been achieved and the secondary water flow rate is controlled based on the cooling demand of terminals. Generally speaking, deficit flow will not take place during normal period in a healthy chilled water system with proper design and commissioning. However, a lot of field investigations and tests show that deficit flow frequently occurs during start period particularly when not all the chillers are switched on. For instance, Figure 6.7 shows the measured water flow rates of the

bypass line in three working days (0:00 28/9/2010-18:00/30/09/2010) in a real building chilled water system. It can be found that the deficit flow began to occur on each morning start period.

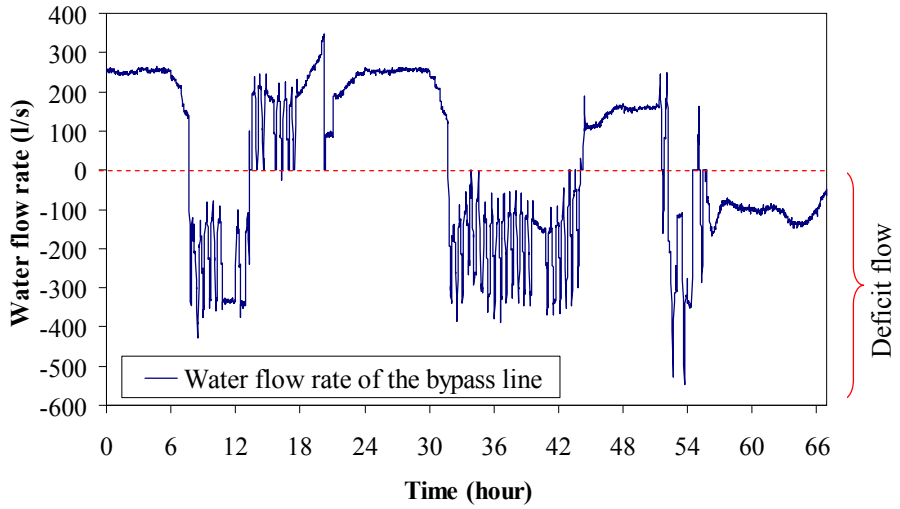

Figure 6.7 Measured water flow rates of the bypass line in three working days in a real building chilled water system in Hong Kong

6.3.1 Case 1: Evaluation of the fault-tolerant strategy in fault-free system

In this case study, the simulation tests evaluates the fault-tolerant strategy in a working day from 7:00am to 19:00pm under three typical weather conditions (i.e., spring, mild-summer and sunny-summer). During start period, different operating numbers of chillers consume different electric energy to lower down the indoor air temperature to the desired level. The operating number of chillers in this test are chose to minimize the total energy consumption during the start period using the existing model-based control strategy in [Sun et al. 2010], in which the optimal operating numbers of chillers can be determined during start period by estimating the total energy consumptions under different operating chillers. During normal

operation period, the chillers were sequenced based on the measured cooling load of terminal units. Only detailed performance data in the sunny-summer test case are presented here.

Figure 6.8 presents the water flow rates of the bypass line in the sunny-summer test case using the three different control strategies. It can be observed that there was no deficit flow in the bypass line using the proposed fault-tolerant strategy (Strategy #3) during the day. While the other two conventional strategies (Strategy #1 and #2) offered significant deficit flow, up to about -340 l/s, during the start period from 7:00 to 9:00 am. This is because that all the secondary pumps worked under their high limit speeds while not all the chillers (and primary pumps) are switched on when using Strategy #1 and #2. Using conventional strategies, secondary pumps were controlled to maintain the pressure drop of the critical loop at a set-point, whether fixed or optimal. During the start period, the indoor air temperature was higher than its set-point and the outlet air temperature of AHUs could not reach their set-points, resulting in that all the valves fully opened. The fully open valves reduced the water resistance of the total terminals and increased the frequencies and operating numbers of secondary pumps to deliver more water in order to maintain the differential pressure at its set-point.

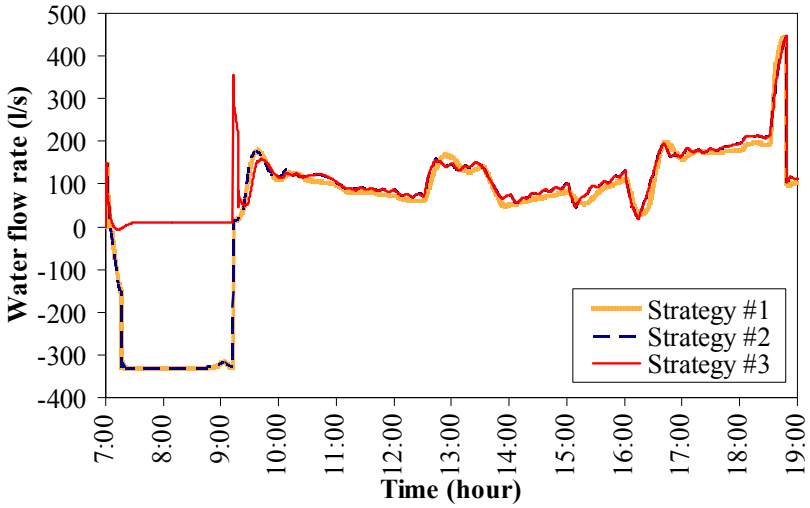

Figure 6.8 Water flow rates in bypass line using three control strategies in the sunny-summer test case

Using the proposed fault-tolerant control strategy with flow-limiting technique, the differential pressure set-point used for pumps control is not only dependent on the valve opening, but also based on the flow rates of the bypass line. When the deficit flow is detected in the bypass line, the flow-limiting controller rapidly decreases the differential pressure set-point, which limits the speed of secondary pumps to ensure the secondary flow rate not more than that of the primary. Therefore, the proposed fault-tolerant strategy could effectively eliminate the deficit flow and accordingly save energy of secondary pumps.

The zone with the highest cooling load in the building (i.e., the critical zone) is selected as an example to compare the indoor cooling effect under the three control strategies. It is worthy noticing that the indoor air temperatures of the critical zone under three strategies were very close during morning start period, as shown in Figure 6.9. It indicates that the proposed strategy could offer equivalent cooling

capacity to the terminal units although the delivered water flow rates were much lower when compared with the other two conventional strategies. It is known that the heat transfer between the water and the air in AHUs is affected by the water flow rate, inlet water temperature besides air flow rate and inlet air temperature at air side. During morning start period, when using Strategy #1 and #2, the deficit flow caused more supply water flow rates through AHUs, as shown in Figure 6.10. The higher flow rate should be able to enhance the heat transfer effect. However, as shown in Figure 6.11, due to the occurrence of deficit flow, the supply water temperatures to terminal units were much higher than that using the proposed strategy, which reduced the heat transfer effect. As the result, the proposed strategy with lower supply water temperature and less water flow rate to terminal units offered similar (even slightly higher) overall cooling effects of AHUs compared with that using the conventional strategies with higher supply water temperature and higher water flow rate to terminal units.

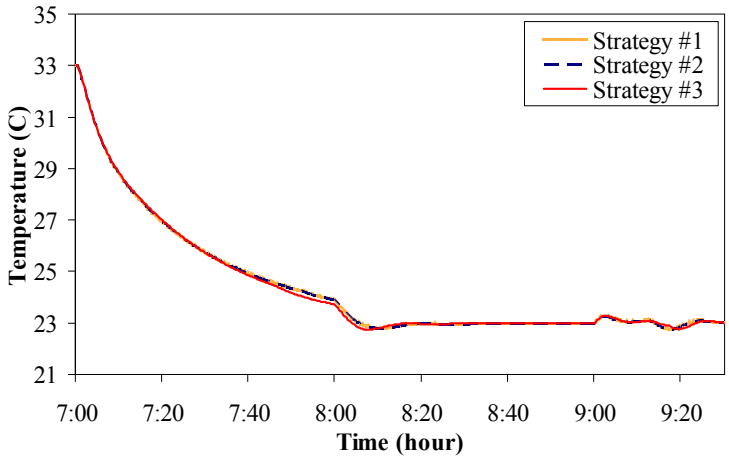

Figure 6.9 Indoor temperatures of critical zones using three control strategies in the sunny-summer test case

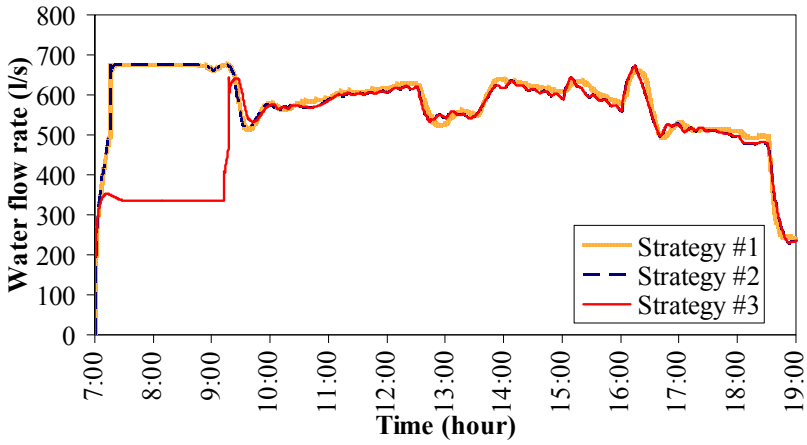

Figure 6.10 Total water flow rates of secondary loop using three control strategies in the sunny-summer test case

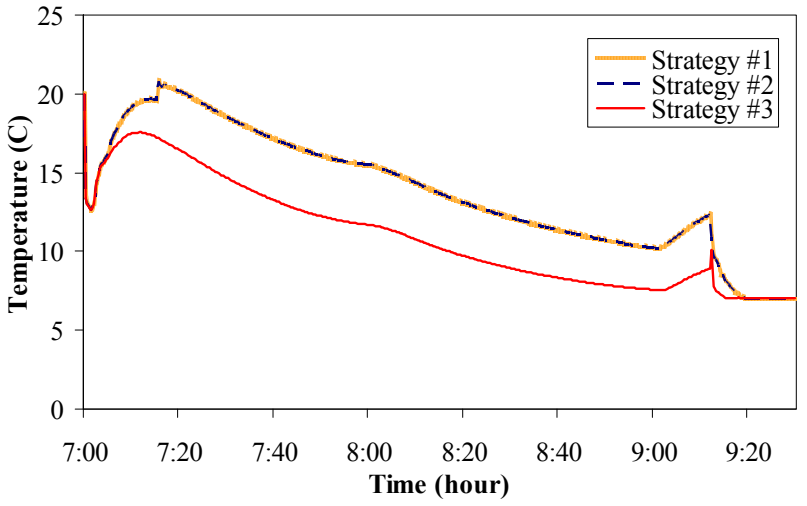

Figure 6.11 Supply water flow rate to terminals using three control strategies in the sunny-summer test case

Table 6.3, 6.4 and 6.5 summarize the energy use and savings of secondary pumps and chillers under three strategies during start period, normal operation period and the whole day respectively. Strategy #1 was used as the benchmark for comparison. It can be seen that the energy consumptions of the chillers of the three strategies under different weather conditions were very close.

Table 6.3 presents a comparison between the energy consumptions of pumps and

chillers using three strategies during start period. It is very obvious that strategy #3 saved about 69.27-77.25% of the secondary pumps energy, which accounts for about 10.57-16.11% of the total energy of pumps and chillers during start period in three typical summer days, compared with strategy #1. The energy consumptions of pumps and chillers using strategy #1 and strategy #2 were very close. That means that strategy #2 using optimal differential pressure set-point failed to offer obvious benefit during start period when compared with strategy #1 using fixed set-point. Therefore, the energy saving during start period by Strategy #3 mainly benefited from the flow-limiting technique. It also can be found that the energy saving by Strategy #3 in the sunny-summer test case was more than that in the other two test cases during start period.

Table 6.3 Electrical energy consumption under different control strategies during the start period (7:00am - 9:00am)

Strategies	W_{pump} (kWh)	$W_{chiller}$ (kWh)	W_{pump}+ $W_{chiller}$ (kWh)	W_{pump} saving		$W_{chiller}$ saving		Total saving	
				(kWh)	(%)	(kWh)	(%)	(kWh)	(%)
Spring									
Strategy #1	437.6	2517.0	2954.5	-	-	-	-	-	-
Strategy #2	432.7	2515.7	2948.4	4.9	1.11	1.3	0.05	6.1	0.21
Strategy #3	134.5	2507.8	2642.3	303.1	69.27	9.1	0.36	312.2	10.57
Mild-summer									
Strategy #1	546.8	2613.2	3160.0	-	-	-	-	-	-
Strategy #2	546.8	2613.3	3160.1	0.0	0	-0.1	0	-0.1	0
Strategy #3	155.7	2606.1	2761.8	391.1	71.53	7.1	0.27	398.2	12.60
Sunny-summer									
Strategy #1	679.5	2671.5	3351.0	-	-	-	-	-	-
Strategy #2	679.3	2671.3	3350.6	0.2	0.03	0.2	0.01	0.4	0.01
Strategy #3	154.6	2656.5	2811.1	524.9	77.25	15	0.56	539.9	16.11

Compared with Strategy #1, in the normal operation period (between 9:00am and 19:00pm), Strategy 2# and #3 saved 11.72-36.84% of pumps energy and 1.11-1.95% of total energy (pumps and chillers) respectively, as shown in Table 6.4. Since there was no deficit flow during the normal operation period using the three strategies, the energy savings were mainly contributed by using optimal differential pressure set-point. During normal operating period, Strategy #3 achieved more energy savings in the spring test case than that in the other two test cases.

Table 6.4 Electrical energy consumptions under different control strategies during the normal operation period (9:00am–19:00pm)

Strategies	W_{pump} (kWh)	$W_{chiller}$ (kWh)	W_{pump}+ $W_{chiller}$ (kWh)	W_{pump} saving		$W_{chiller}$ saving		Total saving	
				(kWh)	(%)	(kWh)	(%)	(kWh)	(%)
Spring									
Strategy #1	681.5	13282.0	13963.5	-	-	-	-	-	-
Strategy #2	430.6	13277.2	13707.8	250.9	36.82	4.8	0.04	255.7	1.83
Strategy #3	430.4	13261.2	13691.6	251.1	36.84	20.8	0.16	271.9	1.95
Mild-summer									
Strategy #1	983.7	17906.0	18889.6	-	-	-	-	-	-
Strategy #2	718.1	17888.0	18606.1	265.5	26.99	18.0	0.10	283.5	1.50
Strategy #3	727.8	17851.9	18579.7	255.9	26.01	54.1	0.30	309.9	1.64
Sunny-summer									
Strategy #1	2414.0	23342.3	25756.3	-	-	-	-	-	-
Strategy #2	2131.1	23339.2	25470.2	283.0	11.72	3.1	0.01	286.1	1.11
Strategy #3	2113.8	23337.7	25451.5	300.2	12.43	4.6	0.02	304.8	1.18

Table 6.5 presents a summary of the energy consumptions of pumps and chillers during the whole day (from 7:00am to 19:00pm). The fault-tolerant strategy (Strategy #3) saved about 26.67-49.52% of secondary pumps energy and 2.90-3.45% of total energy (pumps and chillers) when compared with strategy #1 respectively.

Concerning energy saving, about 17.52-26.67% of pumps energy and 1.9-1.92% of total energy (pumps and chillers) respectively were saved from the applications of flow-limiting technique. It should be pointed out that Strategy #3 saved more energy in the spring test case compared with the other two test cases during the entire day period. Figure 6.12 depicts a detailed description of the energy consumption of pumps under three strategies in the sunny-summer test case.

Table 6.5 Electrical energy consumption under different control strategies during the whole typical day (7:00am – 19:00pm)

Strategies	W_{pump} (kWh)	$W_{chiller}$ (kWh)	W_{pump}+ $W_{chiller}$ (kWh)	W_{pump} saving		$W_{chiller}$ saving		Total saving	
				(kWh)	(%)	(kWh)	(%)	(kWh)	(%)
Spring									
Strategy #1	1119.0	15799.0	16918.0	-	-	-	-	-	-
Strategy #2	863.3	15792.9	16656.2	255.7	22.85	6.1	0.04	261.8	1.55
Strategy #3	564.8	15769.0	16333.9	554.2	49.52	29.9	0.19	584.1	3.45
Mild-summer									
Strategy #1	1530.5	20519.2	22049.6	-	-	-	-	-	-
Strategy #2	1264.9	20501.3	21766.2	265.5	17.35	17.9	0.09	283.4	1.29
Strategy #3	883.5	20458	21341.5	647.0	42.27	61.2	0.30	708.1	3.21
Sunny-summer									
Strategy #1	3093.5	26013.8	29107.3	-	-	-	-	-	-
Strategy #2	2810.4	26010.5	28820.8	283.2	9.15	3.3	0.01	286.5	0.98
Strategy #3	2268.4	25994.2	28262.6	825.1	26.67	19.6	0.08	844.7	2.90

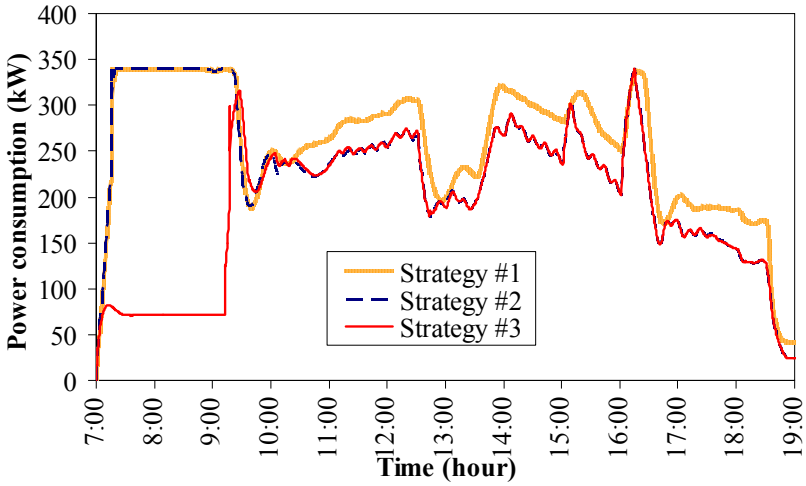

Figure 6.12 Power consumptions of secondary pumps using three control strategies in the sunny-summer test case

Based on the above analysis, it can be concluded that the proposed fault-tolerant control strategies for secondary pumps can effectively eliminate the deficit flow during the start period due to the implementation of flow-limiting techniques. Moreover, the proposed strategies can save significant secondary pump energy compared with other two conventional strategies using fixed differential pressure set-point and optimal pressure set-point respectively.

6.3.2 Case 2: Evaluation of the fault-tolerant strategy in unhealthy system

In a healthy system, the deficit flow only occurs during start period particularly when not all the chillers are switched on. While in an unhealthy system, such as water system fouling or improper controls, the deficit flow is possible to occur at any operation period. As far as the deficit flow occurs, the main supply water temperature to the terminal units will increase and the secondary pumps will consume more energy. It is necessary to ensure the chilled water system works

efficiently even it suffered from some faults that can cause deficit flow. In practice, many causes can lead to the deficit flow problem as mentioned before. In order to evaluate whether the proposed strategy can handle the deficit flow, a fault was artificially introduced in this study by decreasing the supply air temperature set-point of the AHUs from 13°C (design condition) to 10°C. An improper set-point of supply air temperature usually is reset by the tenants or the operators to try to achieve a lower indoor air temperature. Actually, an extremely lower supply air temperature set-point than design value forced the AHU terminals to ask for more chilled water. When the demanded secondary water flow rate exceeds the primary water, the deficit flow is triggered. Three typical weather conditions were selected to test and evaluate the operation stability and energy performance of the proposed fault-tolerant control strategy in the unhealthy system with faults under the typical spring days, mild-summer days and sunny-summer days respectively. Each test lasted five continuous days without stopping air-conditioning. Only detailed performance data in the spring test case are presented here.

As shown in Figure 6.13, deficit flow frequently occurred in the five spring days under the conventional strategies (Strategy #1 and #2). This is because that the AHU terminals demanded more chilled water than their design flows to try to make the outlet air temperature reach the lowered set-point. When the set-point was too low to be reached, the pumps had to work with full speed, resulting in highly degraded operation performance. However, the proposed fault-tolerant strategy (Strategy #3) could eliminate the deficit flow by using the flow-limiting technique in this case.

Using strategy #3, the frequencies of secondary pumps were restricted to limit the secondary water flow rates and consequently the deficit flow was eliminated. Therefore, compared with Strategy #1 and #2, Strategy #3 offered the same cooling capacity while delivering less chilled water flow rates to terminal units, as shown in Figure 6.14. The reason is that Strategy #3 maintained the supply water to terminal units at a continuous low temperature as the result of eliminating deficit flow, as shown in Figure 6.15, which enhanced the heat transfer between air and water streams in AHUs.

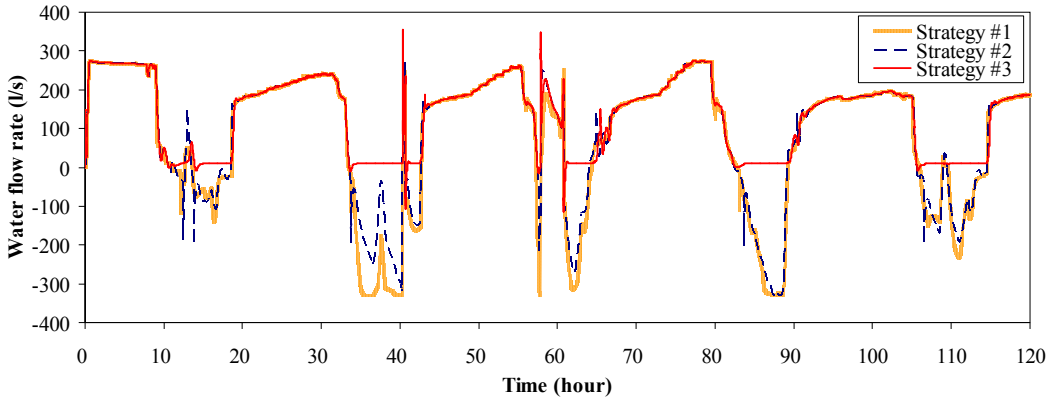

Figure 6.13 Water flow rates in bypass line using three control strategies in spring test case (unhealthy system)

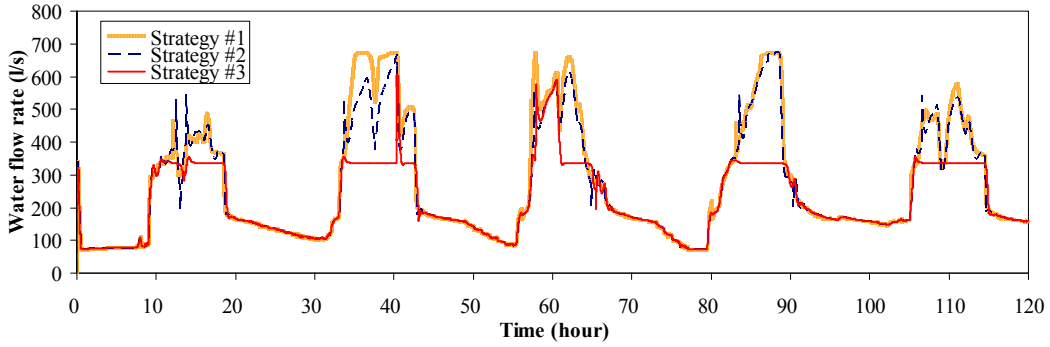

Figure 6.14 Chilled water flow rates in secondary loop using three control strategies in spring test case (unhealthy system)

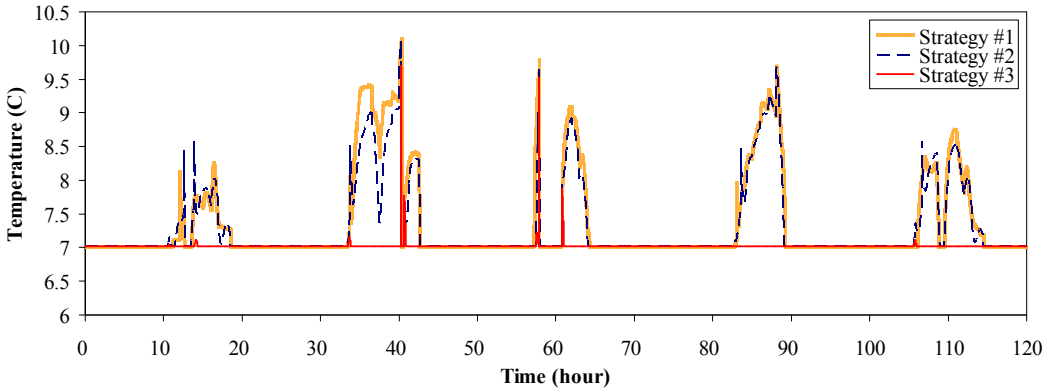

Figure 6.15 Supply chilled water temperature to terminal units using three control strategies in spring test case (unhealthy system)

Table 6.6 presents a summary of the electrical energy consumptions of secondary pumps and chillers using the three control strategies in the unhealthy system under three typical weather conditions. Compared with the conventional Strategy #1 using fixed differential pressure set-point, the proposed Strategy #3 using optimal differential pressure set-point and flow-limiting technique saved about 5369.7kWh (54.30%), 3987.2kWh (34.48%), and 4714.1kWh (30.97%) of the secondary pumps energy, and 5544.3kWh (4.45%), 4930.9kWh (3.22%), 5515.5kWh (3.18%) of the total energy of the pumps and chillers in the three weather conditions. The energy consumptions of the chillers using the three strategies were very close. The energy savings by the proposed strategy were mainly benefited from reducing the consumption of secondary pumps.

Table 6.6 Electrical energy consumption under different control strategies during the five typical days (unhealthy system)

Strategies	W_{pump} (kWh)	$W_{chiller}$ (kWh)	W_{pump}+ $W_{chiller}$ (kWh)	W_{pump} saving		$W_{chiller}$ saving		Total saving	
				(kWh)	(%)	(kWh)	(%)	(kWh)	(%)
Spring									
Strategy #1	9889.0	114643.1	124532.2	-	-	-	-	-	-
Strategy #2	6965.0	114523.1	121488.0	2924.1	29.57	120.0	0.10	3044.1	2.44
Strategy #3	4519.3	114468.6	118987.9	5369.7	54.30	174.5	0.15	5544.3	4.45
Mild-summer									
Strategy #1	11565.4	141349.5	152914.9	-	-	-	-	-	-
Strategy #2	8192.1	141911.7	150103.7	3373.3	29.17	-562.2	-0.40	2811.2	1.84
Strategy #3	7578.2	140405.8	147984.0	3987.2	34.48	943.7	0.67	4930.9	3.22
Sunny-summer									
Strategy #1	15222.5	158030.0	173252.5	-	-	-	-	-	-
Strategy #2	11115.5	157765.8	168881.3	4107.0	26.98	264.2	0.17	4371.2	2.52
Strategy #3	10508.4	157228.6	167737.0	4714.1	30.97	801.4	0.51	5515.5	3.18

It can be also found from Table 6.6 that Strategy #2 using the optimal differential pressure set-point can save 26.98-29.57% of the secondary pump energy compared with Strategy #1 using the fixed set-point. The energy savings mainly benefited from the optimal differential pressure set-point that reduces the water resistance of the secondary loop. On the other hand, about 30.97-54.30% of the pump energy can be saved by Strategy #3 when compared with Strategy #1. This is because that Strategy #3 employs both optimal differential pressure set-point and flow-limiting technique. Therefore, about 3.99-24.73% of the pumps energy can be saved due to the use of flow-limiting technique alone. Figure 6.16 provides the detailed comparison of the energy consumption of secondary pumps under three strategies in spring test days.

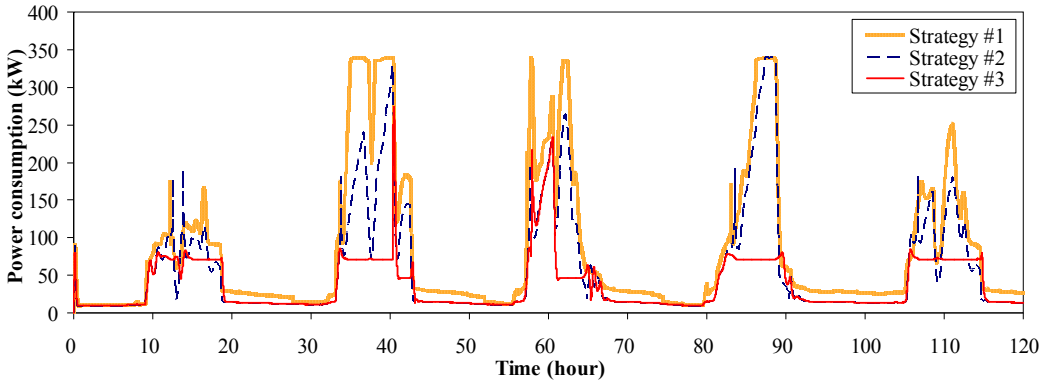

Figure 6.16 Power consumption of secondary pumps using three control strategies in Spring test case (unhealthy system)

Above results show that the deficit flow occurred in the unhealthy system significantly affected the energy performance of the chilled water system when using conventional strategies (Strategy #1 and #2) no matter the set-point was fixed or optimal. The proposed strategy (Strategy #3) using flow-limiting technique was proved to be a fault-tolerant control strategy for secondary pumps in eliminating the deficit flow and enhancing the energy efficiency of pumps. Actually, the proposed strategy cannot diagnose the faults and fully correct them. However, the proposed strategy can relieve the energy waste of pumps caused by deficit flow as far as possible while still satisfying the cooling demand or delivering the highest possible cooling to terminal units.

6.4 Summary

A fault-tolerant control strategy for secondary chilled water pumps is developed not only for eliminating the deficit flow but also for enhancing the energy efficiency of the chilled water distribution systems. This fault-tolerant strategy employs the developed flow-limiting technique that is activated when deficit flow tends to occur

and eliminates it by resetting the differential pressure set-point for pumps control. This strategy also integrates optimal differential pressure set-point that can minimize flow resistance of chilled water loop while still satisfying cooling energy demand.

The operation and energy performance of the proposed fault-tolerant strategy was evaluated on a typical primary-secondary chilled water system in a high-rise building by simulation tests. In a healthy chilled water system, the results indicate that the proposed fault-tolerant strategy can avoid the deficit flow during the start period particularly when not all the chillers are switched on. Compared with the two conventional control strategies, the fault-tolerant strategy can save about 69.27-77.25% of secondary chilled water pump energy consumption during the start period due to the application of flow-limiting technique, which accounts for about 10.57-16.11% of the total energy of pumps and chillers. It also can save about 26.67-49.52 % of the secondary chilled water pump energy during a working day when compared with strategy using fixed differential pressure set-point.

In an unhealthy chilled water system with the occurrence of deficit flow under conventional controls, the proposed fault-tolerant strategy was proved being able to eliminate deficit flow and to improve the energy efficiency of pumps. About 30.97-54.30% of the secondary chilled water pump energy can be saved by using the proposed strategy when compared with the conventional strategy with fixed differential pressure set-point (strategy #1). In this case, about 3.99-24.73% of the secondary chilled water pumps energy saving was contributed by using flow-limiting

technique. This fault-tolerant control strategy is not complex but practical for real in-situ applications. The online implementation and test of the strategy is being conducted in a real high-rise building in Hong Kong.

CHAPTER 7 FAULT DIAGNOSIS AND ENERGY IMPACT EVALUATION OF LOW DELTA-T SYNDROMES

This chapter presents an advanced fault diagnosis strategy for the detection and diagnosis of the low delta-T syndrome resulted from the degraded performances of cooling coils and heat exchangers in building chilled water systems. An energy impact evaluation method for evaluating the energy impact of pumps is also proposed.

Section 7.1 presents the formulation of the proposed FDD strategy and the energy impact evaluation method. Performance indices and their residual thresholds are proposed to diagnose the health condition (normal or fault) of the studied system. Simplified models are employed to establish a benchmark of pump energy consumption. Section 7.2 presents case studies to validate the FDD strategy and the energy impact evaluation method. A summary of this chapter is given in Section 7.3.

7.1 Formulation of the FDD strategy and the energy impact evaluation method

In primary-secondary chilled water systems, the low delta-T syndrome and deficit flow problem often occur when the performances of cooling coils and/or heat exchangers are degraded. For instance, when the performance of the cooling coil is

degraded, such as coil fouling, the heat transfer effect between the inlet air and inlet water is significantly decreased. More chilled water is required and the water temperature difference produced by the coil is decreased when handling the same cooling load. Figure 7.1 shows the required chilled water and water temperature difference of an AHU cooling coil under various cooling load conditions when the water thermal resistance of tubes increased by 20% and 40% respectively. It can be observed that more chilled water was required and lower water temperature difference was produced when a higher level fault was introduced. As a result, more power of pumps was consumed due to the over-supplied water.

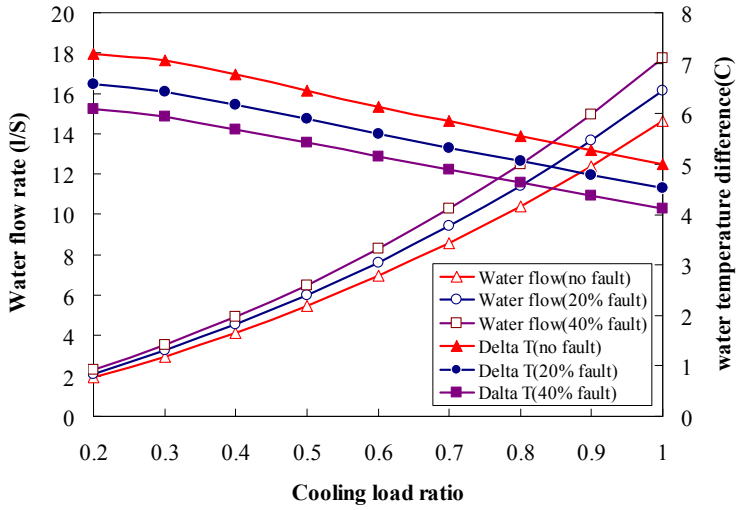

Figure 7.1 Performance of a cooling coil under various load conditions when suffered from faults

Since the water temperature difference produced by cooling coils varies with different cooling load conditions, it is hard to accurately estimate whether a water temperature difference lower than that anticipated occurs or whether the performance of coils are degraded only based on site observations. Therefore, this chapter

presents a fault diagnosis strategy integrated with an energy impact evaluation method to diagnose the low delta-T syndrome and to evaluate the energy impact of pumps. The strategy is developed in the study based on the actual chilled water system presented in Chapter 3. The subsystem of Zone 3 is selected as the example to be studied due to that it is the most complicated subsystem involving heat exchangers, and the other water sub-systems can be considered as the simplifications of such system. The simplified schematic of Zone 3 is illustrated in Figure 7.2.

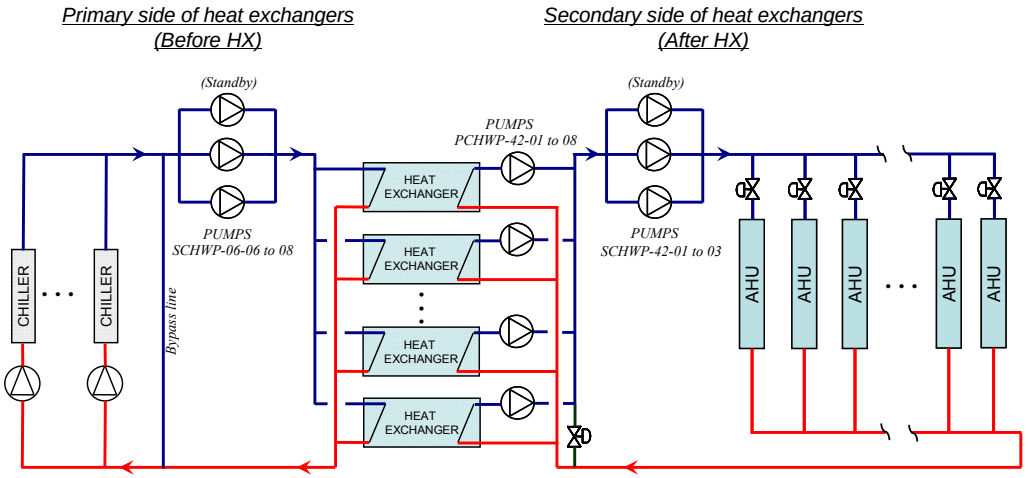

Figure 7.2 Schematic of chilled water system

7.1.1 Outline of the FDD strategy integrated with energy impact evaluation method

The FDD strategy for diagnosing low delta-T syndrome includes a data preprocessor, a fault detection scheme, a fault diagnosis scheme, and an energy impact evaluation scheme, as shown in Figure 7.3. The data measured from HVAC system are firstly preprocessed through outlier removing and data filter. In the fault detection scheme, performance indices (PIs) are calculated using online measurements to characterize

the current status of the system. The reference models of PIs are developed to determine the benchmarks of PIs, which are regressed in advance using the normal operation data. The residuals between the calculated actual PIs and their benchmarks are compared with their online adaptive thresholds to detect the faults. When the residuals of one or more PIs are out of the thresholds, the corresponding PIs are considered in abnormal condition. The adaptive thresholds of PIs can be updated online, which consider both model-fitting errors and measurement errors. Then, the abnormal PIs are further diagnosed and used to identify the specific fault in the fault diagnosis scheme. Lastly, the measured energy consumption of pumps is compared with its benchmark to evaluate pumps energy impact. The benchmark of pumps energy is determined using a model-based method that predicts the energy consumption of pumps in a fault-free system based on the current working condition.

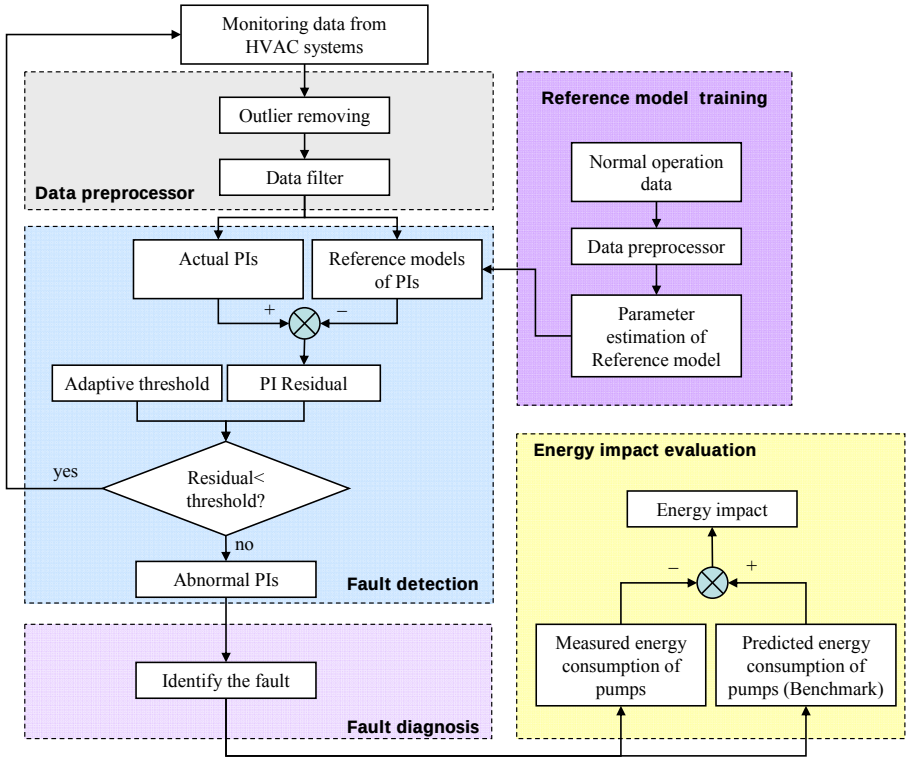

Figure 7.3 Schematic of the FDD strategy integrated with energy impact evaluation

The schematic of the proposed method to determine the benchmark of pump energy is illustrated in Figure 7.4.

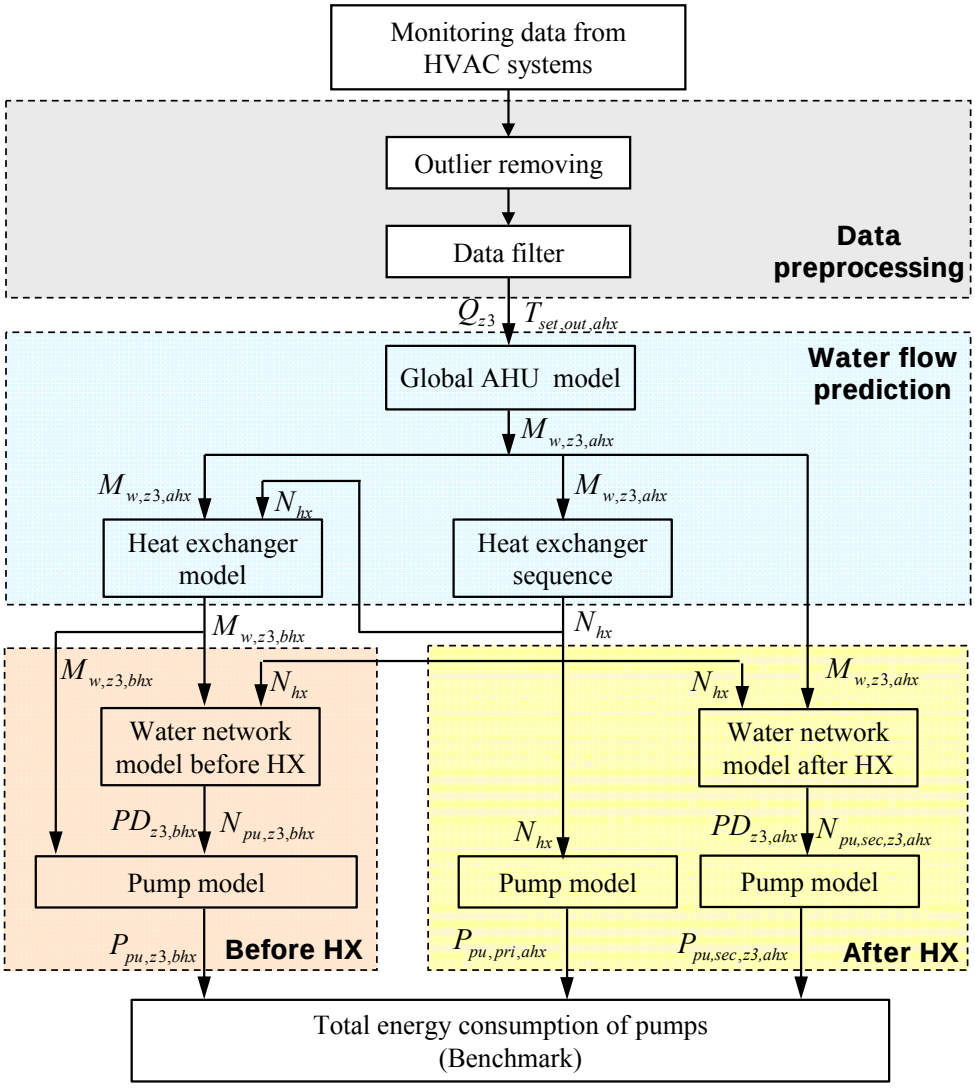

Figure 7.4 Determination of benchmark of pump energy in fault free system

Simplified models are adopted to predict the energy consumption of pumps under various cooling load conditions. For one certain cooling load condition and one certain chiller supply water temperature, the required chilled water flow rate is determined using the global AHU model. The required chilled water at the primary

side of heat exchangers (i.e. before heat exchanger) is determined using heat exchanger model. Besides the measured cooling load, the predefined set-points instead of the measured temperatures (e.g. chiller supply water temperature and outlet water temperature at the secondary side of heat exchangers (i.e. after heat exchangers)) are used to determine the required water flow rate. Lastly, the total energy consumption of pumps is determined using water network models and pump models, which is used as the benchmark of pump energy for evaluating the energy impact of pumps.

The detailed descriptions of the FDD strategy and the energy impact evaluation method are presented in the following as well as the detailed procedures for applications.

7.1.2 Description of the FDD strategy

7.1.2.1 Faults modeling

In order to diagnose the performance degradation of cooling coils and heat exchangers, some performance indices are proposed. The faults under investigation, means of introducing the faults and the proposed performance indices (PIs) are listed in Table 7.1. The dynamic simulation platform in Chapter 3 is used for studying and validating the proposed FDD strategy. Faults are introduced by tuning the parameters of the related component models (i.e. cooling coil or heat exchanger) on the simulation platform. The fault severity levels are introduced by changing quantities

of the parameters. Two severity levels for each fault are investigated in this study.

Table 7.1 Faults, fault modeling and mathematical PI formulations

Fault	Means of introducing faults	Performance indices (PIs)	PIs formulation
AHU cooling coil degradation	Increase thermal resistance at water side	Water temperature difference	$\Delta T_{w,AHU} = T_{w,out,AHU} - T_{w,in,AHU}$
		Overall conductance–area product	$UA_{AHU} = \frac{Q_{tot,AHU}}{LMTD}$
Heat exchanger degradation	Decrease the heat transfer coefficient	Water temperature difference	$\Delta T_{w,bhx} = T_{w,out,bhx} - T_{w,in,bhx}$
		Overall conductance–area product	$UA_{HX} = \frac{Q_{tot,HX}}{LMTD}$

In this study, the fault, cooling coils degradation in AHU, is introduced by increasing the thermal resistance at water side artificially by two levels respectively (i.e., water thermal resistance is increased by 20% and 40%). The water temperature difference ($\Delta T_{w,AHU}$) produced by AHU cooling coils and the overall conductance–area product (UA_{AHU}) are selected as the performance indices to identify the fault. It should be pointed out that the performance index of $\Delta T_{w,AHU}$ is used to diagnose whether an abnormal water temperature difference exists, and the performance of UA_{AHU} is used to determine whether the heat transfer capacity of coils are degraded. For a given cooling load ($Q_{tot,AHU}$), the degradation of UA_{AHU} will result in more chilled water required to handle the cooling load, and thus cause a lower water temperature difference (ΔT_{AHU}) produced by the AHU.

Performance degradation of heat exchangers is introduced by reducing the overall conductance–area product (UA_{HX}) artificially in two quantities (i.e., UA_{HX} is reduced by 20% and 40%). The water temperature difference ($\Delta T_{w,bhx}$) before heat exchangers

and UA_{HX} are selected as the performances indices to identify the fault. When UA_{HX} is reduced, more chilled water is required before heat exchangers to transfer the same cooling energy for lowering down the water temperature after heat exchangers. Consequently, the water temperature difference before heat exchangers ($\Delta T_{w,bhx}$) is reduced.

7.1.2.2 Reference models of performance indices

Reference models of the performance indices are proposed to characterize the operation of a fault-free chilled water system. The studied AHU system is a variable air volume (VAV) system, which controls the outlet air temperature at predefined set-point. The water temperature difference ($\Delta T_{w,AHU}$) is strongly dependent on the cooling load (Q_{AHU}), the inlet water temperature ($T_{w,in,AHU}$) and the inlet air temperature ($T_{a,in,AHU}$). The reference model for $\Delta T_{w,AHU}$ can be expressed as Equation (7.1). Similarly, the overall conductance–area product of AHU (UA_{AHU}) can be set up as Equation (7.2).

$$\Delta T_{w,AHU} = a_0 \cdot Q_{AHU}^{a_1} \cdot T_{w,in,AHU}^{a_2} \cdot T_{a,in,AHU}^{a_3} \tag{7.1}$$

$$UA_{AHU} = b_0 \cdot Q_{AHU}^{b_1} \cdot T_{w,in,AHU}^{b_2} \cdot T_{a,in,AHU}^{b_3} \tag{7.2}$$

For the heat exchanger system, the cooling load (Q_{HX}), the inlet water temperature at the primary and secondary sides of heat exchangers ($T_{w,in,bhx}$ and $T_{w,in,ahx}$), and the water flow rates at primary and secondary sides of heat exchangers ($M_{w,in,bhx}$ and $M_{w,in,ahx}$) are selected to form the reference model of the temperature difference of

water at primary side of heat exchangers ($\Delta T_{w,bhx}$), as shown in Equation (7.3). Since the overall conductance–area product (UA_{HX}) of heat exchangers is only dependent on the water flow rates primary and secondary sides of heat exchangers, Equation (7.4) is used as the reference model of UA_{HX}.

$$\Delta T_{w,bhx} = c_0 \cdot Q_{HX}^{c1} \cdot T_{w,in,bhx}^{c2} \cdot T_{w,in,ahx}^{c3} \cdot M_{w,bhx}^{c4} \cdot M_{w,ahx}^{c5} \tag{7.3}$$

$$UA_{HX} = d_0 \cdot M_{w,bhx}^{d1} \cdot M_{w,ahx}^{d2} \tag{7.4}$$

The coefficients (i.e., a_0–a_3, b_0–b_3, c_0–c_5, d_0–d_2) used in the reference models are constant, which can be determined by linear regression method using the fault-free operation data obtained from the BMS.

7.1.2.3 Estimation of threshold

The residual threshold is used in the FDD strategy to determine whether the performance indices are in abnormal conditions. When the residuals of performance indices exceed the threshold, it means the PIs are in abnormal condition. The uncertainty of residuals is highly affected by the prediction uncertainty of the reference models and the calculation uncertainty of performance indices under various working conditions. Adaptive thresholds are used that vary with working conditions when given certain confidence levels. The method to determine the adaptive thresholds are based on the study of Cui and Wang [2005], which can be briefly introduced as below.

Under a certain confidence level, the threshold of PI residuals can be determined by

Equation (7.5).

$$Th_i = U(\tilde{r}_i) = t_{\alpha/2,n-p}\tilde{\sigma}_{\tilde{r}_i - r_i} \tag{7.5}$$

Where, Th_i is the threshold of the ith PI residual, $\tilde{r}_i$ is the estimator of the residual of the ith performance index. The residual (r_i) is the difference between the measurement and model predicted value of the ith performance index. $U(\tilde{r}_i)$ is the uncertainty of the residual at a certain confidence level. $\tilde{\sigma}^2_{\tilde{r}_i - r}$ is the estimated variance of $\tilde{r}_i - r_i$, which is determined by Equation (7.6). $t_{\alpha/2,n-p}$ is the value of the t distribution with n-p degrees of freedom at a confidence level of (1-α). n is the number of training data points used in the model regression and p is the number of coefficients estimated from the training data.

$$\tilde{\sigma}^2_{\tilde{r}_i - r_i} = \underbrace{\sum_j \left[\left(\frac{\partial g_i}{\partial z_j}\right)\sigma_{z_j}\right]^2}_{\textit{Uncertainty 1}} + \underbrace{\tilde{\sigma}^2_{Y_i}[1 + \mathbf{X}_0^T(\mathbf{X}_{reg}^T\mathbf{X}_{reg})\mathbf{X}_0]}_{\textit{Uncertainty 2}} \tag{7.6}$$

where, g_i is the formula for calculating the ith performance index as shown in Table 7.1. z_j is the jth element in the vector of measured variables (**z**), which is used to calculate the ith performance index (Y_i). σ_{z_j} is the standard deviations of z_j and $\tilde{\sigma}^2_{Y_i}$ is the estimated variance of the regression error of ith performance index(Y_i). $\mathbf{X}_0$ is the vector of regressor for the current prediction and $\mathbf{X}_0^T$ is the transpose of $\mathbf{X}_0$. $\mathbf{X}_{reg}$ is the matrix of regressor associated with the training data and $\mathbf{X}_{reg}^T$ is the transpose of $\mathbf{X}_{reg}$. *Uncertainty 1* is measurement uncertainty and *Uncertainty 2* is

modeling uncertainty.

7.1.3 Description of the energy impact evaluation method

The energy impact evaluation method is developed to evaluate the energy performance of chilled water pumps when the low delta-T syndrome occurs in the chilled water system. The measured power of pumps is compared with the estimated benchmark to determine how much energy is wasted due to the occurrence of the low delta-T syndrome. The benchmark of pump energy is the energy consumption of pumps in a fault-free system (i.e., there is no low delta-T syndrome), which varies with the cooling load. Simplified models are adopted to predict pump energy, including the global AHU model, the water network model, heat exchanger model and pump model. Only the global AHU model is described in detail as below. Other models are the same as those presented in Chapter 5.

7.1.3.1 Global AHU model

The global AHU model is developed to predict the benchmark of the total chilled water flow of AHUs. In this studied HVAC system, the inlet/outlet air temperature and the inlet water temperature of AHUs are modulated to maintain their predefined set-points respectively. For a given cooling load, the benchmark of the total required chilled water flow ($M_{w,AHus}$) of AHUs is more dependent on the cooling load (Q_{AHUs}) when the parameters of the air side and inlet water temperatures are fixed, as shown in Equation (7.7).

$$M_{w,AHUs} = e_0 \cdot (Q_{AHUs})^{e_1} \quad (7.7)$$

For online applications, three parameters (e_0, e_1, e_2) in this model need be identified in advance by linear regression method. It is noted that the water flow rate determined by this model is based on the measured cooling load and the predefined set-point of the AHU inlet water temperature instead of the measured actual AHU inlet water temperature.

7.1.3.2 Models of water network of heat exchangers

The water network models are used for calculating the water network pressure drop before and after heat exchangers respectively. The input data of the models are the water flow rate, operating number of heat exchangers, operating number of pumps, the currently measured pump head and measured total water flow rate. The detailed descriptions of the two models are presented previously in Section 5.2.4.

7.1.3.3 Heat exchanger model and Pump model

The heat exchanger model is used to predict the required water flow rate before heat exchangers when the water flow rate after heat exchangers is given. It uses the ε-NTU method based on the basic principle of thermodynamics. The input data of this model are the measured cooling load, the water flow rate after heat exchangers, the operating number of heat exchangers, and the inlet water temperature before heat exchangers. The detailed description of this model is presented previously in Section 5.2.4. It is noted that the used input parameter of inlet water temperature before heat

exchangers is the predefined set-point of chiller supply water temperature rather than the measured inlet water temperature before heat exchangers.

The pump model is used to predict the energy consumption of pumps when the total water flow rate through pumps and the pump head are known. In this study, the performance of variable speed pumps is modeled using a series of polynomial approximations, including polynomials representing head versus flow and speed, and efficiency versus flow and speed. The detailed description of this model is presented previously in Section 5.2.4.

7.1.3.4 Sequence control strategy of heat exchanger and pump

The determinations of the required operating number of heat exchangers and pumps are based on the sequence control strategy of heat exchanger and pump in the HVAC system studied.

For heat exchangers, the required operating number is reset to be twice as many as the operating number of secondary pumps after heat exchangers. For secondary variable speed pumps, an additional pump is switched on when the frequencies of operating pumps exceed 90% (corresponding to 45Hz) of their nominal capacity. One of the operating pumps is switched off when the frequencies of the operating pumps are lower than 60% (corresponding to 30Hz) of the nominal capacity. For primary constant speed pumps after heat exchangers, their operating number is the same as the operating number of the heat exchangers.

7.1.4 The detailed application procedures

For online applications, the FDD strategy aims to diagnose the low delta-T syndrome resulted from the performance degradation of cooling coils and heat exchangers. The energy impact of pumps is evaluated as well. The detailed application procedure is illustrated as below (also illustrated earlier in Figure 7.2 and 7.3).

(1) Check the measurements using a data preprocessor;

(2) Compute each actual performance index and their reference models using the measured data;

(3) Compute the residual of each performance index;

(4) Determine the residual threshold of each performance index;

(5) The performance indices whose actual residuals excess their thresholds are determined to be abnormal;

(6) Identify the fault according to the deviation of each performance index;

(7) Compute the benchmark of pump energy using the models in Section 7.1.3;

(8) Determine the energy impact of pumps by comparing the measured pump energy consumption with the benchmark.

7.2 Validation and discussion

7.2.1 Setup of the test platform

The proposed FDD strategy is validated on the dynamic simulation platform presented in Chapter 3. Only Zone 3 and two chillers of the super high-rise building

are included in this simulation platform as shown in Figure 7.2. This is a typical primary-secondary chilled water system. Two water cooled centrifugal chillers are installed to generate the chilled water of 5.5°C under design condition. Each chiller is associated with a constant speed primary pump. In the secondary loop, heat exchangers are used to transfer the cooling energy from the chillers to the terminal units. After each heat exchanger, a primary constant speed pump is installed to ensure the constant flow through each heat exchanger. All the secondary pumps are equipped with VFDs. The AHU valves are modulated to maintain the supply air temperature at its set-point (i.e. 13°C). The AHU fans are also equipped with VFDs to vary supply air flow rate and the VAV boxes are modulated to maintain the indoor air temperature at a fixed set-point (i.e. 23°C). The entire simulation platform is developed using TRNSYS 16. The weather data used is the data of the typical year in Hong Kong.

7.2.2 Validation and discussion of the FDD strategy

7.2.2.1 Validation of reference models

The reference models developed in this study were trained using operation data in normal condition (i.e. fault-free condition) under various working conditions. Figure 7.5 and 7.6 present the validation results by comparing the predicted performance indices (determined by reference models) with the calculated ones (determined by equations in Table 7.1). It can be seen that most of the predicted values agreed well with the calculated ones, which indicates that the reference models have acceptable

performances in prediction.

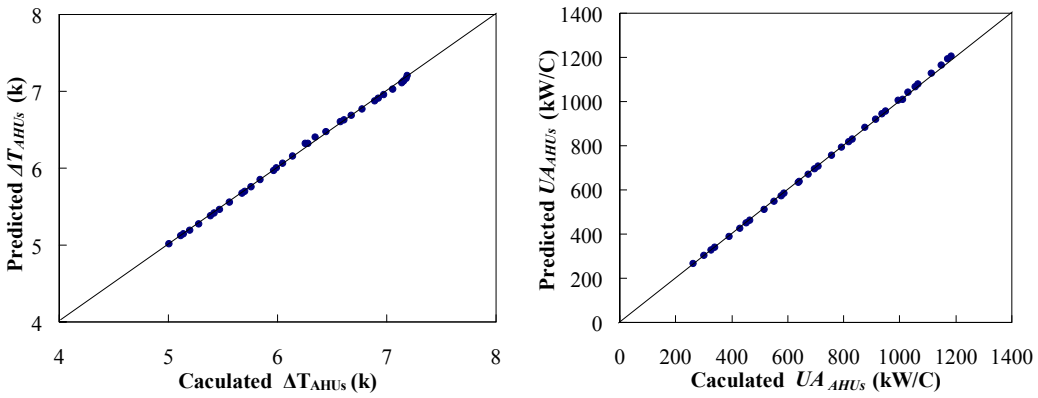

Figure 7.5 Validation results of reference models of AHUs

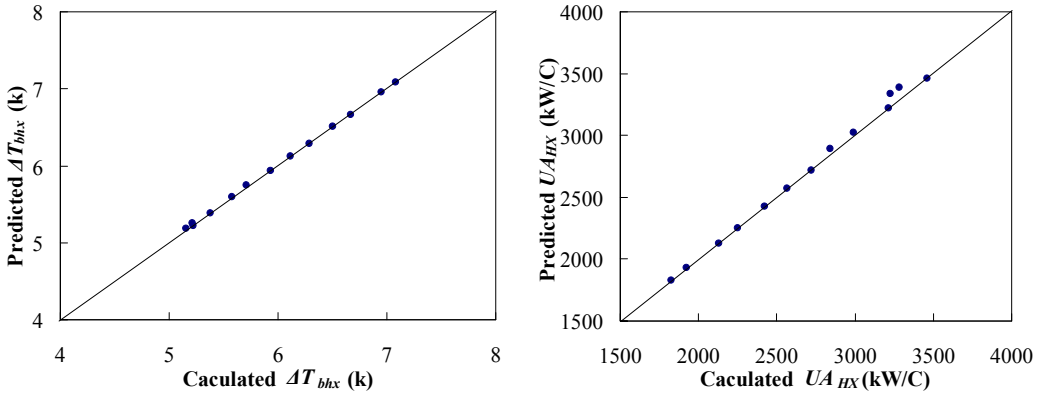

Figure 7.6 Validation results of reference models of heat exchangers

7.2.2.2 Validation of FDD strategy

The dynamic simulation platform of Section 7.2.1 was used to generate operation data for validating the FDD strategy. Three typical days (8:00am to 18:00pm) were selected to represent the chilled water system working under Spring, Mild-Summer and Sunny-Summer days. The system cooling loads under the three typical weather conditions are shown in Figure 7.7. The faults introduced in the simulation tests separately include AHU coils degradation (simulated by increasing thermal

resistance of water side) and heat exchangers degradation (simulated by reducing heat transfer coefficient). During each test day, two severity levels of each fault were introduced separately in increasing order. 30 samples points under each fault level were selected in each test day. The residuals of the performance indices were calculated using the measured data and then compared with their thresholds.

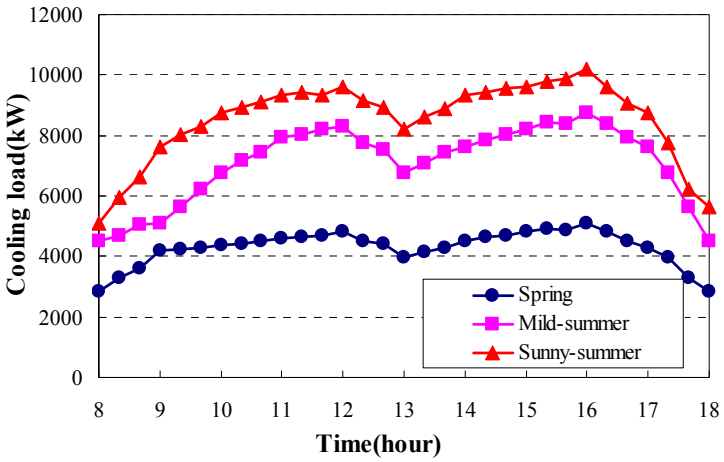

Figure 7.7 Cooling load profiles of three typical days

Figure 7.8 and 7.9 show the residuals of performance indices and their thresholds in the global AHU system when the water thermal resistance of coils was increased by 40% (level 1) and 80% (level 2) respectively. The residual of delta-T means the deviation of the measured system water temperature difference from the expected normal level. It can be observed in Figure 7.8 that delta-T was a very sensible performance index that could be detected easily when the system experienced low delta-T syndrome. When the faulty severity level increased, larger deviations of delta-T occurred. It is worth noticing that a deviation greater than 2°C occurred in the Mild-Summer day (Level 2) and in the Sunny-Summer day (Level 1). The reason is that the outlet air temperature of AHUs could not be maintained at the predefined

set-point when the heat transfer capacity of AHUs were degraded, which in turn resulted in more supplied chilled water and lower water temperature difference.

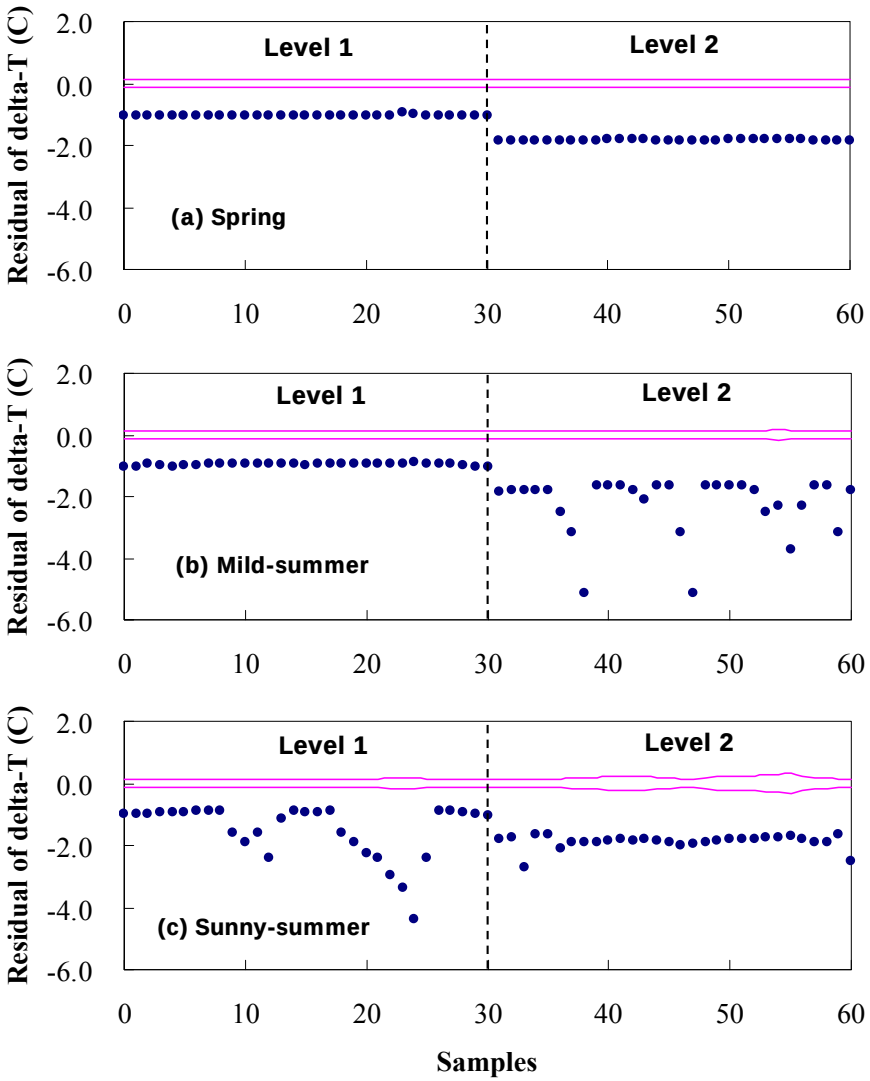

Figure 7.8 Residuals of PI (delta-T) of global AHUs

Compared to the performance index of delta-T of AHUs, the performance index of UA are less sensitive to the detection of coil degradation. As shown in Figure 7.9, the residuals of UA were very close to the thresholds under the faulty severity of Level 1 (particularly in Spring day) although the detection rate of UA is near 100%. When the faulty severity level was increased to Level 2, a larger deviation from the

threshold was achieved, which made the diagnosis more easily.

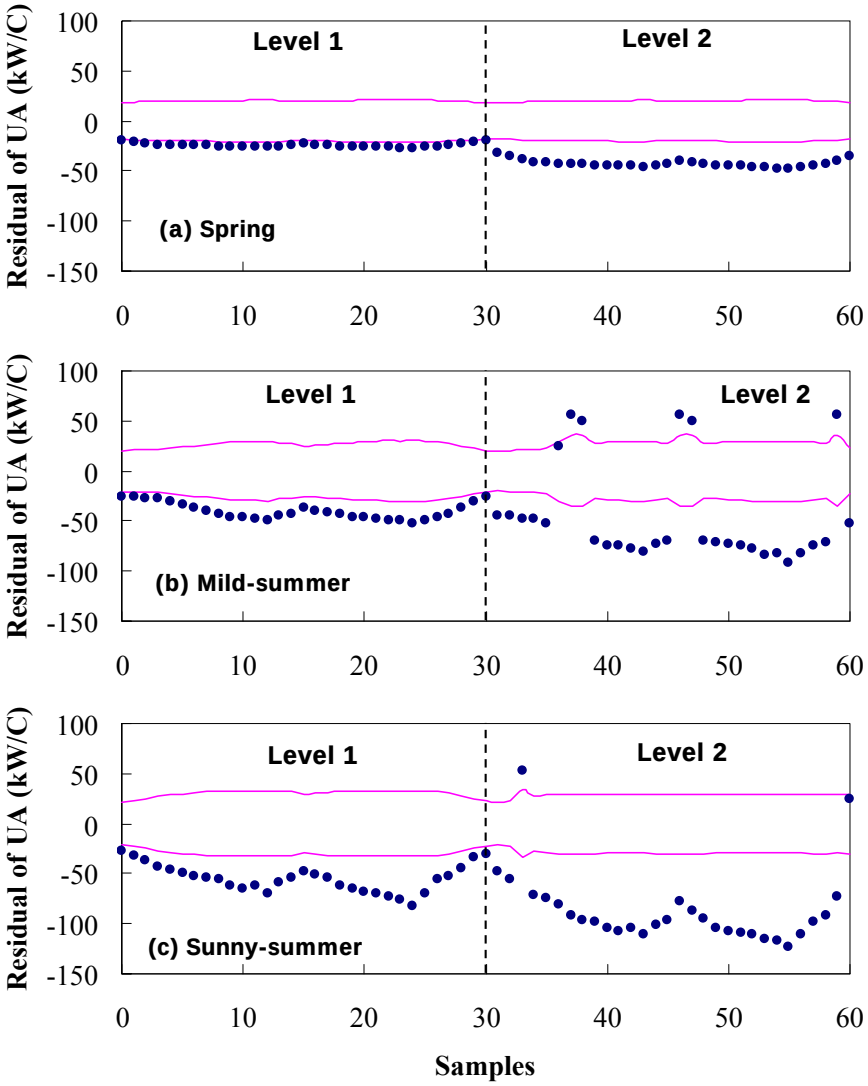

Figure 7.9 Residuals of PI (UA) of global AHUs

Figures 7.10 and 7.11 show the PI residuals and their thresholds of the heat exchanger system when the heat transfer efficiency was decreased by 20% (level 1) and 30% (level 2) respectively. It is obvious that both PIs of ΔT_{bhx} and UA_{HX} are sensitive to the degradation of heat transfer efficiency at two levels. ΔT_{bhx} residual deviated obviously from its threshold, which indicates that the water temperature difference at the primary side of the heat exchangers was lower than the expected

normal value (i.e., low delta-T syndrome occurs). It is noted that there are several points whose deviations are lager than 2°C of Mild-Summer day in Figure 7.10. This is because that the deficit flow before heat exchangers was triggered under those working conditions due to that the outlet water temperature after heat exchangers could not be maintained at its set-point.

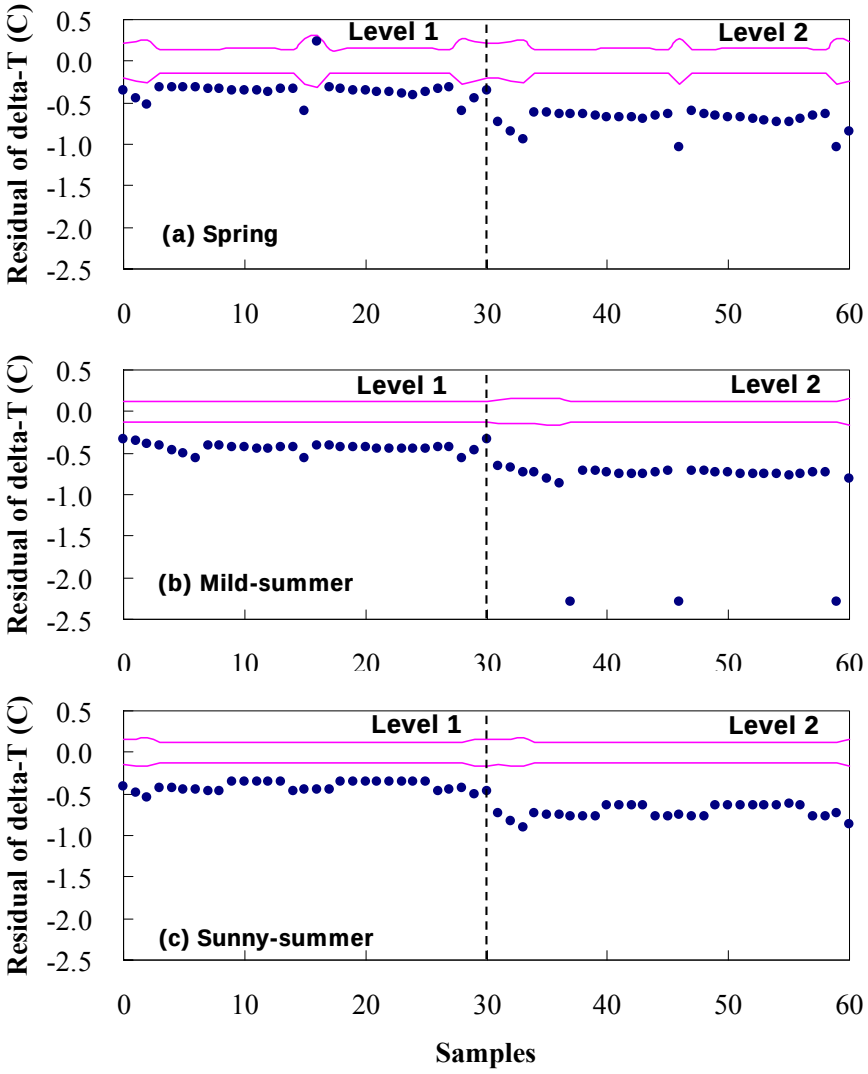

Figure 7.10 Residuals of PI (delta-T) of heat exchangers

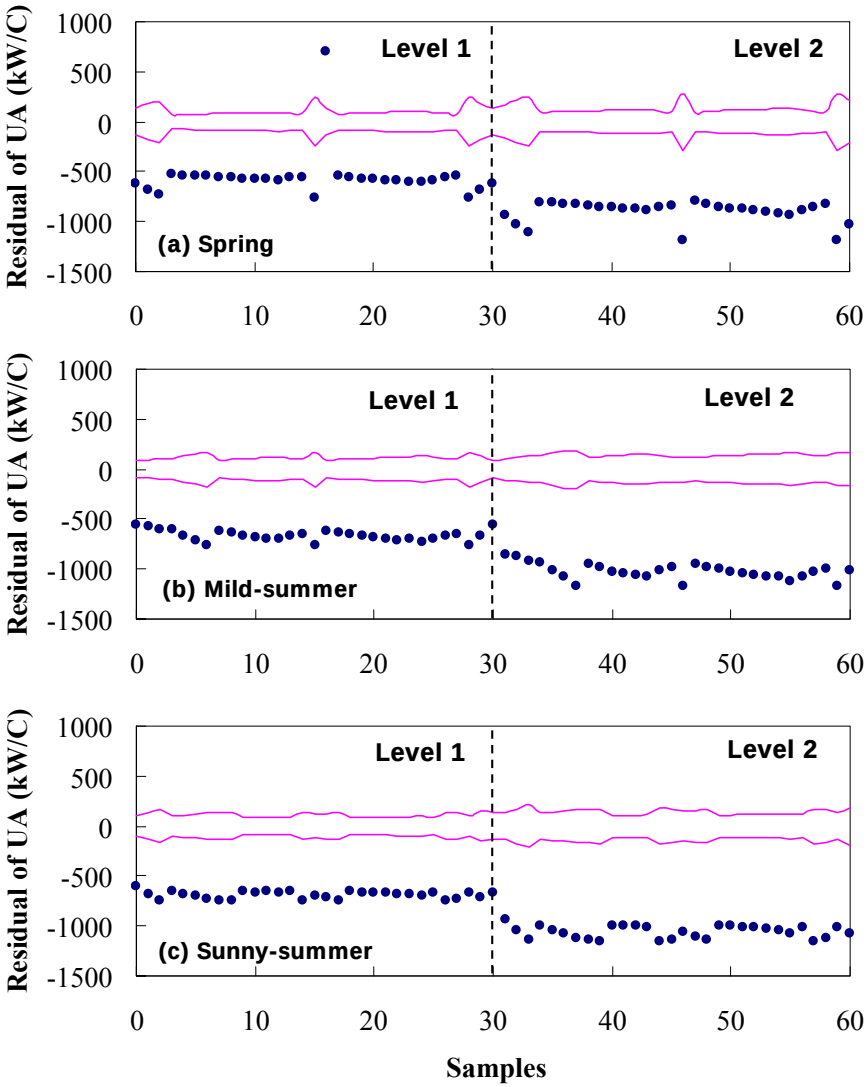

Figure 7.11 Residuals of PI (UA) of heat exchangers

The detailed quantitative validation results are summarized in Table 7.2, where the detection ratio of a performance index is a percentage of the point number outside of the threshold among the total point number. Obviously, most of the detection ratios of performance indices are near 100%, which means the faults can be successfully detected and diagnosed using the proposed FDD strategy under the faulty severity levels defined in this study.

Table 7.2 Summary of the detection ratios of proposed performance indices

Faults of Sub-systems	Performance indices	Spring		Mild-summer		Sunny-summer	
		Level 1	Level 2	Level 1	Level 2	Level 1	Level 2
AHU coils degradation	ΔT_{AHUs}	100%	100%	100%	100%	100%	100%
	UA_{AHUs}	100%	100%	100%	96.8%	100%	96.8%
Heat exchanger coils degradation	ΔT_{bhx}	96.8%	100%	100%	100%	100%	100%
	UA_{HX}	100%	100%	100%	100%	100%	100%

7.2.3 Validation and discussion of the energy impact evaluation method

The proposed energy impact evaluation method aims at evaluating the energy performance of pumps when faults occur in the water system. The benchmark of the total energy consumption of pumps is predicted based on the current cooling load, which represents the ideal energy consumed by pumps when the chilled water system works in fault-free condition. The energy impact of pumps is determined by comparing the measured total energy consumption with the predicted benchmark. Besides the measured cooling load, the following fixed parameters are used in predicting the benchmark of pump energy, including the supply air temperature (13°C), the outlet water temperature after heat exchangers (6.3°C), and the inlet water temperature before heat exchangers (5.5°C).

7.2.3.1 Accuracy of the proposed method

The prediction accuracy of the pump energy benchmark is validated by comparing the predicted pump energy (determined by the proposed method) with the ideal results ("measured" from the simulation platform) when the system is in fault-free operation. Three typical working conditions were selected to represent the chilled

water system working under Spring, Mild-Summer and Sunny-Summer days. Under the given cooling load, the proposed method predicted the energy consumptions of secondary pumps before heat exchangers, primary pumps after heat exchangers, and the secondary pumps after heat exchangers.

Table 7.3 Comparison between performance data using the proposed method and in the idea tests

Items	Seasons					
	Spring		Mild-summer		Sunny-summer	
Typical working conditions						
Cooling load (kW)	4646.48		7350.88		10149.52	
Chiller operating number	1		2		2	
Chiller supply water temperature (°C)	5.50		5.50		5.50	
Items	Methods					
	Proposed (predicted)	Ideal tests ("measured")	Proposed (predicted)	Ideal tests ("measured")	Proposed (predicted)	Ideal tests ("measured")
prediction results						
$M_{w,AHUs}$ (l/s)	170.89	166.76	301.62	300.76	461.32	465.08
$N_{pu,sec,bhx}$	1	1	1	1	2	2
$N_{pu,sec,ahx}$	1	1	2	2	2	2
$N_{pu,pri,ahx}$	2	2	3	3	4	4
N_{hx}	2	2	3	3	4	4
$P_{pu,sec,bhx}$ (kW)	15.6	14.82	61.99	60.79	85.06	88.47
$P_{pu,sec,ahx}$ (kW)	40.48	37.38	83.08	79.55	168.44	172.29
$P_{pu,p,iahx}$ (kW)	89.4	89.4	134.1	134.1	178.8	178.8
Total (kW)	145.48	141.6	279.17	274.44	432.3	439.56
Deviation*(kW)	3.88 (2.74%)	-	4.73 (1.72%)	-	-7.26 (-1.65%)	-

*Value in parentheses indicates the percentage of the prediction deviates from the measurements

Table 7.3 compares the prediction results using the proposed method (predicted values) with the results in ideal tests ("measured" values). It can be observed that the proposed method can accurately predict the energy consumption of pumps. The total

power consumptions of pumps predicted by the proposed method agreed well with that of the ideal tests under the three working conditions. The maximum relative difference between the two methods was only about 2.74%. The operating numbers of pumps and heat exchangers predicted by the proposed method were also the same as those in the ideal tests.

7.2.3.2 Energy impact evaluation of pumps

The proposed method is implemented to evaluate the energy impact of pumps in the simulation platform when different severity levels of faults are introduced. Figures 7.12–7.14 compares the total pump energy consumptions under different fault levels in the typical Spring day, Mild-Summer day and Sunny-Summer day respectively. The power consumption predicted by the proposed method is used as the benchmark for comparison. It is obvious that significant energy of pumps were wasted when performances of AHUs and heat exchangers were degraded. More energy was consumed when the faulty severity level was increased. It also can be found that the faults of AHU degradation had more effect on the energy consumption than the faults of heat exchanger degradation. It is worthy noticing that there were several sudden increases of pump energy in the Mild-Summer and Sunny-Summer test cases. The reason was that the deficit flow was triggered under those working conditions when the outlet water temperature could not be maintained due to the faults.

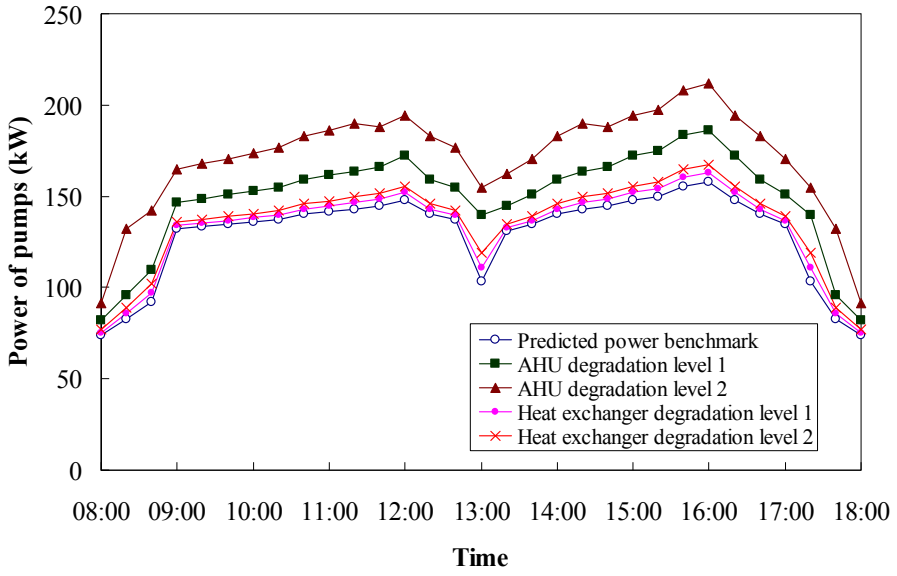

Figure 7.12 Power consumptions of pumps in the Spring test case

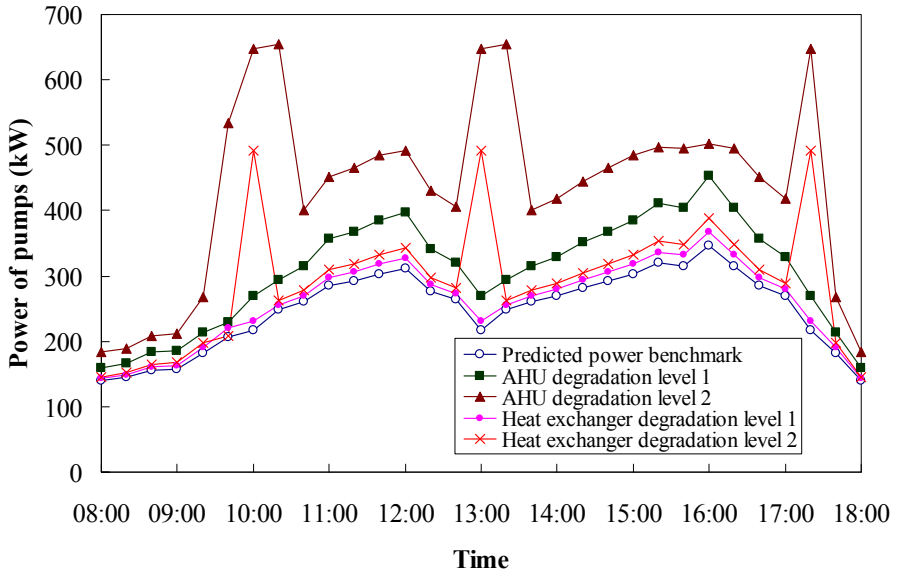

Figure 7.13 Power consumptions of pumps in the Mild-Summer test case

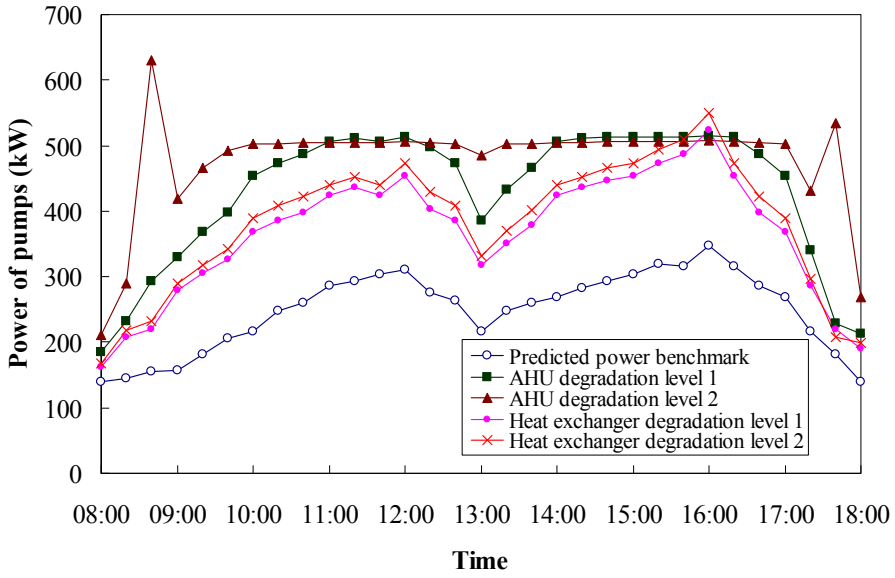

Figure 7.14 Power consumptions of pumps in the Sunny-Summer test case

Table 7.4 summaries the daily (between 8:00am and 18:00pm) energy impacts of pumps under different faults levels in the three typical days. The maximum energy impact of pumps occurred in the mild-summer test case when the AHU degradation was increased to Level 2. About 75.22% of the total pumps energy was wasted when comparing to the benchmark. It is also showed that the energy impact resulted from heat exchanger degradation was mainly contributed by the secondary pumps before heat exchangers. The energy impact due to AHU degradation was mainly contributed by the secondary pumps after heat exchangers particularly under low fault level.

Table 7.4 Daily energy consumption of pumps under different faults levels in three typical days

Strategies	$P_{pu,sec,bhx}$ (kWh)	$P_{pu,pri,ahx}$ (kWh)	$P_{pu,sec,ahx}$ (kWh)	Total (kWh)	$P_{pu,sec,bhx}$ impact (kWh)	(%)	$P_{pu,pri,ahx}$ impact (kWh)	(%)	$P_{pu,sec,ahx}$ impact (kWh)	(%)	Total impact (kWh)	(%)
Spring												
Predicted benchmark	152.58	819.50	363.66	1335.74	-	-	-	-	-	-	-	-
AHU degradation												
Level 1	219.34	849.30	471.00	1539.64	66.76	43.75	29.8	3.64	107.34	29.52	203.9	15.26
Level 2	292.00	894.00	583.26	1769.26	139.42	91.38	74.5	9.09	219.6	60.39	433.52	32.46
Heat exchanger degradation												
Level 1	187.27	819.50	363.66	1370.43	34.69	22.74	0	0	0	0	34.69	2.60
Level 2	220.77	819.50	363.67	1403.94	68.19	44.69	0	0	0	0	68.2	5.11
Mild-summer												
Predicted benchmark	449.75	1221.80	897.80	2569.35	-	-	-	-	-	-	-	-
AHU degradation												
Level 1	648.99	1235.63	1281.40	3166.02	199.24	44.30	13.83	1.13	383.6	42.73	596.67	23.22
Level 2	1116.01	1653.90	1732.01	4501.92	666.26	148.14	432.1	35.37	834.21	92.92	1932.57	75.22
Heat exchanger degradation												
level 1	563.45	1221.80	897.80	2683.05	113.7	25.28	0	0	0	0	113.7	4.43
level 2	839.19	1266.50	926.04	3031.73	389.44	86.59	44.7	3.66	28.24	3.15	462.38	18.00
Sunny-summer												
Predicted benchmark	747.97	1490	1379.40	3617.38	-	-	-	-	-	-	-	-
AHU degradation												
Level 1	970.39	1624.10	1849.63	4444.12	222.42	29.74	134.1	9.00	470.23	34.09	826.74	22.85
Level 2	1103.02	1773.10	2065.30	4941.42	355.05	47.47	283.1	19.00	685.9	49.72	1324.04	36.60
Heat exchanger degradation												
Level 1	926.01	1490.00	1379.40	3795.41	178.04	23.80	0	0	0	0	178.03	4.92
Level 2	1099.96	1490.00	1379.41	3969.37	351.99	47.06	0	0	0	0	351.99	9.73

7.3 Summary

A fault diagnosis strategy integrated with an energy impact evaluation method is presented, which is used for detecting and diagnosing the low delta-T syndrome resulted from the performance degradation of cooling coils and heat exchangers in chilled water systems. The energy impact of pumps due to the low delta-T syndrome is also evaluated. Performance indices and adaptive thresholds are adopted in the FDD strategy to determine the health condition of the system. Simplified models are adopted in the energy impact evaluation method to determine the energy impact caused by the low delta-T syndrome.

The proposed FDD strategy and the energy impact evaluation method were validated in a dynamic simulation platform representing a complex HVAC system. The results show that the proposed FDD strategy can detect the low delta-T syndrome and identify the faults. The results also show that the proposed energy impact evaluation method can accurately determine the energy impact of pumps by comparing the measured pump energy with the benchmark.

CHAPTER 8 EXPERIMENTAL TEST FOR ENHANCING CHILLED WATER SYSTEM PERFORMANCE USING A CHECK VALVE

Since low delta-T syndrome and deficit flow problem significantly degrade the overall performance of chilled water systems, using a check valve (i.e., putting a one-direction check valve in the chilled water by-pass line) to eliminate the deficit flow has received wide attention and open discussion for decades. This chapter presents an experimental validation of using a check valve in the studied super high-rise building to solve the deficit flow problem and thus to enhance the overall operational performance.

Section 8.1 presents a brief overview of the implementation of check valve discussed in the existing studies. Section 8.2 introduces the experimental methodology for implementing check valve in a chilled water system. In Section 8.3, the experiment results are presented. A summary of this chapter is provided in Section 8.4.

8.1 An overview of the implementation of check valve

In order to solve the low delta-T problems and achieve energy conservation, many methods with different degrees of promise have been proposed [Kirsner 1996 and 1998, Avery 1998, McQuay 2002, Taylor 2002, Durkin 2005, Fiorino 1999, Avery 2001]. Among them, the use of a check valve (i.e., putting a one-direction check

valve in the by-pass line) received wide attention and open discussion. The check valve allows the surplus flow but doesn't allow the deficit flow and therefore, can avoid the chilled water from chillers to be contaminated. The major benefit of using the check valve is that an additional chiller is not brought online simply to provide additional primary flow before the operating chillers are fully loaded [Severini 2004]. Severini [2004] described that his philosophy for designing and operation of primary-secondary chiller plants included using a check valve, which has been proved successfully in many projects. Based on a parametric study, Bahnfleth and Peyer [2004] presented that the addition of a check valve to a primary-secondary system can result in a total plant energy saving of up to 4% and a life cycle cost saving of up to 2%. Savings occurred only when the chilled water temperature differences were less than the design value. The authors pointed out that if the secondary pumps are not capable of handling the increased head and flow in the primary loop, the use of the check valve will be an unacceptable option as a retrofit. Kirsner [1998] presented that the use of a check valve is a cheap and simple improvement to the primary-secondary system. It allows a plant to efficiently deal with the low delta-T syndrome while preserving the protective features of the primary-secondary design. Avery [1998] installed a check valve in a real cooling plant for system retrofits and upgrading. The actual operation results showed that as much as 20% chiller plant energy and 28% annual chiller utilization hours were reduced due to the inclusion of the check valve as compared with that prior to the installation of the check valve. Taylor [2002, 2002] presented that the use of a check

valve is recommended for fixed speed chiller plants, but not recommended for variable speed chiller plants since the efficiency of variable speed chillers is high at part-load conditions. The author pointed out that one disadvantage of having a check valve is that if the primary pumps are off and chiller isolation valves are closed while the secondary pumps are on, the secondary pumps will be deadheaded. This can be avoided by shutting off the secondary pumps whenever all primary pumps are switched off.

Compared to above studies recommended to use check valves, several studies [McQuay 2002, Luther 2002, Coad 1998] argued that the use of the check valve will destroy the philosophy of the primary-secondary designs and designers will fell uncomfortably with forcing pumps into series operation and hence, the inclusion of a check valve was not recommended as part of the design of the primary-secondary systems. However, these studies failed to provide any persuasive proof indicating that the use of a check valve is not feasible. The application guide of McQuay [2002] stated that adding a check valve effectively makes the system variable primary flow during low delta-T intervals and the system control will become more complicated. Rishel [1998] presented that the low delta-T central plant syndrome is a complicated problem that cannot be easily fixed by using a check valve and the check valve is not suitable for all primary-secondary systems, such as for the systems utilizing special energy storage systems or water side economizers, etc.

As every coin has two sides, there is also no universal conclusion that whether the

use of a check valve is a good practice and is worthy of consideration to deal with the low delta-T syndrome in a particular primary-secondary system. It is also noted that the studies supporting to use the check valves failed to provide the details how the check valve can help to deal with the low delta-T problems and achieve energy efficient operation. This Chapter presents an experimental approach for validating the feasibility of using a check valve to solve the low delta-T problems, prior to the real installation of a check valve. The aim of this study is to provide some useful reference for properly using check valves if they are considered to be adopted to deal with the low delta-T syndrome in a chilling plant. The experimental tests were carried out on the complex chilled water system in a super high-rise building in Hong Kong by using a 'simulated' check valve by fully closing one of the butterfly valves in the chilled water by-pass line when the system operated with significant excess flow demand and experienced the low chilled water temperature differences.

8.2 Experimental methodology

The studied central chilled water plant, which is detailed introduced in Chapter 3, frequently suffered from low delta-T syndrome and deficit flow problem. Figure 8.1 and Figure 8.2 present the measured cooling capacity of the operating chiller, and measured water flow rate in the by-pass line and measured chilled water temperature difference in the secondary system (i.e., namely system temperature difference) in two consecutive winter days, respectively. It can be observed that the deficit flow existed in most of day time operation while the operating chillers were far from be

sufficiently loaded. As shown in Figure 8.1, the actual cooling energy provided by the operating chiller was significantly lower than its design cooling capacity (i.e., 7230 kW) in case of the deficit flow. In the meanwhile, as illustrated in Figure 8.2, a much lower system temperature difference was resulted due to the high water flow rate (i.e., primary flow plus deficit flow) in the secondary system.

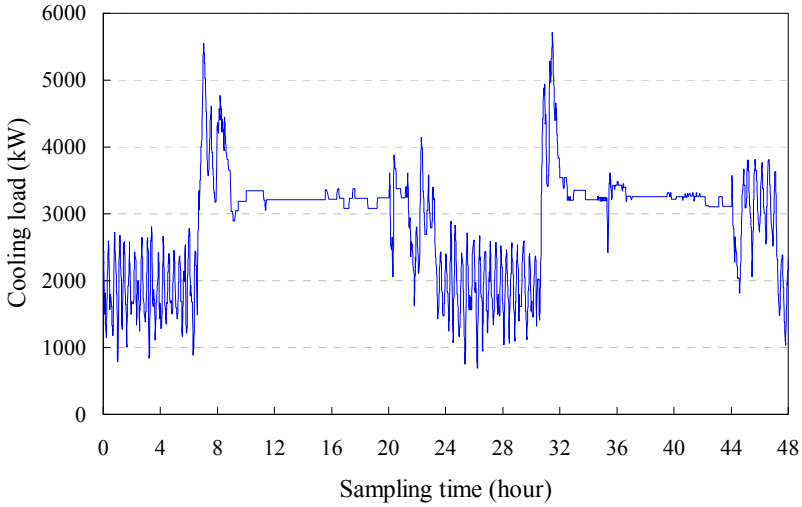

Figure 8.1 Measured cooling capacity of the operating chiller in two winter days

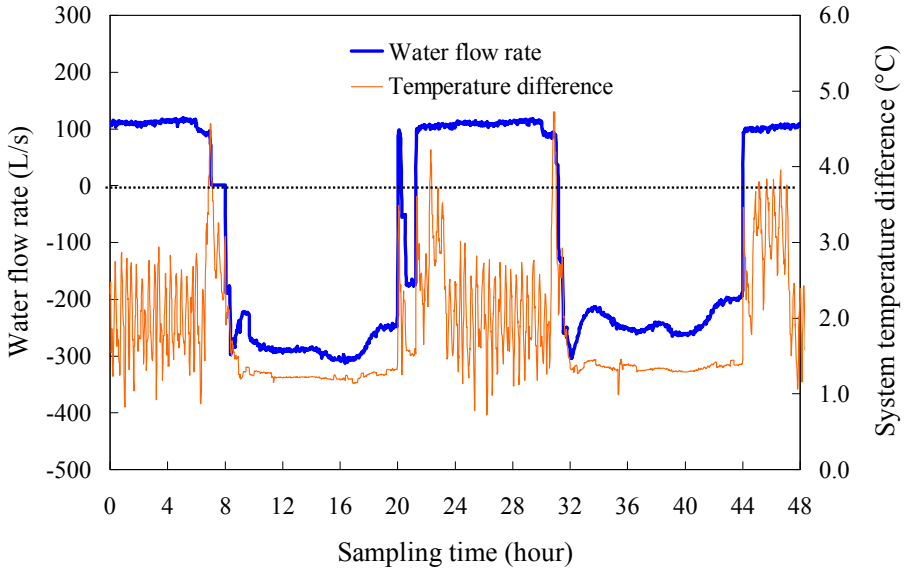

Figure 8.2 Measured water flow rate in the by-pass line and temperature difference in secondary system in two winter days

In order to solve the low delta-T syndrome in this system, the possible causes were analyzed and investigated firstly. Based on the analysis and investigation, the following causes were excluded, including coil fouling, improper sensor calibration, the use of three-way valves and the use of improper set-points. One of the possible causes would be the secondary return water mixing with the supply water from chillers, i.e., the deficit flow mixing with the primary flow.

Considering that the deficit flow is usually not good in the operation of central chilled water plants, a check valve is therefore considered to solve the low delta-T problems. As shown in Figure 8.3, when the check valve is used, the chilled water distribution system will behave as it is decoupled when the primary flow exceeds the secondary flow. However, the primary pumps and secondary pumps will be in series when the secondary flow exceeds the primary flow.

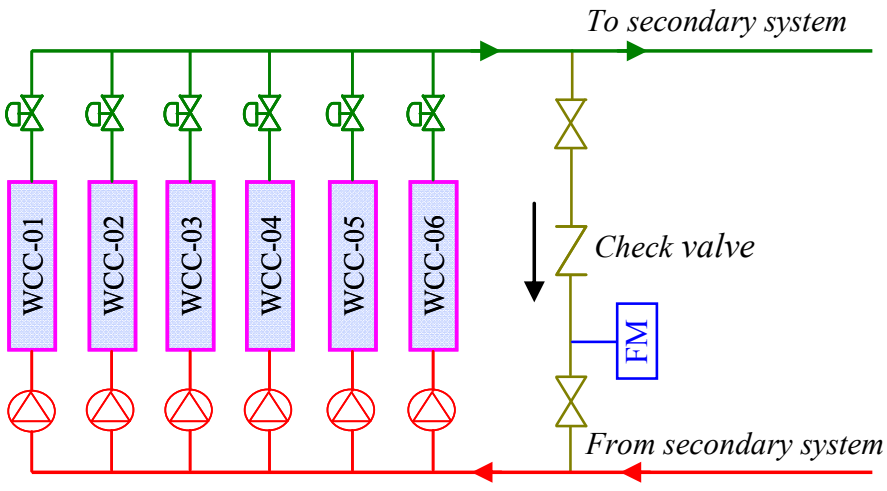

Figure 8.3 Illustration of the system with a check valve

As presented earlier, the existing studies regarding to the use of check valves failed to provide the details how they can improve the system operational performance. To

ensure sufficient degree of confidence on introducing the check valve, a test method is therefore designed and implemented to validate whether the check valve is feasible and can efficiently handle the low delta-T problems, prior to the installation of a real check valve. This test method uses a 'simulated' check valve through fully closing one of the butterfly valves in the by-pass line when the deficit flow is observed and the system experiences with low delta-T problems. In order to provide the distinct difference from that without using the check valve, the test was carried out when the observed deficit flow was in the range of 40%~60% of the design flow of the primary chilled water pump. This is to ensure that the operating chillers have sufficient capability to provide adequate cooling energy for terminal units under the given working condition and there is no need to bring an additional chiller online. During the tests, the chiller control was set to manual mode and the chiller operating number was maintained unchanged.

8.3 Results and Discussion

Three repeated tests by using the 'simulated' check valve were carried out in the real building in three days respectively. The three tests provided the consistent conclusions and the results presented hereafter are from the latest test carried out on Nov. 2009.

Figure 8.4 illustrates the water flow rates in the chilled water by-pass line when the butterfly valve in the by-pass line was fully open and fully closed (i.e., using the 'simulated' check valve) respectively. It can be found that the deficit flow existed

before the 'simulated' check valve was used. The butterfly valve was closed at 11:15am on that test day and opened again at 15:15pm when the test was finished. The chilled water supply temperature set-point used was the design value of 5.5°C and it was reduced to 5.0°C at 13:40pm. The change of the temperature set-point was to investigate whether the reduction of the temperature set-point can help to enhance the system operational performance when the chilled water plant integrated with a check valve.

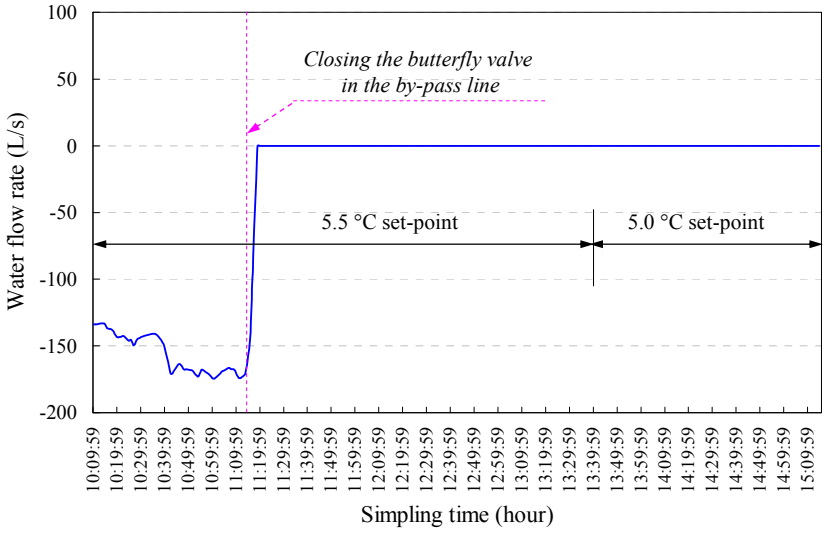

Figure 8.4 Water flow rate in the by-pass line before and after the use of the 'simulated' check valve

Figure 8.5 shows the cooling energy of the operating chiller and outlet air temperature of the AHU in the typical floor before and after closing the butterfly valve in the by-pass line. It can be observed that the supply air temperature could not be controlled at the desired set-point of 13.0°C while the operating chiller was not sufficiently loaded before the 'simulated' check valve was used. Once the 'simulated' check valve was used, the operating chiller was heavily loaded and outlet air

temperature of the AHU could be controlled at the intended set-point. It is worth noticing that the response of the AHU outlet air temperature to the changes of the system from the deficit flow condition to the use of the 'simulated' check valve was very slow and a significant time delay can be observed in Figure 8.5. It is also noted that when the chilled water supply temperature set-point was reduced from 5.5°C to 5.0°C, the cooling energy of the operating chiller increased firstly and then decreased gradually while the outlet air temperature of the AHU decreased firstly and then increased gradually until to reach to a relatively steady state. This demonstrated that lowering down the chilled water supply temperature set-point is worth to be considered in the sequence control of chillers when a check valve is used.

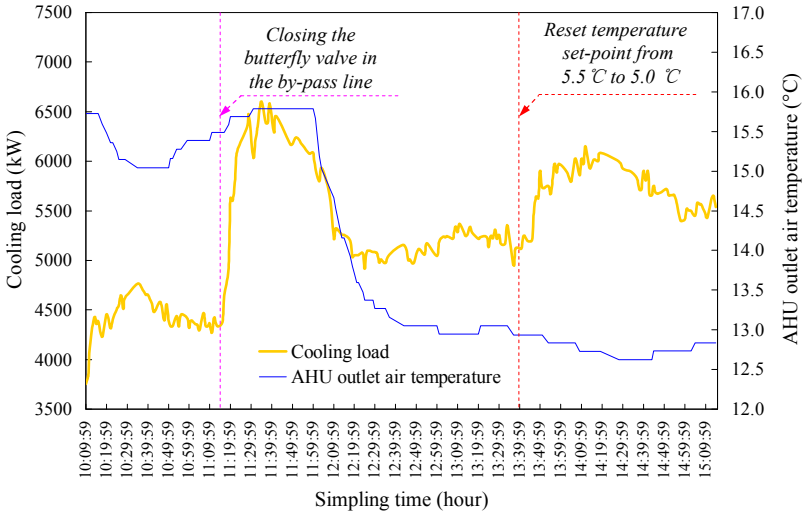

Figure 8.5 Comparison of the chiller cooling capacity and AHU outlet air temperature before and after the use of the 'simulated' check valve

Figure 8.6 presents the comparison of the total power consumption of chillers and secondary water pumps in the test period by using the 'simulated' check valve with that in a similar working condition and the same time period with the deficit flow but

resulting in an additional chiller in operation frequently. It can be found that significantly less energy was consumed when the 'simulated' check valve was used compared to that without using the 'simulated' check valve. The average energy saving due to the use of the 'simulated' check valve in this particular comparison was about 9.2% of the total energy consumption of both chillers and secondary water pumps. The savings will be significantly greater than the above value if the additional energy of a condenser water pump, a primary chilled water pumps as well as cooling towers due to the operation of one more chiller is included. Compared to the system operated with the 'simulated' check valve, when the system operated without using the 'simulated' check valve, if an additional chiller is put into operation, significant more energy will be consumed but cooling energy provided will be adequate. Otherwise, less energy will be consumed but cooling energy provided may be inadequate, resulting in poor indoor thermal comfort.

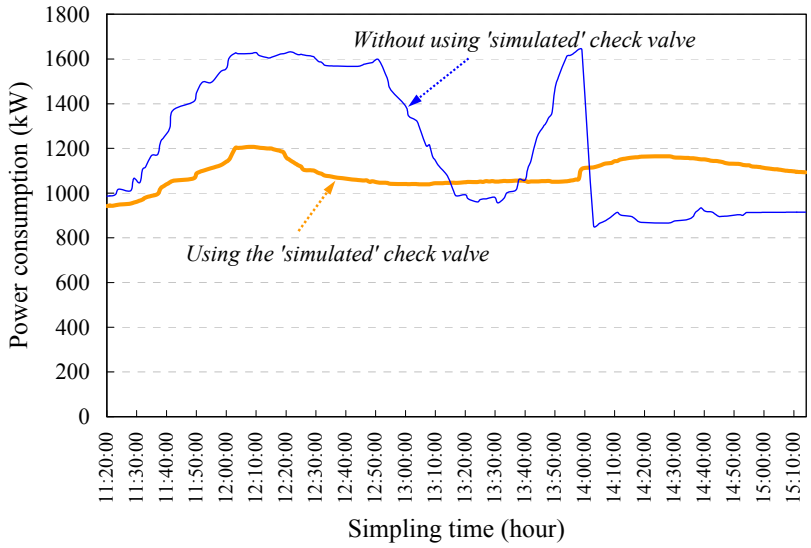

Figure 8.6 Comparison of power consumptions of chillers and secondary pumps between with and without the use of the 'simulated' check valve

The annual energy saving due to the use of a check valve in the complex system studied was estimated by comparing to that without using the check valve based on the current frequency of low delta-T syndrome monitored. Table 8.1 summarizes the annual energy consumption of chillers and pumps (i.e., including constant speed pumps and variable speed pumps) as well as their total energy consumptions when the system operated in two different configurations respectively. Compared to that without using the check valve, about 317200 kWh (0.94%) total annual energy of the chilling plant (including chillers and pumps) can be saved when the system operates with a check valve. The energy saving is mainly achieved due to the use of less operating number of chillers and less operating number of constant speed pumps. The energy consumption of cooling towers was not estimated here. Their actual energy consumption is strongly dependent on the ways used to sequence control of cooling towers, as the towers are equipped with variable speed fans.

Table 8.1 Estimated annual energy saving when using a check valve

System configuration	Chiller energy (kWh)	Pump energy (kWh)	Total energy (kWh)	Total saving	
				(kWh)	(%)
Without using the check valve	24567965	9270556	33838521	-	-
With the check valve	24356715	9164606	33521321	317200	0.94

The results from above tests illustrated that when the system operated with the excess water flow demand and low chilled water temperature difference, either an inadequate cooling energy (without switching on an additional chiller) or an increase in energy consumption (an additional chiller is put into operation) will be resulted.

However, the operating chillers cannot be loaded sufficiently. When the system equipped with a check valve, it can ensure the operating chillers to be loaded sufficiently before an additional chiller is brought online, which can therefore enhance the overall system operational performance and reduce the chiller utilization hours. As presented earlier, when a check valve is used, one issue needs to be concerned is that the secondary water pumps should have capacity of handling the increased pressure drop and water flow in the primary loop . This is often not a big problem in practice since the design of the secondary water pumps is usually somewhat oversized.

Based on the above tests, the installation of a check valve was recommended to the building owner. The building owner has accepted the recommendation and a check valve is being practically implemented.

8.4 Summary

This chapter presents an approach for experimentally validating the feasibility of using a check valve in the chilled water by-pass line to deal with the low delta-T syndrome encountered in primary-secondary chilled water systems, prior to the practical installation of a real check valve. The experimental tests were carried out in a real building through using a ‘simulated’ check valve by fully closing the butterfly valve in the by-pass line. The results show that either a better indoor thermal comfort or a significantly less energy can be resulted when a check valve is used as compared to that without using the check valve.

It is worthy noticing that the check valve is not feasible for every project. When a check valve is taken into consideration, other potential causes, such as improper sensor calibration, the use of improper set-points, etc, which can be easily handled, should be corrected firstly. A good understanding on the system configuration and potential limitations is also essential. In order to increase the degree of confidence by using the check valve, the experimental validation by using the 'simulated' check valve is worth and practical to be considered.

CHAPTER 9 IN-SITU IMPLEMENTATION OF THE ONLINE CONTROL STRATEGIES

This chapter presents how to implement the online control strategies developed in previous chapters for in-situ applications. An intelligent building integration and management system, namely IBmanager, is introduced as a management and communication platform. The online control software package can be integrated with BASs with the support of IBmanager to achieve energy efficient operation of complex building central chilling systems.

Section 9.1 briefly introduces the management and communication platform based on IBmanager. Section 9.2 presents the online control software packages of optimal control strategies and their implementation architectures. An overview of the application software system to implement the online control software packages to the super high-rise building presented in Chapter 3 is provided in Session 9.3. A summary of this chapter is given in Section 9.4.

9.1 Overview of the Management and Communication Platform

The management and communication platform, namely IBmanager, was developed in the Building Energy and Automation Research Laboratory, The Hong Kong Polytechnic University. It is a platform which integrates various building automation systems and industrial automation systems. The integration is supported by the

middleware and web services technologies. IBmanager allows the customized development of various IB subsystems as described in Figure 9.1.

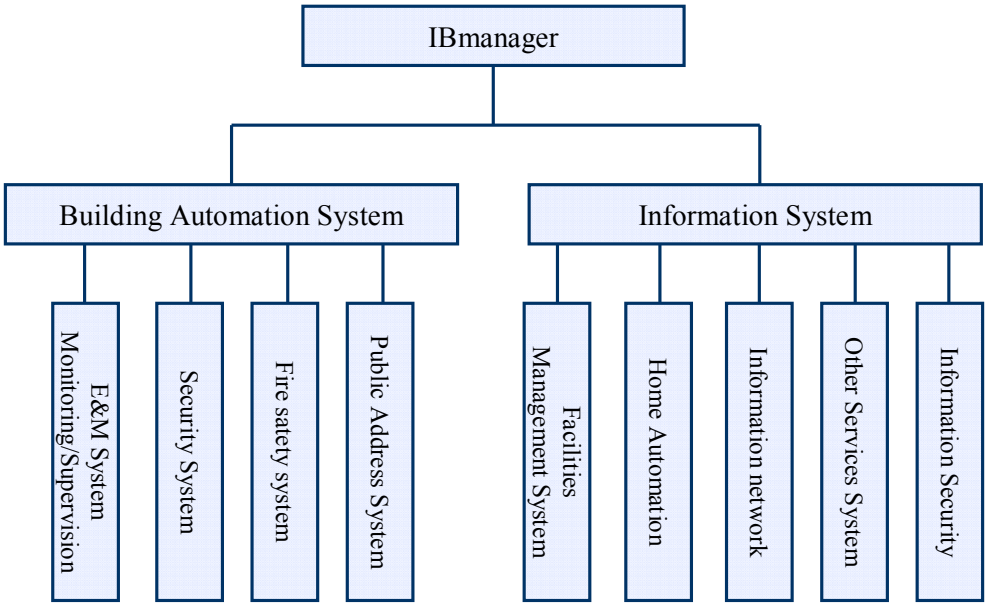

Figure 9.1 Structure of IBmanager

IBmanager contains several components such as OLE for process control (OPC) servers, historical database, BMS function components, BMS human machine interface (HMI), web services server and building management web server. Various interfaces connection and function blocks in IBmanager are shown in Figure 9.2. It can be observed that the intelligent control module and intelligent diagnosis module are included in the BMS function components. The two modules are the main work of this thesis. For other components of IBmanager, BMS HMI realizes the building automation functions in the local area network (LAN). Web services server converts the COM/DCOM interfaces to web services interfaces. The user interface is provided by the kits of active service pages (asp) and dynamic link library (.dll). They are the

interface between the building management web server and web services server.

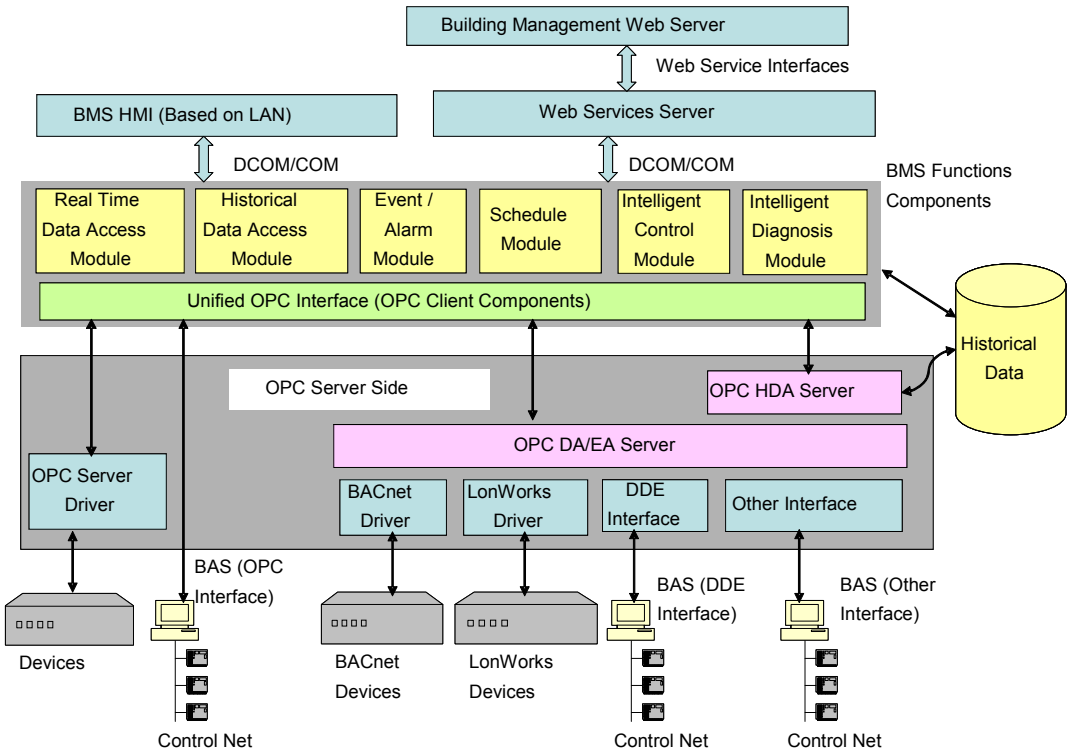

Figure 9.2 Interface connection and function blocks of IBmanager

The key features and functions of IBmanager are listed below.

(1) *Support platform for integration applications:* Accommodate the heterogeneous sub-systems compliant with diverse communication protocols, provide a unified data model and interface for integration/interoperation applications and value-added services.

(2) *Accommodate various communication interfaces:* accommodate various communication interfaces, including open protocols and proprietary protocols.

(3) *Capable to develop customized value-added services:* Allow users to develop their value-added services to be integrated into the IBmanager, such as the developed control and FDD strategies. These value-added services will be loaded into the

IBmanager as plug-ins, running in the same process with the IBmanager.

9.2 Online Software Packages of Optimal Control and FDD Strategies and Their Implementation Architectures

The online software packages of optimal control and FDD strategies are developed using Matlab or FORTRAN programming tools. Each control or FDD strategy in the software package is programmed as a subroutine, and is compiled as a DLL (Dynamic Link Library) module for the convenient implementation in IBmanager. In order to improve the control robustness of the online software packages, an upper limit on the number of iterations is constrained for the models that need the iteration process.

The in-situ implementation architecture of the control and FDD software package for the super high-rise building under study is shown in Figure 9.3. The online software packages developed in this thesis run in the IBmanager on a separate PC (Personal Computer) station. This PC is connected with the main station of the control system (BMS) for the whole chilling system through network. The software package is implemented as a function module of IBmanager, which is interfaced with the BMS via network automation engine (NAE). A decision supervisor in the control system of contractor (ATC) is designed for the operators to set whether the settings given by the online control software packages developed are used or ignored (not used). IBmanager can receive the system operation data through a NAE connecting with local controllers, and BA outstations connecting with sensors, actuators, etc. At the

meantime, IBmanager can send the optimal control settings to the ATC systems through the NAE for the practical control of the building services systems to improve their operating efficiency.

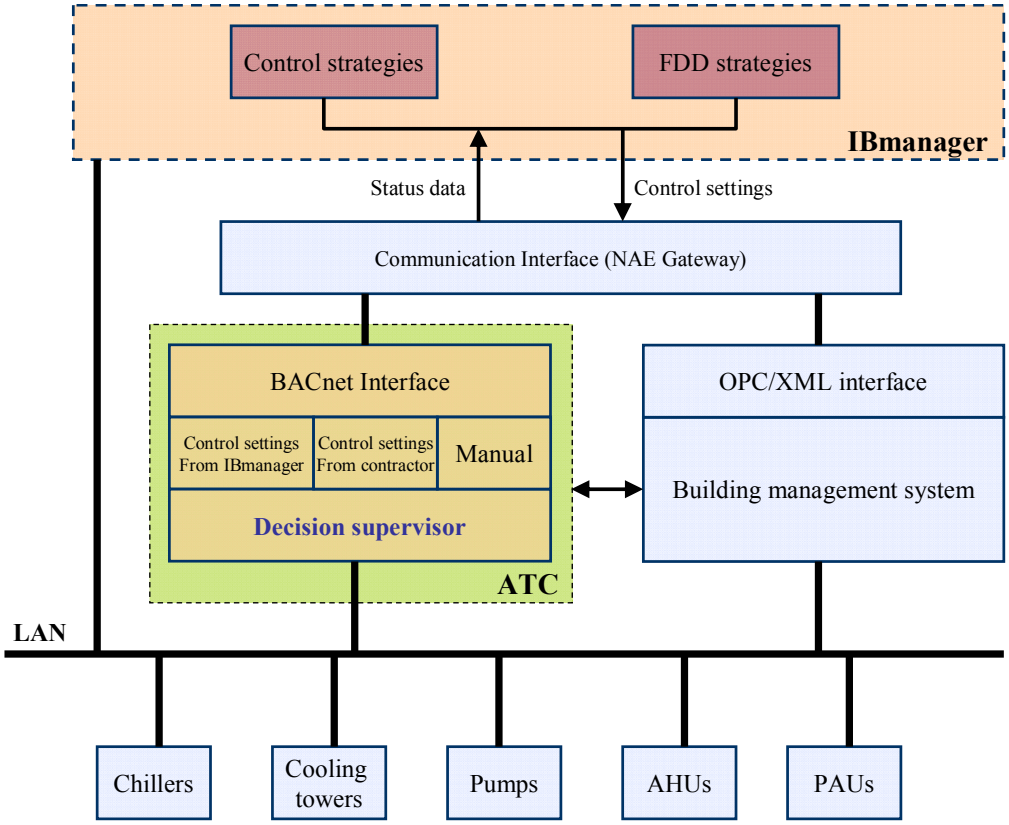

Figure 9.3 In-situ implementation architecture of the on-line building system control and FDD strategy

The data needed by the robust and optimal control strategies include supply air temperature, modulating valve position, water flow rate in the bypass line, total cooling load, pump head, etc. The data needed by the fault diagnosis strategies include the cooling load of AHUS, supply air temperature, temperature difference of AHUs, water flow rate of AHUs, etc. The feedbacks of the software package to the BMS are optimal control settings (such as operating frequency of pumps, operating

number of pumps, operating number of heat exchangers, etc.), diagnosis results, fault alarms, improvement recommendations, etc.

9.3 Overview of the Intelligent Control and Diagnosis System

IBmanager, as the intelligent building management system, has been implemented in the super high-rise building. The control and FDD software packages in IBmanager receive the status data from the existing control system of contractor and then to feed back the optimal settings, as shown in Figure 9.4. It consists of six functions modules, i.e. access management, history data storage, system setting, system configuration, system maintenance and real-time monitoring.

Access Management is used to provide different authorities for users. The supervisory user has the highest authority and can manage the access of all other users. ***History Data*** is used to store the monitoring data from BMS into the database in IBmanager. The recorded operation data can be used for many purposes, i.e., modeling training, fault detection and diagnosis, etc. ***System Setting*** is to select the proper protocols to link various building automation systems. ***System Configuration*** is to configure the parameters decided by different control strategies. ***System Maintenance*** contains server log, event recording and authority control. ***Real-time Monitoring*** is to monitor the operating status of the systems and components on-line via a friendly human machine interface (HMI).

Figure 9.4 The cover page of the ICDS for ICC

Figure 9.5, 9.6 and 9.7 show various human machine interfaces (HMI) of different HVAC sub-systems in the building. The operating data (i.e., chilled water supply and return temperatures, cooling water supply and return temperatures, etc.) can be displayed for operators to monitor whether the system operate properly.

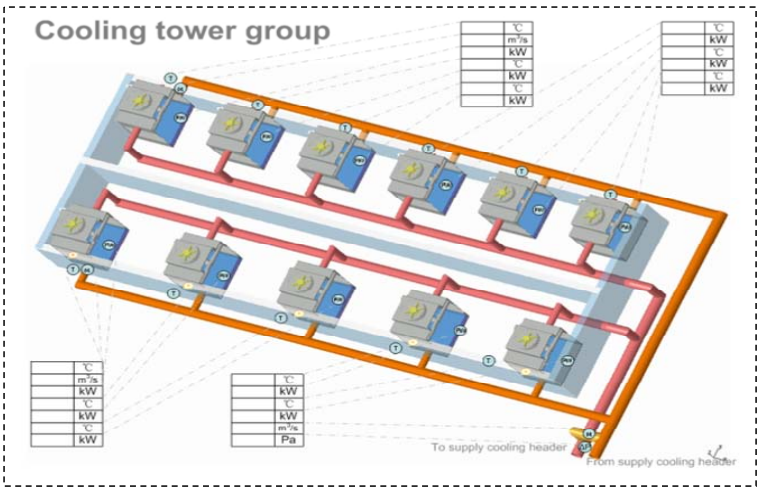

Figure 9.5 HMI of the operation of the cooling tower system

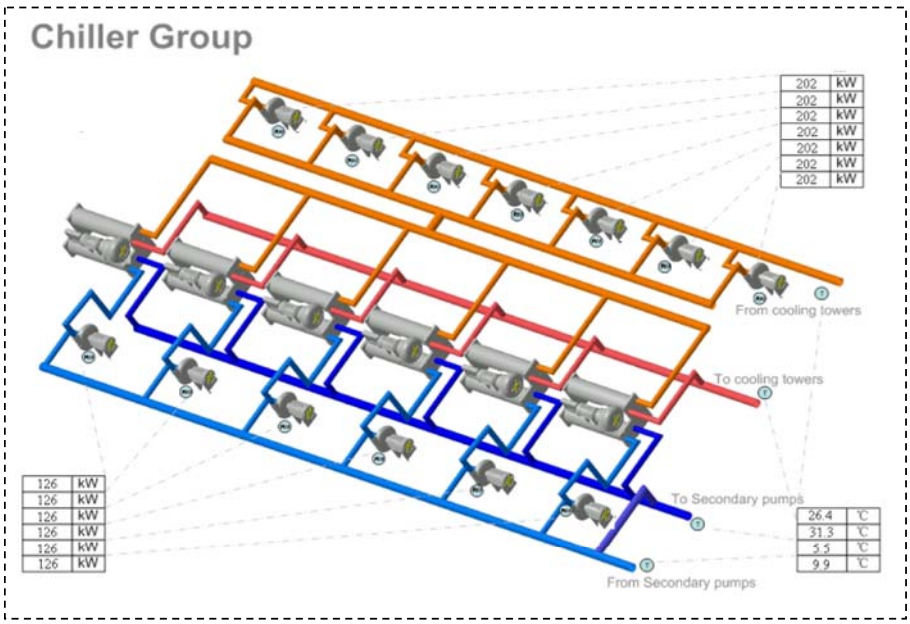

Figure 9.6 HMI of the operation of the chiller system

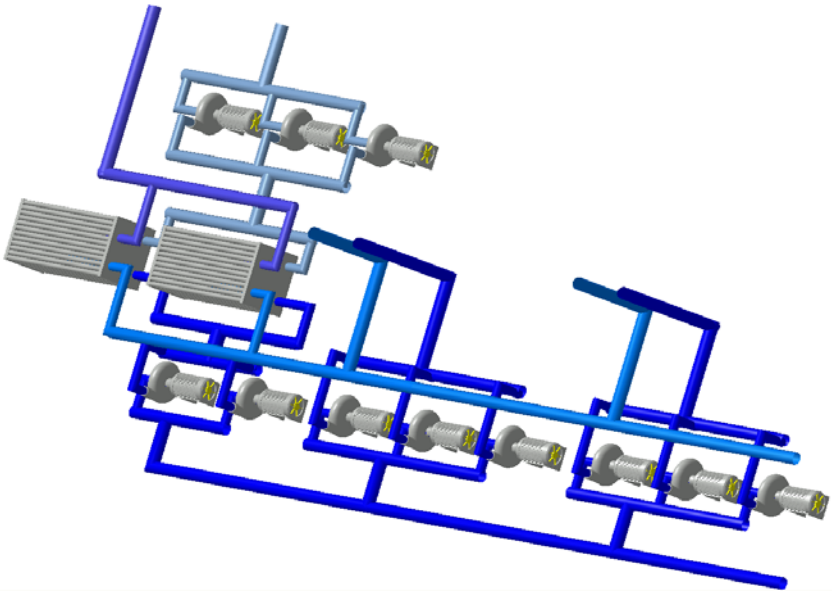

Figure 9.7 HMI of the operation of the heat exchanger system, SCHWP systems before and after heat exchangers

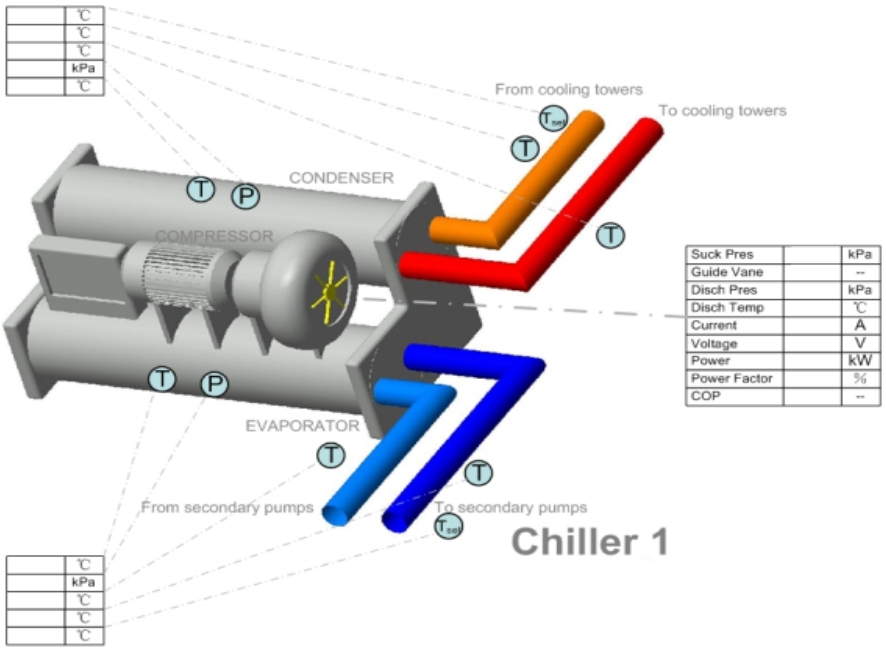

Figure 9.8 HMI of the operation of Chiller 1

9.4 Summary

In this chapter, the in-situ implementation of the proposed control and FDD strategies are presented. The control and fault diagnosis strategies are packaged as modules in IBmanager, which is a management and communication platform developed by the Hong Kong Polytechnic University. The software package of control strategies can receive the real-time operation data of HVAC systems and provide the robust and optimal settings to make more reliable and energy efficient operation. The software package of fault diagnosis strategies can detect unhealthy conditions of the building systems and identify faults automatically.

CHAPTER 10 SUMMARIES AND FURTHER WORK

Low delta-T syndrome and deficit flow problem have significant impact on the operation and energy performance of building chilled water systems. Diagnosis and proper control are highly desired for solving these problems and enhancing the overall performance of the building central air-conditioning systems. This research has addressed such need through the following contributions.

Conclusions on Main Contributions

i. The main contributions of this research are the development of diagnosis and robust control strategies for avoiding low delta-T syndrome and deficit flow problem in complex chilled water systems. The software tools and implementation guidelines for applying these diagnosis and control strategies for enhancing the overall performance of complex building central chilling systems have also been provided.

ii. A dynamic simulation platform for the complex building central chilling system is developed in the study, which is used to evaluate and compare the system operation and energy performances when using different control strategies under dynamic working conditions prior to site implementation.

iii. An in-situ case study to diagnose the low delta-t syndrome and deficit flow problem that frequently occurred in the studied super high-rise building is

presented. An in-situ diagnosis method of low delta-t syndrome for practical application is proposed.

iv. An optimal control strategy for online control of complex chilled water systems involving intermediate heat exchangers is proposed. This optimal control strategy determines the optimal settings of the outlet water temperature after heat exchangers and the required operating number of heat exchangers and pumps in order to minimize the total energy consumption of pumps under dynamic working conditions. This strategy enhances control robustness and reliability including avoiding deficit flow problem.

v. A fault-tolerant control strategy for primary-secondary chilled water pumps is proposed not only for eliminating the low delta-T syndrome and deficit flow problem but also for enhancing the energy efficiency of the chilled water distribution systems.

vi. An advanced fault detection and diagnosis (FDD) strategy integrated with energy impact evaluation for low delta-at syndrome is proposed to diagnose the low delta-T syndrome under dynamic working conditions, and estimate its energy impact on pumps using model-based method.

vii. An in-situ approach is presented for experimental validation of the possibility by using a check valve (i.e., putting a one-direction check valve in the chilled water by-pass line) in the studied super high-rise building to solve the deficit flow problem and thus to enhance the overall operational performance.

Summary on the in-situ case study to diagnose the low delta-T syndrome and deficit flow problem

This thesis presents a method and a case study to diagnose the low delta-T syndrome and deficit flow problem in an actual chilled water system of a super high-rise building. The improper set-point of the outlet water temperature at the secondary sides of heat exchangers was finally confirmed as the exact fault that caused the deficit flow problem. The results show that an improperly low set-point of outlet water temperature at the secondary side of heat exchangers can lead to higher operating frequency and more operating number of pumps on the primary side of heat exchangers, which easily causes the deficit flow. The deficit flow can be reduced or even eliminated when this set-point is reset properly.

The FDD method is validated by an in-situ test. A proper set-point of outlet water temperature on the secondary side of heat exchangers can achieve an average power saving of 87.67 kW (72.37%) of total pumps on primary and secondary sides of heat exchangers.

Summary on the online optimal control strategy for complex building chilled water systems involving heat exchangers

An online adaptive optimal control strategy for complex building chilled water systems involving intermediate heat exchangers is proposed. This strategy determines the optimal settings which minimize the energy consumption of chilled water pumps. This strategy adopts simplified adaptive models allowing the simple strategy can be accurate and effective under various working conditions.

The validation results show that the simplified adaptive models agree well with the "measured" operation data. The proposed optimal control strategy was proven to be able to accurately determine the optimal settings of the outlet water temperature after heat exchangers and the operating number of heat exchangers. The results of the energy performance evaluation tests show that 5.26%-14.69% of the pump energy could be saved when using the proposed optimal control strategy in normal operation as compared with conventional strategies.

The test results also demonstrate that the proposed optimal control strategy has enhanced control robustness and reliability in eliminating deficit flow in the system when facing disturbances, such as a sudden increase of inlet water temperature before heat exchangers. In the cases having deficit flow, up to 50.59% of the chilled pump energy could be saved when using the proposed strategy, which eliminated the deficit flow, as compared with that using the conventional control strategy.

Summary on the fault-tolerant and energy efficient control strategy for primary-secondary chilled water systems in buildings

A fault-tolerant control strategy for secondary chilled water pumps is proposed not only for eliminating the deficit flow but also for enhancing the energy efficiency of the chilled water distribution systems. This fault-tolerant strategy employs the developed flow-limiting technique that is activated when deficit flow tends to occur and eliminates it by resetting the differential pressure set-point for pumps control. This strategy also integrates optimal differential pressure set-point that can minimize flow resistance of chilled water loop while still satisfying cooling energy demand.

The operation and energy performance of the proposed fault-tolerant strategy was evaluated on a typical primary-secondary chilled water system in a high-rise building by simulation tests. In a healthy chilled water system, the results indicate that the proposed fault-tolerant strategy can avoid the deficit flow during the start period particularly when not all the chillers are switched on. Compared with the two conventional control strategies, the fault-tolerant strategy can save about 69.27-77.25% of secondary chilled water pump energy consumption during the start period due to the application of flow-limiting technique, which accounts for about 10.57-16.11% of the total energy of pumps and chillers. It also can save about 26.67-49.52 % of the secondary chilled water pump energy during a working day when compared with strategy using fixed differential pressure set-point.

In an unhealthy chilled water system with the occurrence of deficit flow under conventional controls, the proposed fault-tolerant strategy was proved eliminating deficit flow and improving the energy efficiency of pumps. About 30.97-54.30% of the secondary chilled water pump energy can be saved by using the proposed strategy when compared with the conventional strategy with fixed differential pressure set-point (strategy #1), in which about 3.99-24.73% of the secondary chilled water pumps energy saving were contributed by using flow-limiting technique. This fault-tolerant control strategy is not complex and is practical for real in-situ applications.

Summary on the advanced fault detection and diagnosis (FDD) strategy with energy impact evaluation for low delta-T syndrome

An advanced fault diagnosis strategy integrated with an energy impact evaluation method is presented, which is used for detecting and diagnosing the low delta-T syndrome resulted from the performance degradation of cooling coils and heat exchangers in chilled water systems. The energy impact of pumps due to the low delta-T syndrome is also evaluated. Performance indices and adaptive thresholds are adopted in the FDD strategy to determine the health condition of the system. Simplified models are adopted in the energy impact evaluation method to determine the energy impact caused by the low delta-T syndrome.

The proposed FDD strategy and the energy impact evaluation method were validated in a dynamic simulation platform representing a complex HVAC system. The results show that the proposed FDD strategy can detect the low delta-T syndrome and identify the faults. The results also show that the proposed energy impact evaluation method can accurately determine the energy impact of pumps by comparing the measured pump energy with the benchmark.

Summary on the experimental test to enhance performance of chilled water system using a check valve

An approach is presented for experimentally validating the feasibility of using a check valve in the chilled water by-pass line to deal with the low delta-T syndrome encountered in primary-secondary chilled water systems, prior to the practical installation of a real check valve. The experimental tests were carried out in a real

building through using a “simulated” check valve by fully closing the butterfly valve in the by-pass line. The results show that either better indoor thermal comfort or significantly less energy can be achieved when a check valve is used as compared to that without using the check valve.

Application issues

When the proposed FDD and control strategies are implemented in actual systems, some key points should be pointed out as below to make these strategies understood better and applied correctly.

The in-situ FDD is mainly used to preliminarily find out some simple causes of low delta-T syndrome through field observations and operation history analysis, such as the improper use of three-way valves, the improper control settings, the improper pump control logic, etc. It is hard to determine some potential faults, such as components fouling, and to assess the fault severity and the energy impact as well.

The advanced FDD strategy presented in Chapter 7 makes improvements on the limitation of the in-situ FDD method. It is developed based on mathematical models and analyzes quantitatively the potential faults, such as the coils fouling of AHUs and heat exchangers, and accurately estimate the energy impact resulted from these faults. When using the advanced FDD strategy, the parameters of the models should be identified in advance using the system operation data when there is no fault in the system.

The adaptive optimal control strategy is applicable for complex chilled water system involving heat exchangers. It is used to achieve a stable and energy efficient operation of the variable seed pumps on the primary side of the heat exchangers to avoid the deficit flow problem even some disturbances exist. It is developed based on the MPC (Model Prediction Control) method to accurately determine the optimal and robust supply water temperature on the secondary side of the heat exchanger group and the optimal operating number of heat exchangers. When this strategy is applied, the parameters of individual AHU model, heat exchanger model and pump model should be identified in advance using the operation data. It is noted that these parameters should be updated using the new operation data at certain interval, such as once in each three or six months, in case that there are some performance changes in the system.

The fault-tolerant control strategy is applicable for the typical primary-secondary chilled water systems. It can enhance the system operation stability and the energy performance to the most extent when there are faults that cause deficit flow in the system. When detecting the deficit flow in the bypass line, the secondary pump speed will be lowered down to reduce the water flow of the secondary loop until the deficit flow is fully eliminated. It can be easily integrated into the existing conventional control strategies of secondary pumps as an individual module to enhance their operation stability and anti-disturbance capability. Although the fault-tolerant control strategy can handle the deficit flow problem due to various faults with enhanced system energy performance, it cannot find out the exact reasons

of the deficit flow and cannot correct them as well.

The use of check valve to avoid deficit flow is experimentally validated to be feasible with obvious energy benefits in the studied real chilled water system. Its main function is to force all the return water passing through the chillers, and prevent the additional return water flow from mixing directly with the supply water flow from chillers. The supply water temperature to buildings therefore is kept as low as chiller supply water temperature. It is worthy noticing that the check valve is not feasible for every project. A good understanding on the system configuration and potential limitations is also essential. For instance, the check valve is not applicable for a system with thermal storage device on the secondary loop due to that reverse flow is needed in the bypass line when the chillers are shut down and only the thermal storage device works for cooling supply. Another risk that may occur is that it may result in a dead loop in case that the primary pumps are shut down while the secondary pumps are still in operation.

Based on the above analysis on the application issues, the FDD strategies and control strategies can be used together for the comprehensive diagnosis and optimization of system operation and energy performance. However, the fault-tolerant control strategy and the check valve cannot be implemented at the same time because they intend to eliminate deficit flow by two different means. The main difference between the two methods is that the check valve gets rid of the deficit flow by simply stopping the water flow in the reverse direction without consideration of the

operation of secondary pumps. The fault-tolerant control strategy overcomes the deficit flow by reducing the speed of secondary pumps. Therefore, the fault-tolerant control strategy might achieve better energy performance while overcoming the deficiencies and risks of check valve. It is recommended to use the fault-tolerant control strategy instead of the check valve in a system with sufficient sensors and control system. Obviously, the use of check valve is simpler in terms of operation and control.

Recommendations for Future Work

This study focuses on the development of the diagnosis and robust control strategies for avoiding the low delta-T syndrome and deficit flow problem in complex building central chilling systems. It would be highly desired to make further efforts on the following two aspects related to the research presented in this thesis.

- In-situ implementation and validation of all the diagnosis and robust control strategies proposed in this thesis are needed. This would further evaluate and validate these strategies and make them attain desirable and satisfactory performances in practice.
- The fault diagnosis strategy has been developed in Chapter 7 for detecting and diagnosing the low delta-T syndrome resulted from degraded cooling coils. To conveniently detect and diagnose other causes that result in the low delta-T syndrome, more FDD strategies are needed.

REFERENCES

Austin S.B. 1993. Chilled water system optimization. *ASHRAE Journal* 35(7): 50–56.

Avery G. 1998. Controlling chillers in variable flow systems. *ASHRAE Journal* 40(2): 42-45.

Avery G. 2001. Improving the efficiency of chilled water plants. *ASHRAE Journal* 43(5): 14-18.

Bahnfleth W.P. and Peyer E. 2001. Comparative analysis of variable and constant primary flow chilled-water-plant performance, Heating, Piping, *Air Conditioning Engineering* 73(4): 41–50.

Bahnfleth W.P. and Peyer E. 2006. Energy use and economic comparison of chilled-water pumping systems alternatives. *ASHRAE Transaction* 112(2): 198–208.

Bahnfleth W. and Peyer E. 2004. Variable primary flow chilled water systems: potential benefits and application issues, ARTI-21CR/611-20070-01, *Final report to Air-Conditioning and Refrigeration Technology Institute*.

Braun J.E., Klein S.A., Beckman W.A. and Mitchell J.W. 1989a. Methodologies for optimal control to chilled water systems without storage. *ASHRAE Transactions* 95(1): 652–662.

Braun J.E., Klein S.A., Mitchell J.W. and Beckman W.A. 1989b. Applications of optimal control to chilled water systems without storage. *ASHRAE Transactions* 95(1): 663–675.

Cascia, M.A. 2000. Implementation of a near-optimal global set point control method in a DDC controller. *ASHRAE Transactions* 106(1):249-63.

Chase D.V. and Ormsbee L.E. 1993. Computer-generated pumping schedules for satisfying operational objectives. *Journal of the American Water Works Association* V85(7): 54–61.

Claridge D, Culp C and Liu M et al. 2000. Campus-wide continuous commissioning of university buildings. *Proceedings of ACEEE Summer Study on Energy Efficiency in*

Buildings :3.101-3.112, Pacific Grove, CA.

Claridge D, Liu M and Haberl J. 1996. Can you achieve 150% of predicted retrofit savings? Is it time for recommissioning? *Proceedings of 1996 ACEEE Summer Study on Energy Efficiency in Buildings*: 4.59-4.67.

Coad W. J. 1998. A fundamental perspective on chilled water systems. *HPAC Engineering* 70(8): 59-66.

Dexter, A.L. and D. Ngo. 2001. Fault diagnosis in air-conditioning systems: a multi-step fuzzy model-based approach. *HVAC&R* 7(1):83-102.

Durkin T.H. 2005. Evolving design of chiller plants. *ASHRAE Journal* V47(11): 40-50.

Fiorino D.P. 1999. Achieving high chilled-water delta Ts. *ASHRAE Journal* V41(11): 24-30.

Fiorino D.P. 2002. How to Raise Chilled Water Temperature Differentials. *ASHRAE Trans* 108 (1): 659-665.

Fong K.F., Hanby V.I. and T.T. Chow. 2006. HVAC system optimization for energy management by evolutionary programming. *Energy and Buildings* 38(3):220–231.

Gertler, J.J. 1998. Fault detection and diagnosis in engineering systems. Marcel Dekker, Inc.

Giebler, T., Liu M., and Claridge D. 1998. Evaluation of energy conversion measures by model simulation. *The eleventh symposium on improving building systems in hot and humid climates proceedings*, June 1-2, Fort Worth, Texes.

Huang G.S., Wang S.W. and Sun Y.J. 2008. Enhancing the Reliability of Chiller Sequencing Control Using Fused Measurement of Building Cooling Load. *HVAC&R Research* V14(6): 941-958.

Hydeman M.and Zhou G. 2007. Optimizing chilled water plant control. *ASHRAE Journal* 49(6): 44–54.

Jack D.W., Thomas B. and Devine G. 1991. Pump scheduling and cost optimization. *Civil Engineering Systems* V8(4): 197–206.

Jin X.Q., Du Z.M. and Xiao X.K. 2007. Energy evaluation of optimal control

strategies for central VWV chiller systems. *Applied Thermal Engineering* 27(5-6): 934–941.

Katipamula, S. and Brambley M.R.. 2005a. Methods for fault detection, diagnostics and prognostics for building systems- A review, Part I. *HVAC&R Research* 11 (1):3-25.

Katipamula, S. and Brambley M.R. 2005b. Methods for fault detection, diagnostics and prognostics for building systems- A review, Part II. *HVAC&R Research* 12 (2):169-187.

Kirsner W. 1996. Demise of the primary-secondary pumping paradigm for chilled water plant design. *HPAC Engineering* V68 (11):73-78.

Kirsner W. 1998. Rectifying the primary-secondary paradigm for chilled water plant design to deal with low ΔT central plant syndrome. *HPAC Engineering* 70 (1): 128-131.

Kissock J.K. 1993. A methodology to measure retrofit energy saving in commercial buildings. PhD Thesis, Texas A&M University.

Lee, W.Y., C. Park and G.E. Kelly. 1996a. Fault detection of an air-handling unit using residual and recursive parameter identification methods. *ASHRAE Transactions*, 102(1):528-539.

Lee, W.Y., J.M. House, C. Park and G.E. Kelly. 1996b. Fault diagnosis of an air-handling unit using artificial neural networks. *ASHRAE Transactions* 102(1):540-549.

Lee, W.Y., J.M. House and D.R. Shin. 1997. Fault diagnosis and temperature sensor recovery for an air-handling unit. *ASHRAE Transactions* 103(1):621–633.

Lee, W.Y., J.M. House and N.H. Kyong. 2004. Subsystem level fault diagnosis of a building's air-handling unit using general regression neural networks. *Applied Energy* 77(2):153-170.

Liu M, Athar A and Claridge D et al. 1994. Reducing building energy costs using optimized operation strategies for constant volume air handling systems. *Proceedings of the Ninth Symposium on Improving Building Systems in Hot and Humid Climates*:192-204 . Arlington, Texas.

Lu L., Cai W.J., Chai Y.S. and Xie L.H., 2005a. Global optimization for overall HVAC systems—Part I problem formulation and analysis. *Energy Conversion and Management* 46(7-8): 999–1014.

Lu L., Cai W.J., Chai Y.S. and Xie L.H. 2005b. Global optimization for overall HVAC systems— Part II problem solution and simulations. *Energy Conversion and Management* 46(7-8): 1015–1028.

Luther K.R. 2002. Chilled water system forensics. ASHRAE Transactions V108(1): 654-658.

Ma Z.J. and Wang S.W. 2009. An optimal control strategy for complex building central chilled water systems for practical and real-time applications. *Building and Environment* 44(6): 1188-1198.

Ma Z.J. and Wang S.W. 2009. Energy efficient control of variable speed pumps in complex building central air-conditioning systems. *Energy and Buildings* 41 (2): 197-205.

Ma Z.J., Wang S.W. and Pau W.K. 2008. Secondary loop chilled water in super high-rise. *ASHRAE Journal* 50(5): 42-52.

McCormick G. and Powell R.S. 2003. Optimal pump scheduling in water supply systems with maximum demand charges. *Journal of Water Resources Planning and Management* 129(3): 372–379.

McQuay. 2002. Chiller plant design: Application Guide AG 31-003-1, 2002. *McQuay International*.

Moore B.J. and Fisher D.S. 2003. Pump pressure differential setpoint reset based on chilled water valve position. *ASHRAE Transactions* 109(1): 373–379.

Ngo, D., and A.L. Dexter. 1999. A robust model-based approach to diagnosing faults in air-handling units. *ASHRAE Transactions* 105(2): 1078-1086.

Norford, L.K., J.A. Wright, Buswell R.A. , Luo D., Klaasen C.J. and Suby A.. 2002. Demonstration of fault detection and diagnosis methods for air-handling units (ASHRAE 1020-RP). *International Journal of Heating, Ventilating, Air Conditioning and Refrigerating Research*, 8(1):41-71.

Persin, S. and Tovornic B. 2005. Real-time implementation of fault diagnosis to a

heat exchanger. *Control Engineering Practice* 13(8):1061-1069.

Qin, J.Y., and Wang S.W. 2005. A fault detection and diagnosis strategy of VAV air-conditioning systems for improved energy and control performances. *Energy and Buildings* 37(10):1035-1048.

Rishel J.B. 2003. Control of variable speed pumps for HVAC water systems. *ASHRAE Transactions* 109(1): 380–389.

Rishel J.B. 1991. Control of variable-speed pumps on hot-and chilled-water systems. *ASHRAE Transactions* 97(1): 746–750.

Rishel J.B. 1998. System analysis vs. quick fixes for existing chilled water systems. *HPAC Engineering* 70 (1): 131-133.

Severini S.C. 2004. Making them work: Primary-secondary chilled water systems. *ASHRAE Journal* 46 (7): 27-33.

Sun Y.J., Wang S.W. and Huang G.S., 2009. Chiller sequencing control with enhanced robustness for energy efficient operation. *Energy and Buildings* 41(11): 1246-1255.

Sun Y.J., Wang S.W. and Huang G.S. 2010. Model-based optimal start control strategy for multi-chiller plants in commercial buildings. *Building Services Engineering Research and Technology* 31(2): 113–129.

Taylor S.T. 2002. Degrading chilled water plant delta-T: causes and mitigation. *ASHRAE Transaction* 108 (1): 641-653.

Taylor S.T. 2002. Primary-only vs. primary-secondary variable flow systems. *ASHRAE Journal* V44(2): 25-29.

Tillack L. and Rishel J.B. 1998. Proper control of HVAC variable speed pumps. *ASHRAE Journal* 40 (11) : 41–46.

Upadhyayaa, B.R., and E. Eryurekb. 2006. Degradation monitoring of industrial heat exchangers. *Proceedings of the 1st World Congress on Engineering Asset Management (WCEAM)*: 504-215.

U.S. Department of Energy. 2010. *Building energy data book 2010*.

Waltz J.P. 2000. Variable flow chilled water or how I learned to love my VFD. *Energy Engineering* 97(6): 5-32.

Wang S.W. 2010. Intelligent Buildings and Building Automation, Spon Press (Taylor & Francis), London and New York.

Wang S.W. and Jin X.Q. 2000. Model-based optimal control of VAV air-conditioning system using genetic algorithm. *Building and Environment* 35(6):471-87.

Wang S.W. and Ma Z.J. 2010. Control Strategies for Variable Speed Pumps in Super High-Rise Building. *ASHRAE Journal* 52(7): 36–43.

Wang S.W., Ma Z.J. and Gao D.C. 2010. Performance enhancement of a complex chilled water system using a check valve: Experimental validations. *Applied Thermal Engineering* 30(17-18): 2827-2832.

Wang, S.W., and Xiao F. 2004. AHU sensor fault diagnosis using principal-component analysis method. *Energy and Buildings* 36(2):147–160.

Wang S.W. and Xu X.H. 2002. A Robust Control Strategy of Combined DCV and Economizer Control for Air-conditioning Systems. *Energy Conversion and management* V43 (18): 2569-2588.

Wang S.W., Zhou Q., and Xiao F. 2010. A system-level fault detection and diagnosis strategy for HVAC systems involving sensor faults. *Energy and Buildings* 42(4): 477-490.

Weyer, E., G. Szederkenyi, and K. Hangos. 2000. Grey box fault detection of heat exchangers. *Control Engineering Practice* 8(2):121-131.

Yu G., Powell R.S., Sterling M.J.H. 1994. Optimized pump scheduling in water distribution systems. *Journal of Optimization Theory and Applications* V83(3): 463–488.

Yoshida, H., and S. Kumar. 1999. ARX and AFMM model-based on-line real-time data base diagnosis of sudden fault in AHU of VAV system. *Energy Conversion & Management* 40(11):1191-1206.